University of Nevada

Reno

Active Faults and Associated Tectonic Stress in the Coso Range, California

A dissertation submitted to the University of Nevada at Reno
in partial fulfillment of the requirements for the degree of
Doctor of Philosophy

by

Glenn R. Roquemore

March 1981

Mines Library
University of Nevada - Reno
Reno, Nevada 89557

MINES
LIBRARY
Thesis
1553

The dissertation of Glenn R. Roquemore is approved:

David B Slemmons
Dissertation Advisor

R. F. Lawson
Department Chairman

John E Nellor
Dean, Graduate School

University of Nevada

Reno

March 1981

ACKNOWLEDGMENTS

The author is indebted to the NWC Research Department, particularly Pierre St. Amand, and the Sigma XI Grants-in-aid (University of Nevada) for their technical and financial support in carrying out this study. Also, consultative contributions by Charles Bacon, David B. Slemmons, Roy J. Shlemon, and John Zellmer are greatly appreciated.

ABSTRACT

The Coso Range contains faults that have been active in the Holocene. Some of these faults have moved about 100 years ago, possibly with the 1872 Owens Valley earthquake. Exploratory trenches exposed offsets up to 3.4 meters for one faulting event. Thus, a magnitude of 7.5 could be expected on these faults based on displacement versus length equations. Recent local and regional earthquakes have caused property damage in the city of Ridgecrest.

The tectonics of the Coso Range have been described as having arcuate and ring faults both of which suggest the presence of a circumscribed subsidence bowl or caldera-like feature. Data presented in this paper suggest the tectonism of the Coso Range is in transition between stresses from the right-slip, San Andreas fault-plate interaction and the extensional tectonics of the Basin and Range province. Arcuate faults in the Coso Range are interpreted to have been produced by the regional stress field, rather than being from volcanogenic origin. Focal mechanisms of small-magnitude earthquakes support the stress directions indicated by local fault patterns. Fumeroles in the area are primarily associated with oblique-slip faults, rather than with arcuate or ring faults. The geothermal reservoir is, therefore, much different from that of a caldera or subsidence bowl, and the overall geothermal potential is probably less than the earlier estimates.

This diverse structural zone between the Sierra Nevada and Walker Lane could be caused by a clockwise rotation of the Sierra Nevada Range about its northern axis.

CONTENTS

ABSTRACT iii

LIST OF FIGURES viii

LIST OF TABLES xii

1.0 INTRODUCTION 1

1.1 PURPOSE AND SCOPE 3

1.2 PREVIOUS WORK 4

1.3 GEOGRAPHY 5

1.3.1 Location and Access 5

1.3.2 Human Activity 7

1.3.3 Topographic Mapping and Aerial Photography . . . 7

1.3.4 Climate 7

1.3.5 Flora and Fauna 8

1.4 PHYSIOGRAPHIC SETTING 8

1.5 GEOLOGIC SETTING 9

1.6 LITERATURE AND DATA REVIEW 10

1.7 AERIAL PHOTOGRAPHY INTERPRETATION 10

1.8 FIELD VERIFICATION 11

1.9 SCARP PROFILING 11

2.0 DESCRIPTION OF ACTIVE FAULTS 14

2.1 INTRODUCTION 14

2.2 LITTLE LAKE FAULT 14

2.3 SOUTHERN SEGMENT OF THE AIRPORT LAKE FAULT (PLATE 2) 23

2.4 THE NORTHERN, COSO HOT SPRINGS, AND HAIWEE SPRINGS SEGMENTS OF THE AIRPORT LAKE FAULT (PLATE 3) 29
2.5 ACTIVE BREAKS ALONG THE EAST SIDE OF AIRPORT LAKE (PLATE 4) 35
2.6 SUMMARY AND CONCLUSIONS 40
3.0 EXPLORATORY TRENCHING 44
3.1 INTRODUCTION 44
3.2 TRENCH A 44
3.2.1 Stratigraphy 50
3.3 TRENCH B 51
3.3.1 Stratigraphy 55
3.4 LITTLE LAKE TRENCH 57
3.5 SUMMARY AND CONCLUSIONS 59
4.0 FAULT SCARP PROFILES 65
4.1 INTRODUCTION 65
4.2 FACTORS THAT AFFECT SLOPE DEGRADATION IN THE COSO RANGE 65
4.3 FAULT SCARP PROFILES 66
4.3.1 Coso Hot Springs Segment of the Airport Lake Fault 66
4.3.2 Southern Segment of the Airport Lake Fault . . . 66
4.3.3 Faults on the East Side of Airport Lake 70
4.3.4 Back-Crest Swale 70
4.4 SUMMARY AND CONCLUSIONS 73

5.0 SEISMICITY 75

5.1 INTRODUCTION 75

5.2 DESCRIPTION OF NOTABLE EARTHQUAKES 75

5.2.1 1872 Owens Valley Earthquake 75

5.2.2 1917 Owenyo Earthquake 76

5.2.3 1946 Walker Pass Earthquake 77

5.2.4 1952 Kern County Earthquakes 81

5.2.5 1961 Brown Earthquake 84

5.2.6 1962 Walker Pass Earthquake 86

5.2.7 February 1977 Ridgecrest Earthquake 90

5.2.8 March 1977 Ridgecrest Earthquakes 92

5.2.9 1979 Walker Pass Earthquake 93

5.2.10 Local Seismicity 93

5.3 SUMMARY AND CONCLUSIONS 98

6.0 CALCULATION OF DESIGN EARTHQUAKE 100

6.1 INTRODUCTION 100

6.2 DESIGN EARTHQUAKE (LITTLE LAKE FAULT) 100

6.3 DESIGN EARTHQUAKE (AIRPORT LAKE FAULT) 101

6.4 DESIGN EARTHQUAKE (EAST SIDE AIRPORT LAKE FAULT) 102

6.5 SUMMARY AND CONCLUSIONS 103

7.0 PRESENT LOCAL TECTONIC PATTERN 104

7.1 INTRODUCTION 104

7.2 STRUCTURE CONSISTENT WITH BASIN AND RANGE STRESS PATTERNS 105

7.2.1 Graben Valleys and Tilted Blocks 105

7.2.2 Strike-Slip Faults 107

7.2.3 White Hills Anticline 110

7.2.4 Alignment of Volcanoes 110

7.3 RATE AND STYLE OF VERTICAL AND HORIZONTAL DISPLACEMENTS 111

7.3.1 Vertical Displacements 111

7.3.2 Horizontal Displacements 111

7.4 FUMEROLIC ACTIVITY ALONG BASIN AND RANGE FAULTS IN THE COSO RANGE 112

7.5 ARCUATE FAULTS IN THE COSO RANGE 113

7.6 SUMMARY AND CONCLUSIONS 115

8.0 REGIONAL TECTONICS 117

8.1 INTRODUCTION 117

8.2 TECTONIC MODEL FOR THE AREA BETWEEN THE SIERRA NEVADA AND THE WALKER LANE 119

8.3 SUMMARY AND CONCLUSIONS 122

9.0 SUMMARY AND CONCLUSIONS 123

10.0 REFERENCES 128

MAP ENCLOSURES . . . . . (Inside back cover)

LIST OF FIGURES

1. Index map of the study area 6

2. Aerial view of the Sierra front showing a shutter ridge caused by the Little Lake fault 16

3. Aerial view of a sidehill trough formed in association with the shutter ridge shown in Figure 2 17

4. Aerial view of 250 meters of right-slip displacement caused by the Little Lake fault in a 400,000 year old lava flow 18

5. Aerial view of tectonic depressions and linear troughs along the Little Lake fault 19

6. Aerial view of a rhomboid tectonic depression on the Little Lake fault 20

7. Ellipsoidal ridges formed along the Little Lake fault 21

8. A linear trough formed along the Little Lake fault 22

9. Schematic model indicating how thrust faulting has occurred on the Little Lake fault 24

10. Aerial view of a 2-kilometer-wide graben located on the south end of the Airport Lake fault 26

11. Aerial view of a 1-kilometer-wide graben located in coso basin on the Airport Lake fault 27

12. Stones that have been overturned by seismic shaking 28

13. Aerial view of faceted spurs formed along the Airport Lake fault 30

14. Aerial view looking north along the south segment of the Airport Lake fault 31

15. Aerial view looking south along the Coso Hot Springs segment of the Airport Lake fault 32

16. Aerial view of the northeast end of the Coso Hot Springs segment of the Airport Lake fault 33

17. Aerial view of the Sierra Nevada front 34

18. Schematic diagram indicating how landslides can form between *en echelon* faults 36

19. Aerial view of the faults on the east side of Airport Lake 37

20. Aerial view of faults trending into the Wild Horse Mesa 38

21. Comparison between fault patterns on Wild Horse Mesa and those on the Bishop tuff 39

22. View of 1/2-meter recent normal-slip displacement on a fault on the east side of Airport Lake 41

23. Aerial view showing location of Trench A 45

24. Aerial view showing location of Trench B 46

25. Aerial view showing the location of the Little Lake trench 47

26. View of Airport Lake fault exposed in Trench A 48

27. Log of Trench A 49

28. Log of Trench B 52

29. A 20-centimeter-thick calcrete layer that has been truncated by faulting 53

30. Slickensided fault plane in Trench B 56

31. Little Lake trench showing its position within a tectonic depression 58

32. View of the Little Lake trench showing its length and width 60

33. Truncation of stratigraphy by the Little Lake fault 61

34. View of the stratigraphic unit that contains most of the mud volcanos exposed by the Little Lake trench 62

35. View of the fine structures found in a mud volcano exposed by the Little Lake trench 63

36. Scarp profile No. 1 on the Coso Hot Springs segment of the Airport Lake fault 67

37. Scarp profile No. 2 on the Coso Hot Springs segment of the Airport Lake fault 67

38. Scarp profile No. 3 on the Coso Hot Springs segment of the Airport Lake fault 68

39. Scarp profile No. 4 on the Coso Hot Springs segment of the Airport Lake fault 68

40. Scarp profile No. 5 on the Coso Hot Springs segment of the Airport Lake fault 69

41. Scarp profile No. 1 on the southern segment of the Airport Lake fault 69

42. Scarp profile No. 2 on the southern segment of the Airport Lake fault 70

43. Scarp profile No. 1 on the east side of Airport Lake 71

44. Plot of the regional historical seismicity from 1932-1977 78

45. Closeup view of machine shop wall showing cracking and grouting along the foundation where the wall shifted about 2 centimeters off the foundation 87

46. Water pipe and concrete retainer wall 88

47. View of the 1961 epicentral region showing tilted telephone poles 89

48. Geographic plot of southern California region showing locations of earthquakes larger than magnitude 6.0 94

49. Strain-relief map of the southern California region 95

50. Plot of local microseismicity from September 1975 to September 1977 97

51. Plot of focal mechanisms for the Coso Range 99

52. Fault map of the Coso Range 106

53. Schematic diagram of the southern Coso Range showing the local stress orientation 108

54. Aerial view of Wild Horse Mesa showing abundant step-faults 109

55. Diagram showing how Chinnery's concept of arcuate faults apply to the Coso Range 114

56. Fault map of the western United States and Mexico 120

57. Schematic of Figure 56 121

LIST OF TABLES

1. Fault scarp profile data 72
2. Design earthquake data for the Little Lake fault 101
3. Design earthquake data for the Airport Lake fault 102
4. Design earthquake data for the faults on the east side of Airport Lake 103

1.0 INTRODUCTION

The Coso Range contains diverse rock types and geomorphology. The volcanic rocks include basalts, andesites, dacites, and rhyolites. The basement rocks include granitic, diorite, gabbro, and occasional metamorphic septa. Most of the volcanic rocks are Quaternary age with eruptions as early as 40,000 years ago.

Roquemore (1977) reported that the Coso Range contains a group of west- and east-tilted blocks with a multitude of grabens. Most of the warping has occurred since mid-Pleistocene and represents between 2000 to 3000 feet of differential uplift; the deformation rate is determined to be 1.82 millimeter per year, vertically.

Walter and Weaver (1980a), in a study of the seismicity of the Coso Range, found that during the first two years of seismographic-network operation (1975-1977), 4200 local earthquakes (with magnitudes ranging from 0.5 to 3.9) were recorded within or immediately adjacent to the Coso Range. The structure indicated by a seismicity study (Walter and Weaver, 1980b) is a complex, conjugate strike-slip pattern with major zones that strike north-northwest and show right-slip movement, with a general north-south compression consistent with all fault-plane solutions.

Roquemore (1978a) reported that the Coso Range is a tectonic block bounded by the Owens Valley graben boundary faults, that splay around the eastern and western sides of the block. The Coso block has horst and graben structures, internal second order, with north-south trending. Strike-slip faulting has resulted in conjugate Riedel and *en echelon* faults which internally complicate the horst and graben structures.

Seismicity of the Coso Mountains is related to known faults in most cases, and the earthquake focal mechanism matches the geologic evidence (Roquemore, 1977) for fault style and orientation (Walter and Weaver, 1980b). Experimental and field data suggest that all of the major structures are compatible with regional spreading and associated north-south compression and east-west extension, and are typical within the Basin-Range and Sierra Nevada transition zone.

Roquemore (1978b) noted that the Coso Range contains several major active fault systems. These include the Charlie fault (now named the Little Lake fault), the Haiwee fault, and the Airport Lake fault which dominate other (lesser developed) faults in the area. The orientations of these faults range from northwest to north and south and have right-slip displacement indicated by offset landforms and left-stepping *en echelon* dip-slip morphology.

The northwest-trending Little Lake fault can be traced south from Little Lake, through Indian Wells Valley, and on south to the Garlock fault. Along its length are well developed rhombohedral depressions and pressure ridges that document lateral movement. Blancan (von Huene, 1960) sediments are warped by the fault into an anticlinal structure more than 25 meters high. The southern end of the fault bends nearly 90 degrees to the east as it approaches the Garlock fault (Zbur, 1962). Activity of the fault is indicated by offset Holocene (i.e., post-Pleistocene or recent) materials and evidence of numerous recent earthquakes ranging in magnitude from 3.8 to 5.0.

Most of the major active faults in the Coso Range are typical range front faults that trend north and south. Field evidence suggests that

these faults are all acting as part of the same structural system. There are major left-lateral offsets located along the Garlock fault which is to the south of the Coso Range. The Garlock fault serves as a boundary zone between the Mojave block and the Basin- and Range-physiographic province. The Sierra Nevada fault zone, which is situated to the west of the Coso Range, has been considered one of the more active zones in southern California (Hileman et al., 1973).

1.1 PURPOSE AND SCOPE

The purpose of this study is to (1) map and determine the morphology and activity of faults in the Coso Range, (2) determine the present structural mechanics of the Coso Range, (3) explain the structural development based on (1) and (2) above, and to (4) suggest a tectonic model for the structural development of the Coso Range and surrounding areas based on recent geologic history.

State-of-the-art methods in fault detection and analysis were applied in implementing the procedures discussed in this report. Photography at varying scales and time of day was utilized. Also, field verification of data was done along all geologic zones and appropriate annotations were made on a map (i.e., offset stream and shutter ridge). Exploratory trenching was accomplished to expose fault planes, to provide a means for dating the faults, and to determine recurrence intervals.

The method of investigation used for this study is listed as follows:

1. Collect and review all appropriate published and unpublished reports and data.

2. Acquire all available aerial photography for the region (in this case low-sun-angle, low-altitude photography was available).

3. Interpret the photographs.

4. Accomplish detailed field work including field verification.

5. Accomplish exploratory trenching.

6. Construct scarp profiles.

7. Prepare active fault maps and a technical report.

1.2 PREVIOUS WORK

The Coso Range is included in a portion of land that was withdrawn from public land during the early 1940s. Prior to that time, geologic investigations were restricted to broad-scale regional studies such as those done by Whitney (1865), Gilbert (1875), Goodyear (1888), Fairbanks (1896a,b), Campbell (1902), Spurr (1903), and Knopf (1911).

Small mining efforts resulted in geological reports on the Coso Range and nearby areas. These investigators include Warner (1930), Ross and Yates (1943), Frazer et al. (1943), Chesterman (1956), Power (1959), and Hall and Mackevett (1962).

The Coso formation was studied especially from the paleontological aspect by Schultz (1937).

Other studies that mention the Coso Range (although not the prime focus) include Kelley (1937, 1938) and Hopper (1947).

Structural studies of the Coso Range were undertaken by von Huene (1960), Zbur (1963), and Healy and Press (1964).

Geologic mapping of the Coso Range has been completed by Roquemore (1977), Duffield and Bacon (1977), and Stinson (1977).

Several reports have now been published that deal primarily with the definition of the Coso geothermal resource area (see *Literature and Data Review* paragraph in subsequent text).

1.3 GEOGRAPHY

1.3.1 Location and Access

The Coso Range is in the southwest corner of the Basin and Range physiographic province (Figure 1). The massif of the Sierra Nevada (to the west) is separated from the Coso Range by Rose Valley. Owens Lake is on the northern boundary, the Argus Range is to the east, and the Indian Wells Valley is to the south.

Access to the Coso Range is good along Highway 395 from which two dirt roads (bladed) lead into the study area. Cinder Road leaves the highway at Red Hill (a prominent cinder cone in Rose Valley), and Coso Road leaves the highway at Gill's Oasis (a roadside rest area) also in Rose Valley. Other routes include a 4-wheel drive road which leads south from the settlement of Darwin and two 4-wheel drive roads that lead north from the compounds of the Naval Weapons Center.

NOTE

It should be made very clear at this point that only the west portion of the Coso Range can be entered without permission from the Naval Weapons Center. A locked gate blocks each of the access roads into the range.

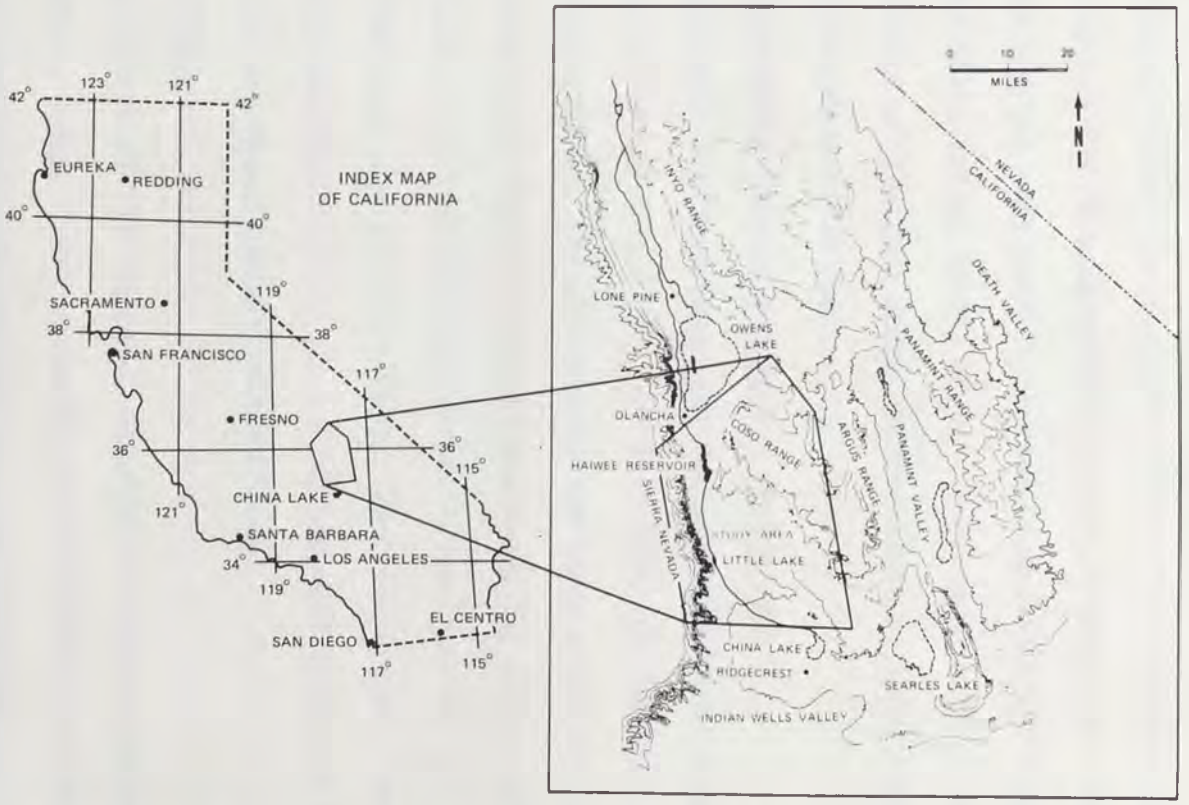

FIGURE 1. Index map of the study area.

1.3.2 Human Activity

The study area is totally rural and located mostly on military restricted land. There are a few small population concentrations nearby. These villages include Pearsonville, Little Lake, Cartago, Dunmovin, Grant, and Olancha and are located generally along Highway 395. Ridgecrest and China Lake are two substantially larger communities which are located in the Indian Wells Valley to the south. Small pumice mines in the unrestricted areas of the Coso Range produce lightweight aggregate, planting material, and decorative rock.

1.3.3 Topographic Mapping and Aerial Photography

Topographic coverage comprises four maps drawn to a scale of 1:62,500. These are (1) Haiwee Reservoir, (2) Coso Peak, (3) Mountain Springs Canyon, and (4) Little Lake. The photographs and surveys for the 1:24,000 series are completed, but they will not be available for three to four years. Conventional aerial photographs are available from the U.S. Geological Survey (USGS) and the U.S. Air Force. Special-purpose, low-altitude photography was used for the study, and was made available by the National Aeronautics and Space Administration (NASA).

1.3.4 Climate

The climate of the region is associated with hot summers, cool to cold winters, large diurnal temperature variations, low humidity, little cloudiness and visibility restrictions, and prevailing southwest winds. Russell (1926) classified the Coso Range in a transition between hot and cold desert with a January isotherm greater than 32°F. To be more precise, at the 3400- to 4400-foot elevation in the Coso Range, there exists a 32°F isotherm (adapted from Naval Weapons Center data). According to

the Naval Weapons Center weather summary, 1946 to 1976, the mean annual precipitation is 2.96 inches.

1.3.5 Flora and Fauna

Much of the soil at the higher elevations of the Coso Range support a mixed Joshua tree and pinon pine, timber-type ground cover. The median elevations support Joshua trees and Shadscale brush, and the lower elevations are typified by creosote bush and Shadscale brush.

Mammalian populations in the area include ground squirrels, pocket mice, cricetine rats and mice, hares, and rabbits. A few bats are commonly seen on summer evenings.

Indigenous and migratory birds found in the Coso Range are the golden eagle (*Aquila chrysaetos*), hawks, prairie falcons (*Falco mexicanus*), American kestrels (*Falco sparverius*), owls, roadrunners (*Geococcyx californianus*), and native quail. Chukars (*Alectoris chukar*) were introduced into the area and are abundant near springs.

Indigenous large mammals observed in parts of the area include the mountain lion (*Felis conolor*), bobcat (*Lynx rufus*), coyote (*Canis latrans*), kitfox (*Vulpes macrotis ssp*), and the badger (*Taxidea taxus*). Exotic mammals include the feral burro (*Equus asinus*), the feral horse (*Equus caballus*), and domestic cattle.

1.4 PHYSIOGRAPHIC SETTING

The Coso Range forms a natural barrier at the south end of Owens Valley. It is bounded on the north by Owens Lake (dry) and bounded on the south by Indian Wells Valley; both are closed basins. Coso Peak is the highest point in the Coso Range with an elevation of 8160 feet

approximately 2500 meters). The lowest topographic contour has an average elevation of 3000 feet (approximately 900 meters). The physiography is generally a moderately uplifted horst block with minor horsts and grabens within it. In places, the boundary between the Coso Range and the Argus Range is barely discernible. In the northern portion of the area, the Argus Range is separated from the Coso Range by Etcheron Valley; however, the southern portion is not separated by any physiographic feature. At its northeast corner, the Coso Range is separated from the Inyo Range by the Centennial Flats, a broad graben valley.

1.5 GEOLOGIC SETTING

The Coso Range basement rock is a tectonically isolated sliver of the Sierra Nevada batholith composed of cretaceous plutons and minor metamorphic septa. Volcanic cover, Pliocene to Pleistocene in age, is present throughout much of the area and generally occurs as thin sheets of basalt and andesite flows no more than a few tens of meters thick.

Pliocene to Pleistocene sedimentary rocks of the Coso Formation are found throughout the area, however, the greatest exposures are around the west and north flanks of the range. These sediments record a complex geologic history. The basalt units are generally coarse gravels derived from the Coso Range with little contribution from the Sierra Nevada. Above the gravel lies fine grained, lacustrine sediments including volcaniclastics. Within this unit is subaerial and subaqueous andesitic to rhyolitic tuffs. The entire formation is tilted away from the range, indicating the uplift of the range (Roquemore, 1977).

Blancan and younger sediments are found on the south flank of the range (von Huene, 1960) where they are warped into an assymetrical, east-plunging anticline.

1.6 LITERATURE AND DATA REVIEW

All relevant published material pertaining to the Coso Range and Basin and Range province was reviewed. Unpublished and some published data were obtained from the Navy Geothermal Program. Data pertaining solely to the Coso Range are limited. The following references were generated either directly or indirectly by the Navy Geothermal Program: Austin and Pringle (1970), Koenig et al. (1972), Teledyne Geotech (1972), Furgerson (1973), Combs (1975), Duffield (1975), Lanphere et al. (1975), Combs (1976), Combs and Jarzabek (1977), Duffield and Bacon (1977), LeSchack et al. (1977), Stinson (1977), Fournier et al. (1978), Fox (1978a), Fox (1978b), Galbraith (1978), and Hulen (1978).

1.7 AERIAL PHOTOGRAPHY INTERPRETATION

Aerial photographs of the study area were available from USGS and from NWC photographic files. Photographic missions were flown by personnel from Miramar Naval Air Station, NASA, and by local photographers for various studies and at scales ranging from 1:6000 to 1:60,000. Both color prints and black and white prints were produced and made available. In some cases, both infrared and microwave imaging were used.

Low-sun-angle conditions are apparent in most of the low-altitude photography. The sun angle in the photography is very similar to that

discussed by Cluff and Slemmons (1972) and clearly illuminates and accentuates fault features.

The photographs were interpreted and transferred to a map utilizing a zoom transfer scope. The resultant maps and photographs were then taken to the field for verification.

1.8 FIELD VERIFICATION

Each mapped, fault zone was traversed on foot to verify the fault features and to examine the terrain for indications of offset. The procedure and terminology for this phase of work were taken from Clark (1973) and Slemmons (1977).

1.9 SCARP PROFILING

All of the fault zones, except the Little Lake fault (because it is lateral slip), were surveyed based on work by Wallace (1977). By assuming that the fault scarps in the Coso Range are forming by systematic offsets and the resulting earthquakes rather than by creep, profiling becomes a useful tool in recognizing the sequential displacement history of the faults.

Most of the faults in the Coso Range are geomorphically fresh. The erosion rate in this part of the Basin and Range province is very slow, and, in fact, probably slower than in the pilot study area described by Wallace. The basis for this statement is that the areas of Nevada which were studied by Wallace have freeze-and-thaw cycles, and the area of concern in this study has generally none. Because of this fact, it should

be understood that the numerical values arrived at in this study are probably too high.

For this study, a K & E self-indexing, geological survey alidade was used. This instrument has a pendulum device that automatically corrects for the slight residual tilts of the plane table and sets the indices used to read both the horizontal and vertical multipliers and the elevation-angle scale. The scales are read optically and the instrument gives results that are approximately four times more accurate than those results obtained with conventional alidades (*K & E Surveying Instrument Manual*, 1964).

Readings were taken at very close intervals (1.0 to 0.2 meters) up the scarp slope. Through the eyepiece, values for the vertical stadia scale, the horizontal stadia multiplier, and a center scale for the zenith angle can be seen. The *Stadia-Arc Method*, described in the *K & E Surveying Manual* (1964), is the easiest and most common method of data reduction and can be done on-site with a pocket calculator. Using this method, the stadia interval (top stadia hair minus the lower stadia hair) is determined first. Second, the horizontal multiplier and vertical stadia scale are read, then the following computations are made:

$$S - H = D_h$$

$$V - 50 = V_c$$

$$S(V_c) = D_v$$

$$D_v - D_I = D_{vc}$$

where

S = Stadia interval

H = Horizontal multiplier

D_h = Horizontal distance

V = Vertical stadia scale

F_c = Vertical stadia scale corrected

D_v = Vertical distance from the instrument

D_I = Height of the instrument

D_{vc} = Vertical distance corrected

After the above computations have been made, the data points can be plotted either by hand or by computer. The main advantage of this method of measurement is that, in the event of future movement of the fault, there will be very accurate baseline information that can be re-measured and to which data may be compared.

2.0 DESCRIPTION OF ACTIVE FAULTS

2.1 INTRODUCTION

In this chapter, the discussion of each fault includes references to the Index for Active Faults of the Coso Range and to Plates 1 through 4, located in the envelope-type pocket inside the back cover of this report.

In this study, active faults are defined as being either 10,000 years of age or younger.

2.2 LITTLE LAKE FAULT

The Little Lake fault (Plate 1) splays eastward from the Sierra Nevada frontal fault near the Little Lake Hotel and continues south across Indian Wells Valley to the Garlock fault (St. Amand, 1958; von Huene, 1960). The surface trace of the fault mapped here is over 11.6 kilometers in length. Only the northern segment was mapped in this study for the following reasons:

1. It has a marked expression in the 400,000-year-old basalts.
2. It offsets young alluvium on the Sierra Nevada front.
3. The south end of the fault crosses the north-south trend of the Airport Lake fault.
4. As the fault enters the deep alluvial basin of Indian Wells Valley, the fault expression changes to short, segmented, and highly eroded scarp traces not easily seen on existing photography.

One-half kilometer west of the Little Lake Hotel, the Little Lake fault merges with the Sierra Nevada frontal fault. In this area, young

alluvium and landslide debris are offset 30 meters by right-slip displacement. The overall geomorphic expression consists of aligned springs, shutter ridges, hillside troughs, and linear troughs (Figures 2 and 3). The fault is exposed in a railroad-cut just south of Wickline Canyon (Plate 1). In Section 20, a 140,000-year-old (Duffield et al.) basalt flow (basalt of Red Hill, Duffield and Bacon) is offset forming a linear trough with no measurable displacement because of the homogeneity of the rock on both sides of the trough. South of that point, a 440,000-year-old (Duffield and Smith, 1978) basalt cliff (basalt of lower Little Lake Ranch, Duffield and Bacon, 1977) is offset 250 meters in a right-slip sense (Figure 4). Because the offset sliver of basalt was eroded by Owens River and thereby cannot be measured directly, the fault displacement was reconstructed for this study with the aid of a cardboard model. The result was a determination that a minimum of 250 meters displacement has occurred since the eruption of the 440,000-year-old lava flow.

The fault pattern is well exposed atop the basalt of Lower Little Lake Ranch (Figure 5). The pattern is a series of *en echelon* normal-slip faults that form rhomboid-shaped depressions (Figure 6) and ellipsoid-shaped ridges (Figure 7). Between the depressions and ridges, linear troughs (Figure 8) exist and, depending on the topography of the flow surface, there are occasional side-hill troughs.

In Section 33, Plate 1, the Little Lake fault has a long (2 kilometers) segment which has an apparent normal displacement with the west side down. The mechanism of this segment, however, does not easily permit normal faulting in the orientation in which it is situated. First of all, the overall fault displacement is clearly right slip, therefore,

FIGURE 2. Aerial view of the Sierra front showing a shutter ridge caused by the Little Lake fault.

FIGURE 3. Aerial view of a sidehill trough formed in association with the shutter ridge shown in Figure 2.

FIGURE 4. Aerial view of 250 meters of right-slip displacement caused by the Little Lake fault in a 400,000 year old lava flow.

FIGURE 5. Aerial view of tectonic depressions and linear troughs along the Little Lake fault.

FIGURE 6. Aerial view of a rhomboid tectonic depression on the Little Lake fault.

FIGURE 7. Ellipsoidal ridges formed along the Little Lake fault.

FIGURE 8. A linear trough formed along the Little Lake fault.

the apparent normal-slip displacement must be a result of this mechanism. The normal-slip displacement along other segments of the fault are part of *en echelon* patterns or part of rhomboid structures formed by sinuous traces along the fault trace. Adjacent to this segment, the fault zone steps almost a kilometer to the west (left step). Mechanically, as the fault has stress applied, this segment would have stress vectors that could permit the formation of a thrust (Figure 9). In fact, the scarp has a rounded, rubble surface produced by a wide zone of crushed basalts as opposed to a steep, fairly sharp break as displayed in normal faults produced by *en echelon* breaks. It is concluded, therefore, that the Little Lake fault contains a segment nearly 2 kilometers long which is probably a thrust fault associated with right-slip displacement.

Below longitude 35°53' and east of latitude 117°50', Plate 1, a window was found in the lava flow that exposed lacustrine sediments. These sediments informally called the White Hills formation are probably much younger than Blancan (Duffield and Bacon, 1977) as reported by von Huene (1960). Through the White Hills formation, the fault pattern of the Little Lake fault dissipates into short, segmented, dip-slip scarps. The scarps are easily eroded and many have served as wind barriers facilitating dune formation. Because of the lack of relief and proper aerial photography, this area was not included in this study. The mapped length of the Little Lake fault is 24 kilometers at present.

2.3 SOUTHERN SEGMENT OF THE AIRPORT LAKE FAULT (PLATE 2)

In this area, normal faults are associated with right-slip displacments, in left-stepping *en echelon* patterns; however, grabens also occur

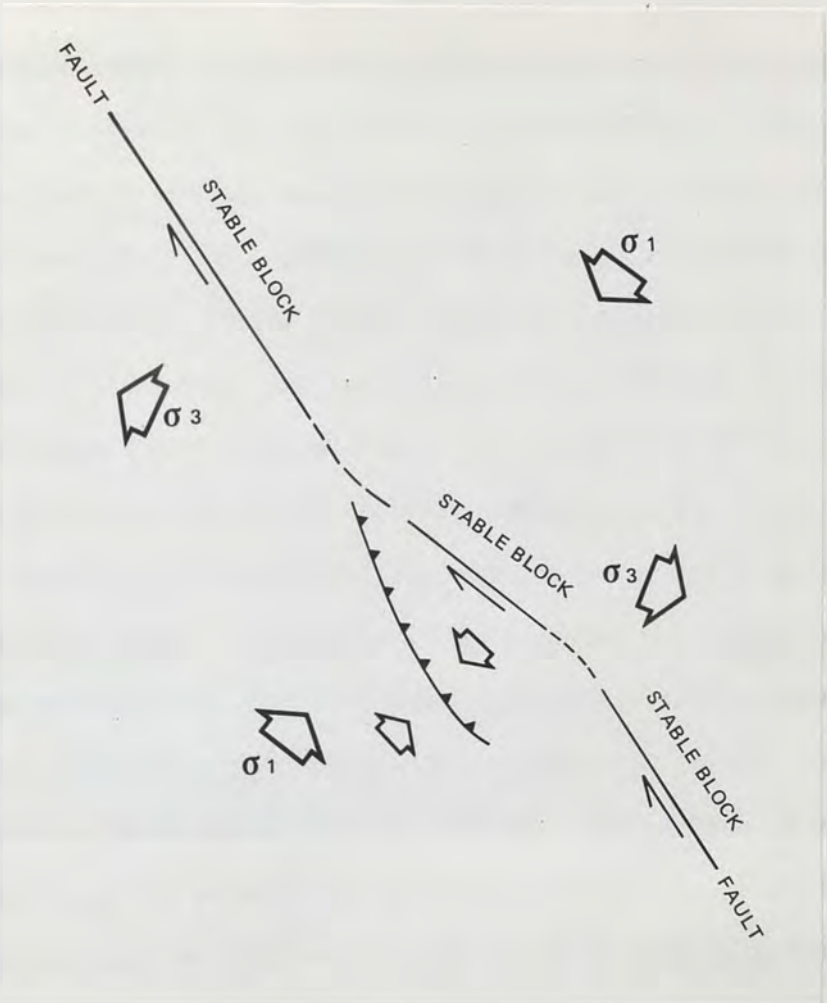

FIGURE 9. Schematic model indicating how thrust faulting has occurred on the Little Lake fault.

along the entire length of the Airport Lake fault. The graben in Sections 32, 33, 4, and 5 (Figure 10), is nearly 2 kilometers wide. Near latitude 35°55', ther is another graben 1 kilometer wide (Figure 11). In Section 16, there is a small graben with flipped stones on the upthrown side of the east flank. These stones have a desert pavement on the upthrown surface. The stones are coated with desert varnish and the underside of the stones are stained a bright red-orange color (Figure 12). Probably 20 to 30% of the stones in the pavement have the orange side facing up. Stones are generally ellipsoidal in shape and 4 to 20 centimeters in major diameter. Disturbances by wind are not likely because of the large surface area of the stones in contact with the ground, they weigh several kilograms, they are in low profile with ground, and there is no selective size of stone that is flipped. The surface on which the pavement has formed is elevated by faulting above any local drainages and is subjected only to sheet wash which may form from rain drop accumulation on the surface. Evidence of any substantial erosion by water is nonexistent. Therefore, it is concluded that the stones were flipped to their present position by Holocene seismic activity. The wet flank of this graben was trenched for this study, and the results are reported in Chapter 3. The trench is located in alluvial fan material that is the youngest (not including contemporary fans) in a sequence of at least four alluvial fans of different ages (according to D. B. Slemmons in an oral communication in 1980).

Section 16, and the south portion of Section 9, contain debris flows and alluvial fans. In Section 9, there is evidence for right-slip displacement in the form of shutter ridges and offset stream channels. In

FIGURE 10. Aerial view of a 2-kilometer-wide graben located on the south end of the Airport Lake fault.

FIGURE 11. Aerial view of a 1-kilometer-wide graben located in Coso Basin on the Airport Lake fault.

FIGURE 12. Stones that have been overturned by seismic shaking. Note the orange oxidation stains formed on the underside of these stones. The largest stone pictured is about 20 centimeters in length.

the south portion of Section 4, the fault approaches the base of the mountain block forming very sharp, steep faceted spurs (Figure 13). In Sections 3 and 33, there is a graben formed in basalt; however, the faulting extends into young alluvium on both ends (Figure 11). In Section 28, the faulting again approaches the mountain front where the bedrock is highly fractured and altered. The altered rock is formed partially from crushing in the fault zone; however, as the fault continues north, hydrothermal alteration is dominant.

2.4 THE NORTHERN, COSO HOT SPRINGS, AND HAIWEE SPRINGS SEGMENTS OF THE AIRPORT LAKE FAULT (PLATE 3)

On the bottom end of Plate 3, Sections 15, 16, 21, and 22, there are abundant offset stream channels and offset ridges in a right-slip sense. Shown in Section 22, an abandoned hot spring as well as active fumeroles and hot springs shown in Section 16, provide evidence for deep fault planes and hydrothermal convection, at present and in the recent past. Generally, areas in Sections 16 and 21 lack hydrothermally-altered zones and fumeroles such as Coso Hot Springs. The Coso Hot Springs are along an *en echelon* left step of the Coso Hot Springs fault segment of the Airport Lake fault (Figure 14). The Coso Hot Springs fault has dip-slip displacement with up to 3 meters of offset. Fumeroles are aligned along its length (red areas, Figure 15). In Section 33, there is a massive landslide (hummocky area, Figure 16) in the zone between the left step of two *en echelon* fault segments. This phenomenon is common in the Coso Range including several locations along the Sierra Nevada front (Figure 17). Areas located between *en echelon* faults are subjected to

FIGURE 13. Aerial view of faceted spurs formed along the Airport Lake fault.

FIGURE 14. Aerial view looking north along the south segment of the Airport Lake fault. The Coso Hot Springs segment may be seen in a northeast orientation.

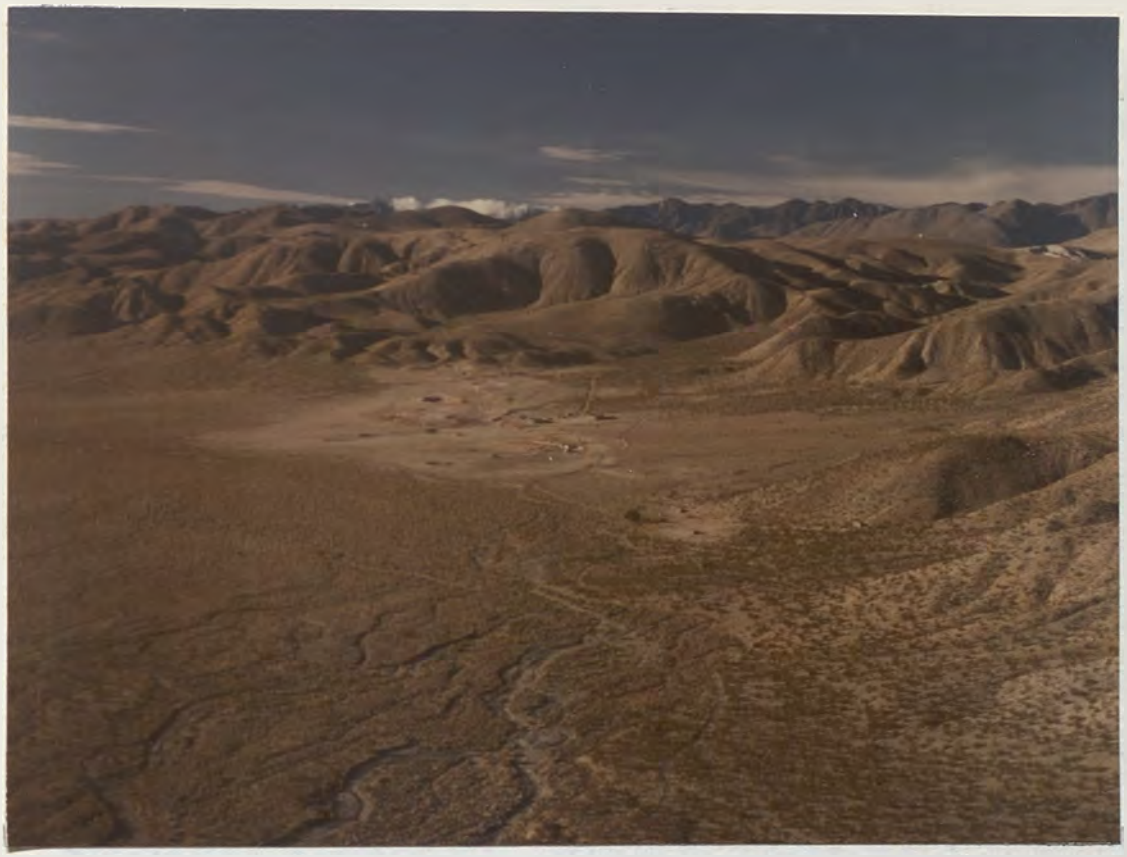

FIGURE 15. Aerial view looking south along the Coso Hot Springs segment of the Airport Lake fault. Note the abundance of fumerolic activity.

FIGURE 16. Aerial view of the northeast end of the Coso Hot Springs segment of the Airport Lake fault. Note landslide in hill above the hot springs.

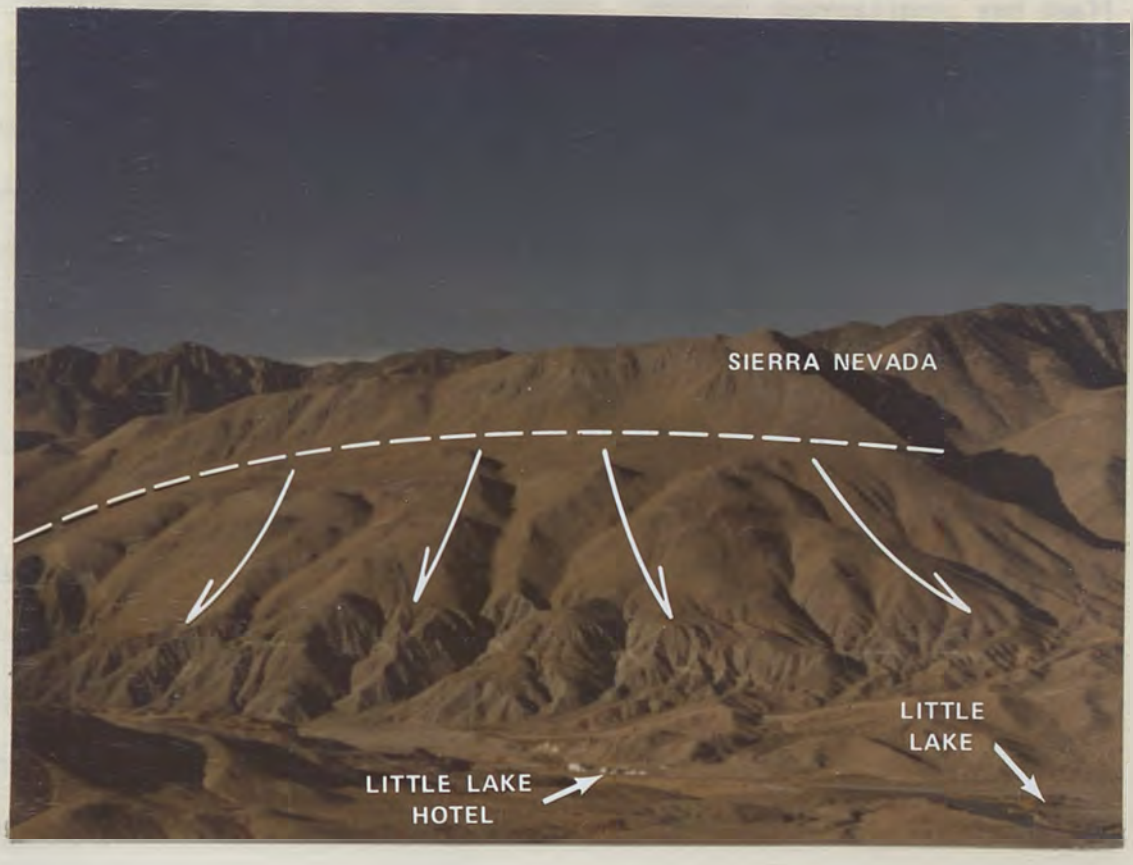

FIGURE 17. Aerial view of the Sierra Nevada front. Note landslide.

extensional stresses as seen in the conceptual model on Figure 18. From Section 21 to the top of Plate 3, the faulting adheres closely with the mountain front. Offset stream channels, tectonic depressions, and small grabens all provide evidence for right-slip displacement along this segment of the fault. Northward, the fault is dispersed in basalt sheets and is not seen as a single, continuous fault until it reaches the north end of Coso Range where it enters the Owens Lake playa. The total mapped length of the Airport Lake fault is 30 kilometers.

2.5 ACTIVE BREAKS ALONG THE EAST SIDE OF AIRPORT LAKE (PLATE 4)

The faulting on the east side of Airport Lake is left-stepping *en echelon* normal faults. The faults on the east side of Airport Lake together with the Airport Lake fault form the deep graben of Coso Basin. The average fault scarp height is 3 meters. Most of the faulting is in Holocene alluvium; however, the upthrown block is located in subaqueous tuff (Figure 19). Ramping, left-stepping *en echelon* patterns all suggest right-lateral displacement, although no offset stream channels could be found. This fault trends into the 3-million-year-old lava flows of Wild Horse Mesa (Figure 20). On the mesa, massive step-fault patterns have formed, much like those on the surface of the Bishop tuff in east central California. This pattern can be seen in Figure 21. Probably the fault pattern, generally confined to a narrow zone in the alluvial materials, spreads out laterally in the lava flows, because the lava sheets are thin and brittle as compared to alluvium or bedrock. As the fault movement takes place at depth in bedrock, stress is distributed over a large area in the overlying lava sheet and fracture and displacement takes

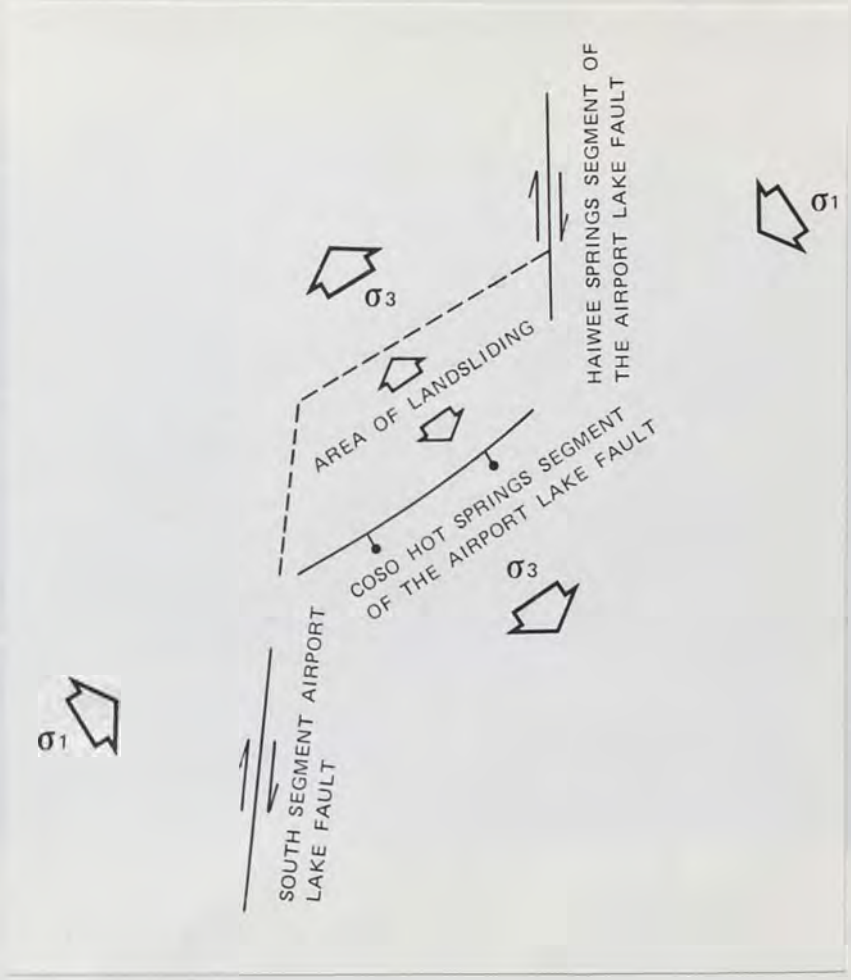

FIGURE 18. Schematic diagram indicating how landslides can form between *en echelon* faults.

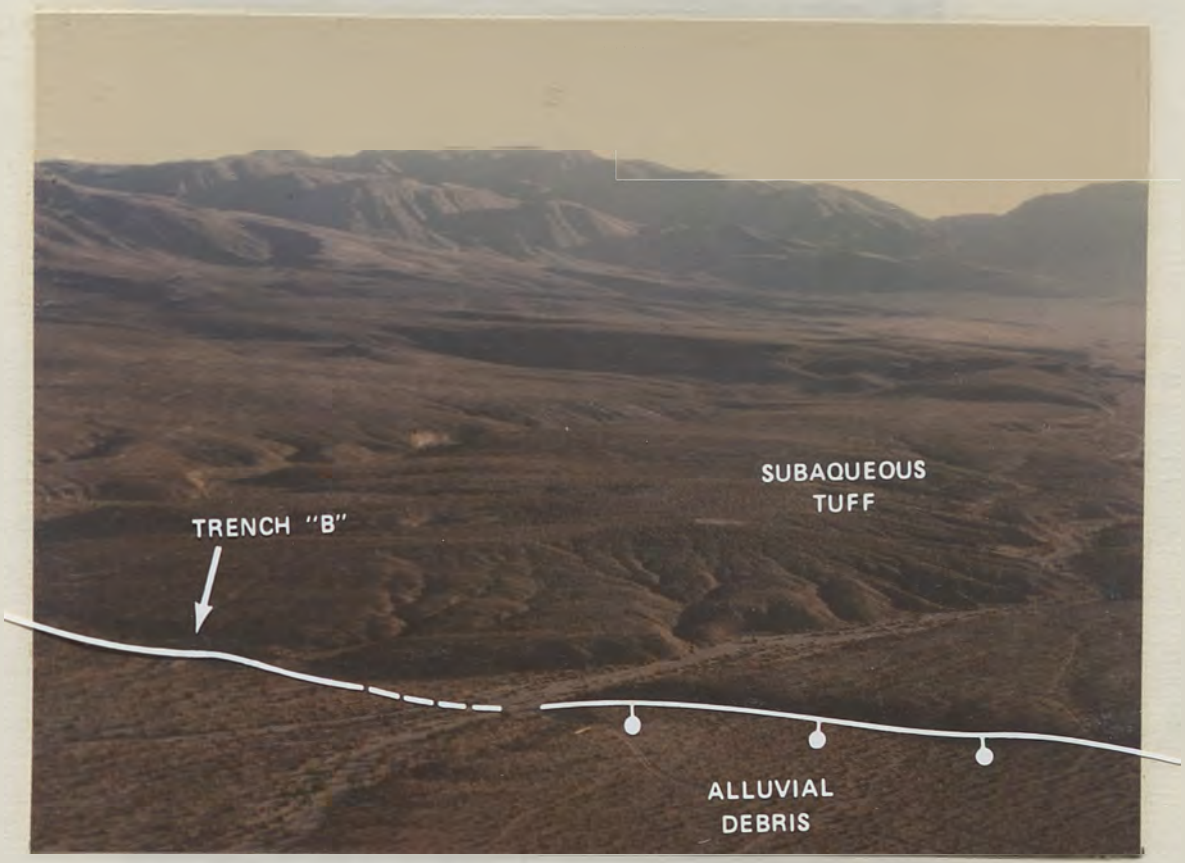

FIGURE 19. Aerial view of the faults on the east side of Airport Lake. Note subaqueous tuff on the upthrown block.

FIGURE 20. Aerial view of faults trending into the Wild Horse Mesa.

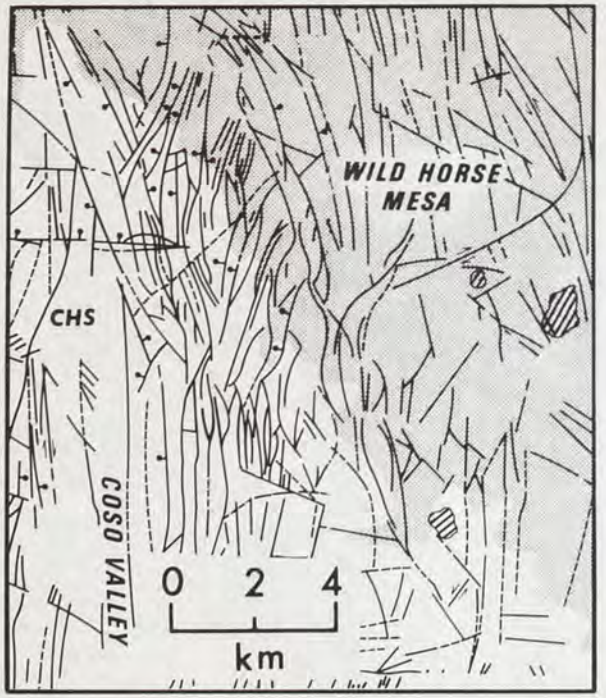

(a)

Wild Horse Mesa.

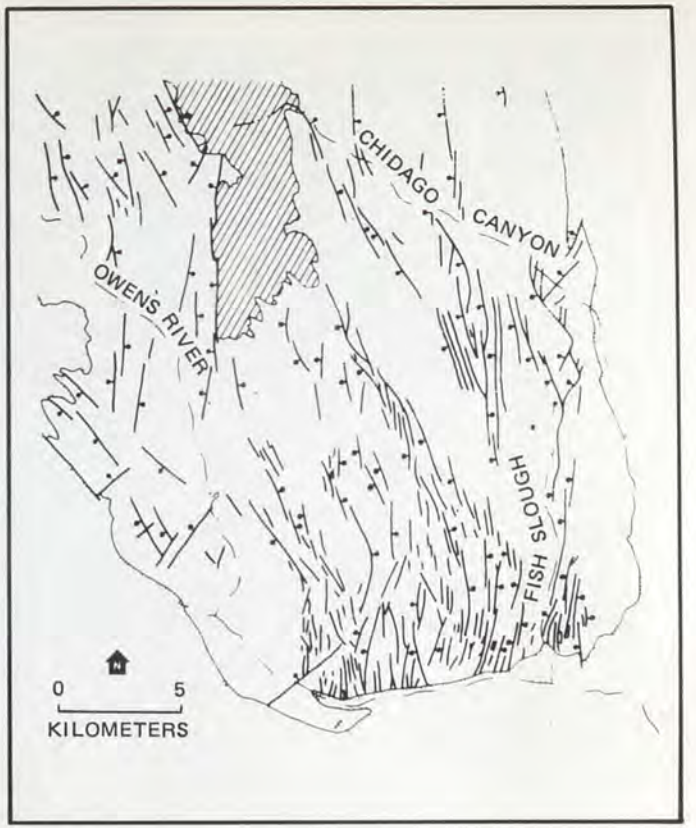

(b)

Bishop tuff.

FIGURE 21. Camparison between fault patterns on Wild Horse Mesa and those on the Bishop tuff.

place over a large portion of the stressed area. This pattern (ramping and sinuous *en echelon*) further supports the overall right-shear component evident in the faults on the east side of Airport Lake.

Approximately 30 meters south of trench "B" in Section 17, the fault crosses a small, modern drainage. The fault offsets the modern fan by 1/2 meter (Figure 22). According to Shlemons* in an oral communication during 1980, based on geomorphological evidence such as the degree of subsequent incision by modern erosion, the scarp is not likely to be more than 100 years old.

2.6 SUMMARY AND CONCLUSIONS

Field observation was performed on all active faults within the study area to obtain morphological data. The data were then compiled to help determine the activity and style and amount of displacement on each fault.

The Little Lake fault is the only purely right-slip fault in the study area. The morphology includes shutter ridges, linear troughs, sag ponds, and pressure ridges. Thirty meters of right-slip displacement were found in undated material of probable Holocene age. Two hundred fifty meters of right-slip displacement were found in a 400,000-year-old basalt flow. The overall mapped length of the fault is 24 kilometers; however, the fault has the potential for being much longer and provides a topic of further study. The complicated mechanics of the right-slip movement have produced a thrust displacement on a 2-kilometer segment of

*Roy J. Shlemons is a consulting geologist in Newport Beach, California.

FIGURE 22. View of 1/2-meter of recent normal-slip displacement on a fault on the east side of Airport Lake.

the fault. The southern reaches of the fault enter thick, lake bed material which reflects displacement in a highly splayed and diffuse pattern.

The southern segment of the Airport Lake fault proved to have right-slip displacement based on left-stepping *en echelon* patterns and associated tension grabens. Recency of displacement is indicated by flipped stones found near the fault scarps. The faulting generally adheres to the mountain front, however, occasionally scarps are formed along young alluvial fans. These fans are the youngest in a series of at least four age groups in the area. It has been estimated that the fan could be no older than 10,000 years. Displacement in the fans is dip-slip with scarps up to 3 meters in height. Along the fault, the mountain front is crushed and altered to a reddish-brown color.

The Coso Hot Springs and Haiwee segments of the Airport Lake fault have abundant offset stream channels and ridges. Flowing hot springs are common along this portion of the fault. Evidence for extinct fumeroles is seen as reddened, altered ground with occasional travertine outcroppings. The overall pattern is left-stepping *en echelon* with normal-slip displacement on the *en echelon* segments up to 3 meters. The north end of the fault dissipates in lava flows and is not seen as a continuous, mappable fault until it reaches the far northern Coso Range. The mapped length is 30 kilometers.

The faulting on the east side of Airport Lake is in the form of left-stepping *en echelon* faults with dip-slip displacement on each *en echelon* segment reaching 3 meters. The fault crosses recent fan development, thought to be less than 100 years old, and displaces it by 0.5 meter.

The overall, mapped length is 24 kilometers; however, evidence suggests that it could be much longer in a southerly direction. This is certainly an important future topic of study.

3.0 EXPLORATORY TRENCHING

3.1 INTRODUCTION

Three trenches were dug for this study. Trench A is on the Airport Lake fault immediately west of Airport Lake (Figure 23). Trench B is on an unnamed fault zone east of Airport Lake (Figure 24). A third trench was dug across the Little Lake fault (Figure 25) late in this study; the available data are presented herein.

The location of Trench A was chosen because the fault in that locality broke the youngest in a sequence of alluvial fans. The location of Trench B was chosen because the fault formed a small graben in that locality that could be exposed in one trench cut. The trench location on the Little Lake fault was chosen because of the existence of a tectonic depression filled with fine sands and clays that often record sandblows.

3.2 TRENCH A

Trench A is on the southern Airport Lake fault (Plate 2). At this locality, the fault style is dip-slip and is formed in coarse, alluvial materials younger than 80,000 years in age (Figure 26). The offset on the fault is indicated by displacement of two cinder-rich, alluvial units that also contain rare obsidian pebbles (Figure 27).

According to a letter from Charles R. Bacon (1979), the obsidian was scanned for zirconium, yttrium, and rubidium. The obsidian comes from one of two possible domes in the Coso Range that date 0.090 ± 0.025 and 0.088 ± 0.038 million years. This means that the glacial stages are

FIGURE 23. Aerial view showing location of Trench A.

FIGURE 24. Aerial view showing location of Trench B.

FIGURE 25. Aerial view showing the location of the Little Lake trench.

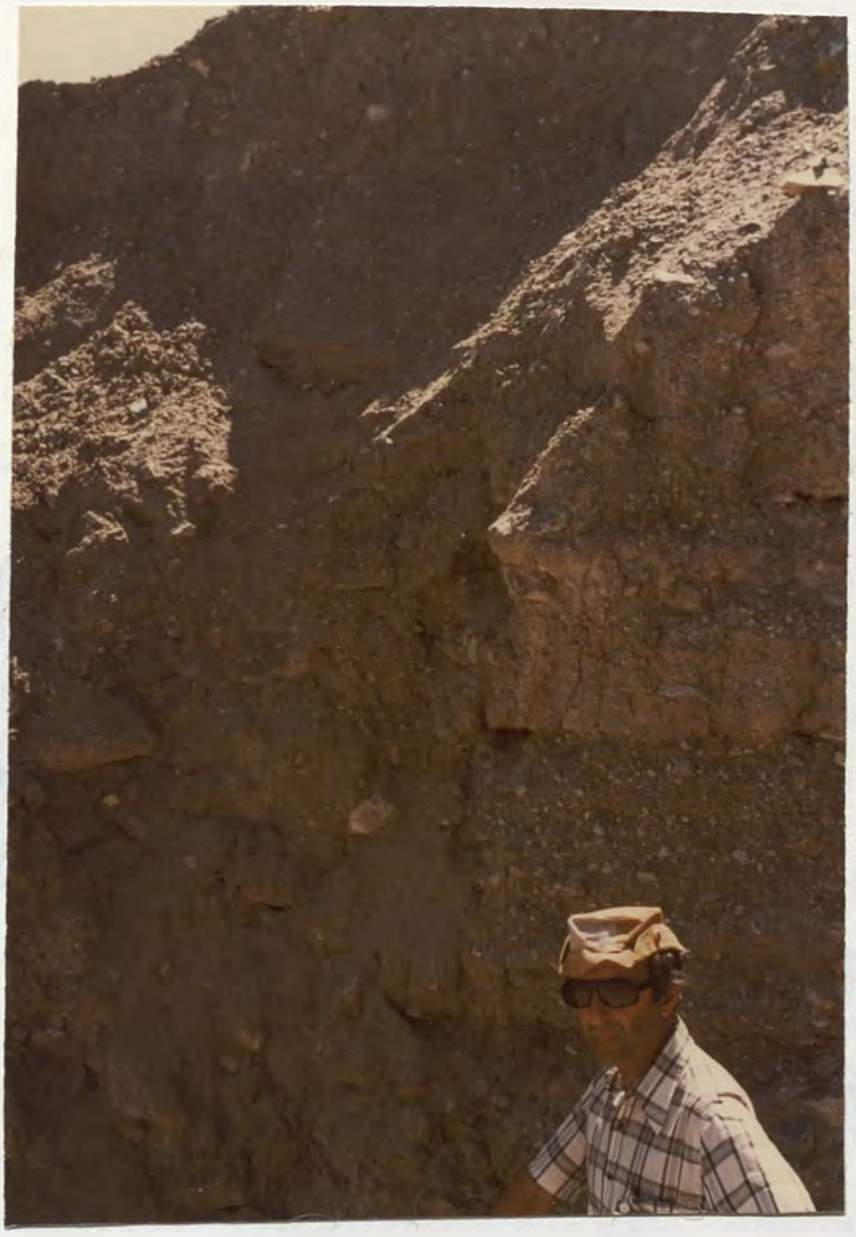

FIGURE 26. View of Airport Lake fault exposed in Trench A.

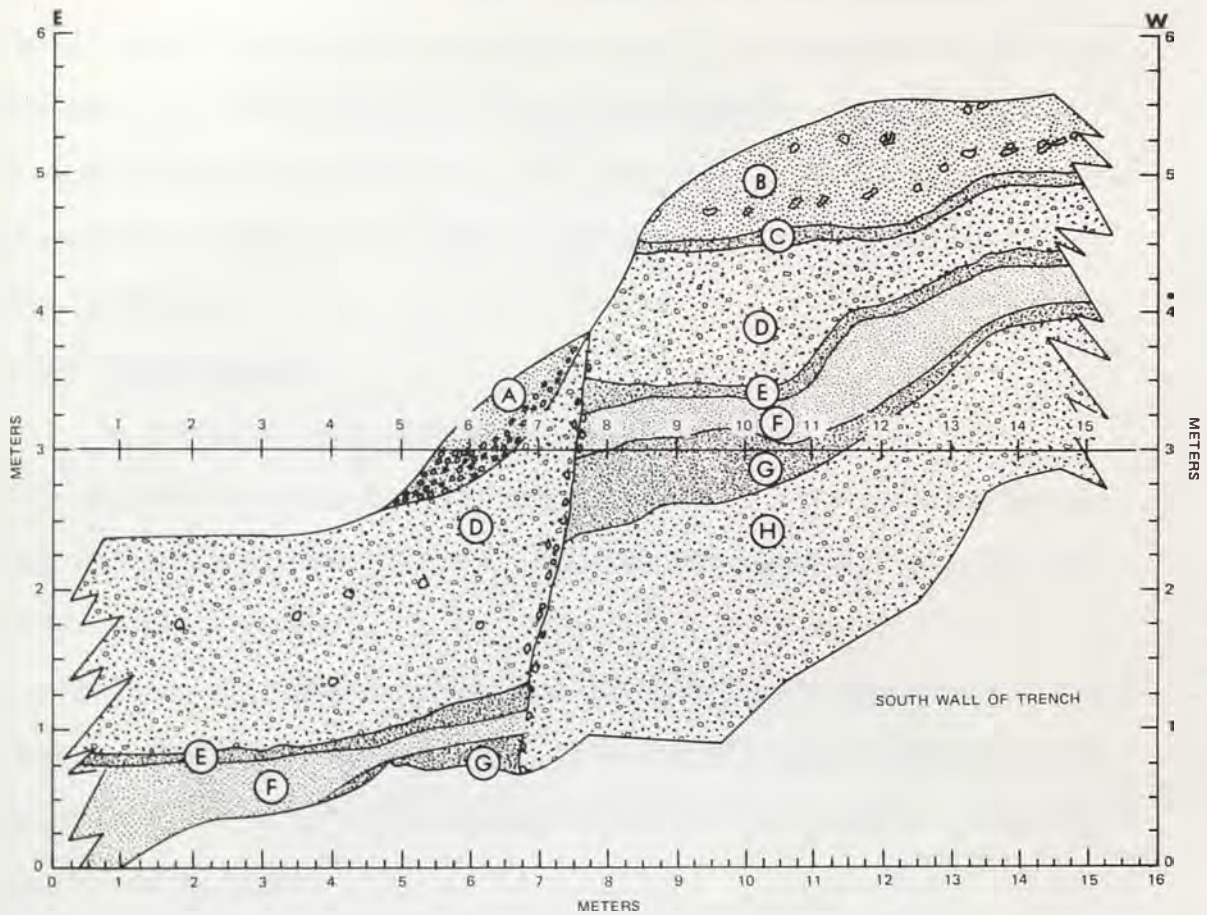

A – DEBRIS SLOPE ALONG FAULT SCARP, CRUDE BEDDING IN THE UNIT WARPS IN A CONCAVE FASHION TO SCARP FACE. ANGULAR COBBLE SIZED CLASTS AND SAND.

B – CONGLOMERATE WITH BOULDERS, POSSIBLY A DEBRIS FLOW, ALTERNATING SANDY LAYERS WITH BOULDER RICH LENSES. CLASTS ON ANGULAR.

C – GRAY SCORIA RICH SANDY LENSE, SCORIA IS TYPICALLY 1-2cm IN DIAMETER AND IS PRESENT AS 30 TO 40 PERCENT OF THE UNIT.

D – SANDY CONGLOMERATE WITH 1-2 PERCENT ANGULAR BOULDERS.

E – GRAY SCORIA RICH SANDY LENSE, SCORIA IS TYPICALLY 1-2cm IN DIAMETER AND IS PRESENT AS 30 TO 40 PERCENT AS 30 TO 40 PERCENT OF THE UNIT.

F – SANDY MUDSTONE, CONTAINS SOME SLIGHT STRATIFICATION IN COURSER ZONES.

G – GRAY SCORIA RICH SANDY LENSE, SCORIA IS TYPICALLY 2-3cm IN DIAMETER AND IS PRESENT AS THIS UNIT ALSO CONTAINS OBSIDIAN CLASTS 1-2cm IN DIAMETER.

H – SANDY CONGLOMERATE WITH 2-3 PERCENT VERY ANGULAR BOULDER CLASTS.

FIGURE 27. Log of Trench A.

represented in the section. Roy J. Shlemons, in his oral communication in 1980, stated that the upper materials can be no older than 10,000 years. However, this information is entirely preliminary. The total offset is about 3 meters with the east side downdropped. There is no evidence of multiple offsets. The width of the fault zone is approximately 20 centimeters.

3.2.1 Stratigraphy

The following descriptions are keyed to Figure 27.

Unit H is a sandy conglomerate with angular clasts indicating the lack of transportation distance. The bedding characteristics are nil with a lack of sorting.

Unit G is a sand-rich zone with abundant scoria and rare obsidian clasts. There is a lack of rounding in the scoria which indicates the possibility of primary airfall deposition. Slight bedding can be seen in the scoria layers.

Unit F is a slightly-stratified, sandy mudstone. The unit is poorly indurated and changes in coarseness laterally.

Unit E is a sand-rich zone with abundant scoria and rare obsidian clasts. There is a lack of rounding in the scoria which indicates the possiblity of primary airfall deposition. Slight bedding can be seen in the scoria layers.

Unit D is a sandy conglomerate that is similar in particle size to Unit H. Angular boulders suggest the lack of transportation distance.

Unit C is a cinder-rich, sandy lens similar in composition to Units E and G.

Unit B is a conglomerate with zones of aligned boulders. Alternating boulders with sandy layers suggest rapid changes in the energy of the deposition mechanism. This can be attributed to the change in slope due to small uplifts along the fault scarp.

Unit A is the debris slope on the scarp face. The composition of the alluvium is similar to Unit B and was surely derived from it as the scarp face was eroded.

3.3 TRENCH B

Trench B is on the east side of Airport Lake along an unnamed set of *en echelon* faults (Plate 4). This faulting, together with the southern segment of the Airport Lake fault, forms the deep graben valley known as Coso Basin. Trench B was placed along the fault scarp where it was evident from surface expressions that a small, tension graben was formed at the base of the fault scarp. The trenching showed this to be the case (Figure 28). The overall displacement is about 3.4 meters on the east side of the graben (the main fault segment). The total displacement on the west side of the graben is unknown because corresponding units could not be traced (Figure 29). It is assumed, based on the attitude of bedding and fault geomorphology, that the displacement is probably comparable to that of the main segment.

A short, preliminary soil profile (unified soil classification) was completed on the upper few tens of centimeters in this trench. Shlemon also stated that the surface is a weak A_v horizon probably no more that 5000 or 6000 years old. No oxidation was evident beneath surface clasts. Binding the clasts is a 1-to 2-centimeter fine, platey

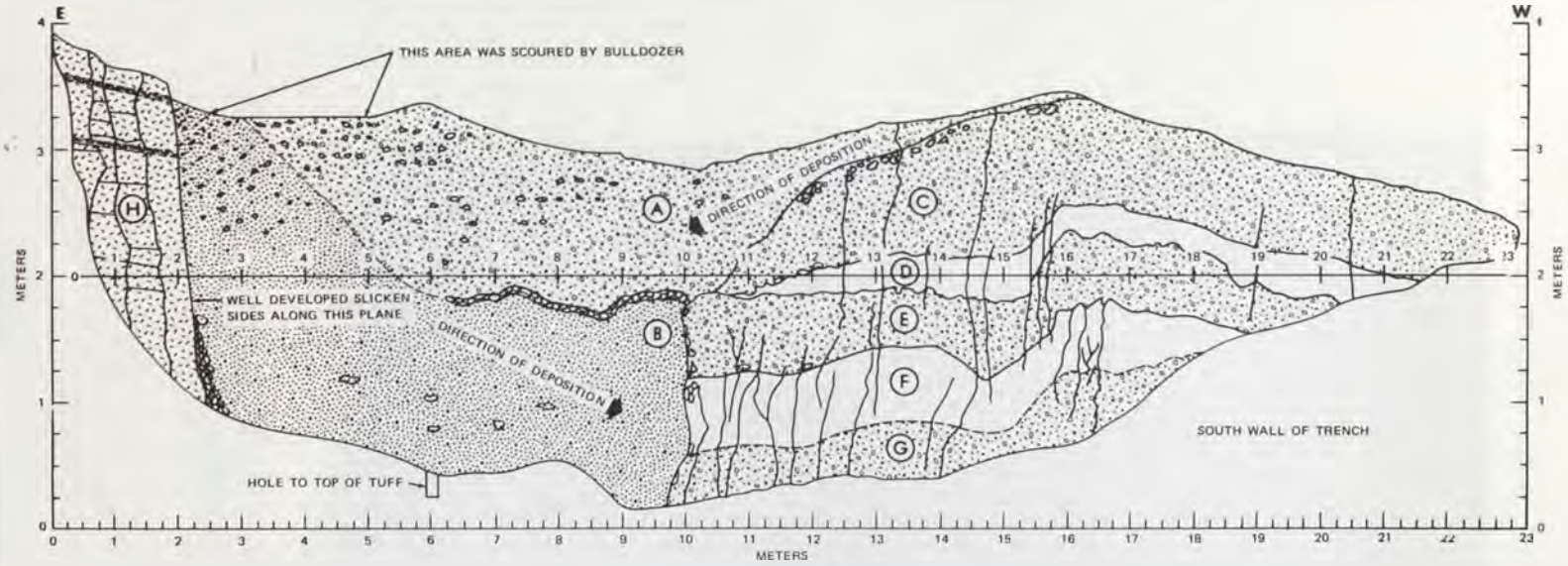

A – SANDY GRAVEL, CLASTS RANGE UP TO 10cm ACROSS, GRAY BUFF IN COLOR, SEVERAL ROOTS IN UPPER METER, CLASTS ARE COATED WITH CALICHE AND ARE MOSTLY VOLCANIC IN ORIGIN, SLIGHT STRATIFICATION TAKES PLACE IN FINER BEDS. CONTAIN ABUNDANT OBSIDIAN, GENERALLY SUBANGULAR TO SUBROUNDED 2-4cm IN SIZE.

B – FINE TO COARSE SANDY GRAVELS, BUFF IN COLOR, CONTAINS FEW OBSIDIAN CLASTS. CLASTS ARE MOSTLY VOLCANIC SOME GRANITIC OR METAMORPHIC. SLIGHT STRATIFICATION IN FINER BEDS.

C – COARSE SANDY GRAVEL WITH CAPPING BOULDER LAYER LITTLE OR NO STRATIFICATION, LIGHT GRAY BUFF IN COLOR, CONTAINS ABUNDANT ROOTS.

D – MASSIVE WHITE CALICHE LAYER, HIGHLY FAULTED, HAS A FEW BOULDERS ON UPPER SURFACE.

E – BUFF MEDIUM GRAINED SANDY GRAVEL, LITTLE OR NO STRATIFICATION. NO LARGE CLASTS OR OBSIDIAN.

F – BROKEN MASSIVE WHITE BUFF CALICHE LAYER. HIGHLE FAULTED AND FRACTURED. ZONE OF MOST INTENSE FRACTURING OCCUR IN THIS LAYER.

G – BUFF MEDIUM GRAINED SANDY GRAVEL, NO STRATIFICATION.

H – BUFF SUBAQUEOUS TUFF, CONTAINS BOMBS UP TO 1m IN SIZE. FEW GRANITIC OR METAMORPHIC BOMBS. CLEARLY THE SOURCE FOR VOLCANIC MATERIALS IN FAN UNITS.

FIGURE 28. Log of Trench B.

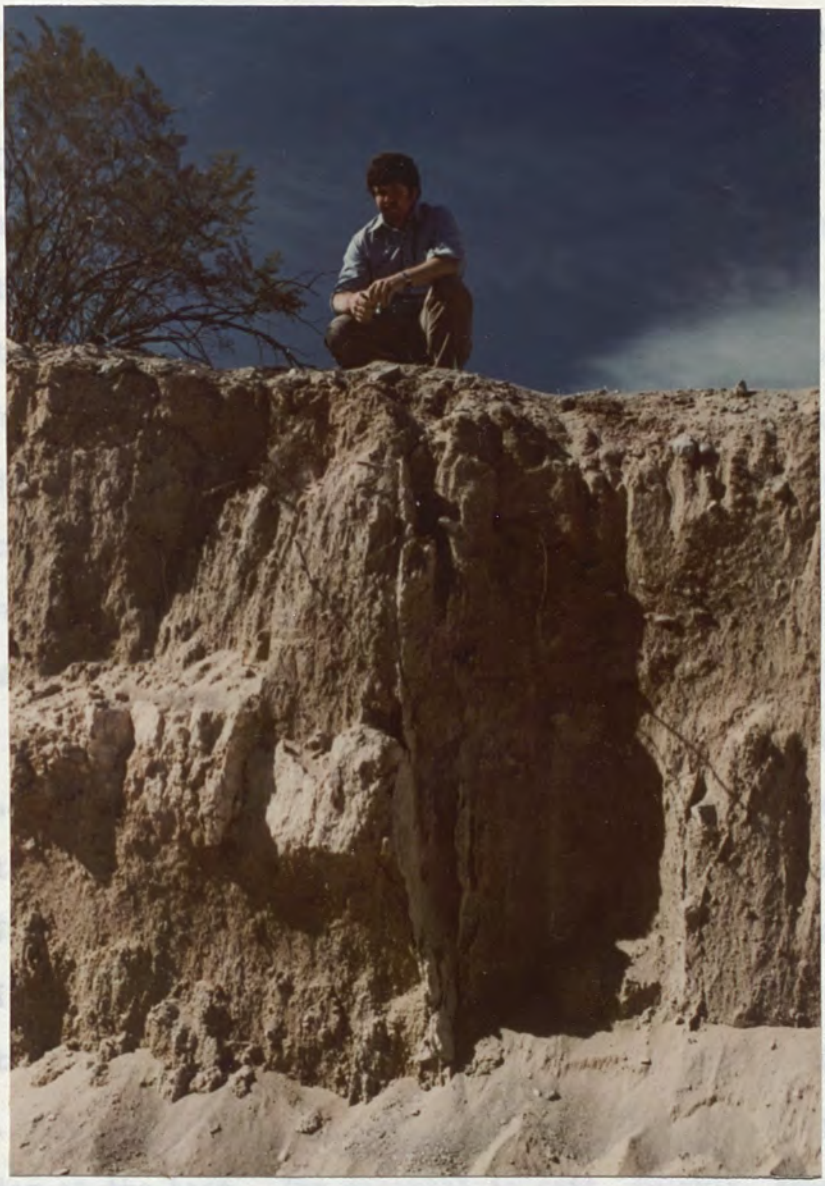

FIGURE 29. A 20-centimeter-thick calcrete layer that has been truncated by faulting.

layer. Soil stratum IC has a color of 10 YR 7/3 to 6/4 (Muncell color chart) when moist. The structure is massive, loose consistency, friable, nonsticky, and nonplastic. There are common, fine, vertical roots. Stratum IC is 20 centimeters thick with stratified lenticular clasts. The general classification is a medium, sandy loam. The contact with soil stratum IIC_2 is abrupt and smooth.

Stratum IIC_2 is 6 centimeters thick and is 10 YR 7/3 (Muncell) in color. The matrix is slightly redder than above. The structure is moderate medium to coarse, angular, blocky, hard, friable, nonsticky, and nonplastic. There are few medium, vertical roots. The general classification is a pebbly, loamy sand. The contact with stratum IIC_3 is abrupt and smooth. Stratum IIC_3 is 20 centimeters thick and 10 YR 6/4 (Muncell) in color. The structure is massive, granular, loose, soft, nonsticky, and nonplastic. There are common, vertical, fine roots. Approximately 10% angular clasts, 3 centimeters in diameter, are in the matrix. The general classification is a fine sand. The contact with stratum $IIIC_4$ is clear and wavy.

Stratum $IIIC_{4CA}$ is 15 centimeters thick. The color is 10 YR 7/1 (Muncell). Structure is weak, fine, subangular, and blocky at the top and granular at the base. The material is soft, friable, nonsticky, and nonplastic. There is a weak cement at the top that is strongly effervescent. Disseminated lime in the matrix is common. The general classification is a pebbly sand. The contact with stratum IVC_5 is gradual and wavy.

Stratum IVC_5 is 15-plus centimeters thick. The color is 10 YR 6/4, 6/3 (Muncell) when moist (more clay than above). The structure is

massive, soft, and very friable. The material is nonsticky and nonplastic. There are a few, vertical, fine roots. The general classification is a loamy, coarse sand.

The above information and the fact that very few thin clay films are in the root tubules and a general lack of colloidal staining on the mineral grains suggest a late Pleistocene age for this section according to Shlemon (1980). The upper section is probably no more than 3000 to 4000 years old, Shlemon stated.

3.3.1 Stratigraphy (Figure 28)

Unit H is a buff-colored, mafic, subaqueous tuff. The tuff contains several bombs that reach 1 meter in size and abundant, caliche-filled fractures. The scarp face is slickensided (Figure 30) with a small-pebble-debris fan which increases in thickness with depth. The down-thrown west side of the tuff was located by digging a small hole a little less than 1/2-meter deep. The rapid caving of the trench walls did not permit excavation to the tuff layer.

Unit G is buff-colored, medium-grained, sandy gravel with no apparent stratification.

Unit F is a thick, white caliche layer. This layer is faulted in several areas as demonstrated by thin fractures and a 1-meter down-step. The lower side of the layer is slightly graded into Unit G. The origin of this layer must by subaqueous because of the purity of the calcium carbonate and nearly complete lack of sandy materials.

Unit E is a buff-colored, medium-grained, sandy gravel layer. This unit is very similar to Unit G in the lack of stratification and large boulders.

FIGURE 30. Slickensided fault plane in Trench B.

Unit D is similar to Unit F except that it is thinner. This unit is also faulted in the same manner as Unit F, and probably represents another sequence of lake formation in the Coso Valley. The calcium carbonate is punky but devoid of sandy particles. The upper and lower contacts are scarp.

Unit C is a coarse, sandy gravel with a layer of rocks that vary from cobbles to boulders at the upper contact. There is little evidence for stratification. This unit is high enough in the section to have roots from contemporary flora.

Unit B is a fine-to-coarse, sandy gravel containing a few pebbles of obsidian. The obsidian pebbles are usually subrounded but clasts have been found to be angular, indicating a lack of transport distance that suggests they are from an air fall. The other clasts in the unit are generally volcanic; however, a few granitic and metemorphic clasts can be found.

Unit A is a sandy gravel with a few large caliche-coated clasts, thinly dispersed in the matrix. This unit contains abundant subrounded obsidian clasts and a lesser number of angular fragments. The obsidian is probably from an air fall. Roots from contemporary flora are abundant in this unit.

3.4 LITTLE LAKE TRENCH

Toward the end of the present study, the opportunity arose to trench the Little Lake fault. The trench was placed on a playa surface of sag pond in the fault zone (also called rhombic depression in this report, Figure 31). The trench is located across the survey location 3021 in

FIGURE 31. Little Lake trench showing its position within a tectonic depression.

Section 33 (Plate 1). Because the trench was completed near the end of this study during the wet season and the trench began to fill with water, a complete logging of the trench could not be done. In spite of this problem, however, some data were collected and a preliminary account is given here.

The trench, dug by a bulldozer, is 50 meters long and 4 meters deep (Figure 32). The displacement seen in the trench is lateral slip, but as can be seen in Figure 33, the fault is dipping to the southwest. The width of the zone is about 4 meters. The displacement appeared to reach the surface.

This trench contains an abundance of liquefaction features that are probably relict mud volcanoes. The light layer seen in Figure 34 contains most of the liquefaction features. This layer contains carbonized twigs and chunks of charcoal, radiocarbon dated at 2545 ± 160 years. Figure 35 is a close-up of a portion of Figure 34 and shows the fine structure produced in the liquefaction process. The age dates and preliminary geologic observations suggest that a large earthquake has occurred on the Little Lake fault in the last 2500 years. Work is continuing to determine recurrence intervals.

3.5 SUMMARY AND CONCLUSIONS

The Airport Lake trench (Trench A) was located on a young, alluvial fan. The displacement in the trench was seen as 3 meters of dip-slip offset of two cinder-rich, obsidian-rare layers. The age of these layers, based on volcaniclastic chronology, is between 88,000 and 90,000 years. A 2-centimeter soil layer forming the surface is thought to be no more

FIGURE 32. View of the Little Lake trench showing its length and width.

FIGURE 33. Truncation of stratigraphy by the Little Lake fault.

FIGURE 34. View of the stratigraphic unit that contains most of the mud volcanos exposed by the Little Lake trench.

FIGURE 35. View of the fine structures found in a mud volcano exposed by the Little Lake trench.

than 10,000 years in age. There was no evidence in the trench of more than one earthquake.

A trench on faults along the east side of Airport Lake (Trench B) exposed a graben with a minimum of 3.4 meters of dip-slip displacement. Information indicating multiple events was not seen in the trench. Based on the soil stratigraphy, the faulting is thought to have occurred in the last few thousand years.

The trench on the Little Lake fault, although incompletely studied, exposes a 4-meter wide, crushed zone. The fault plane dips to the southwest. Abundant liquefaction features, probably mud volcanoes, were identified along one stratigraphic horizon. This horizon is dated at about 2500 years and records a major earthquake since that time.

4.0 FAULT SCARP PROFILES

4.1 INTRODUCTION

To determine the age of the fault displacements in northern Nevada, Wallace (1977) used the geomorphic characteristics of young fault scarps. To compare Wallace's data with the data collected for this study of the Coso Range, several assumptions were made. These assumtions were: (1) the climate is similar in both areas, (2) the rock type is similar in both areas, (3) the compaction and cementation of the displaced rock unit are similar in both areas, and (4) the freeze-and-thaw cycles are similar in each area.

The climate and rock types are similar. The freeze-and-thaw cycles are more frequent in northern Nevada. Perhaps the most varied factor is the compaction and cementation of the displaced rock units. The formation of caliche is an important factor to evaluate in scarp degradation studies. (Although not attempted in this study, a possible solution to the problem may be to obtain the seismic velocity of the faulted material to determine its relative compaction and compare this value to scarps with well-determined age dates.)

4.2 FACTORS THAT AFFECT SLOPE DEGRADATION IN THE COSO RANGE

The annual rainfall in the Coso Range averages 5 inches. Most of that value occurs in a few intense downpours. The freeze-and-thaw cycles are such that it would be difficult to estimate through time (i.e., the last 12,000 years) the number of cycles per year. In this area,

freeze-and-thaw cycles do not now cause significant degradation of fault scarps. Strong winds are common; velocities often exceed 60 mph.

Rain and wind are the major factors in fault scarp degradation in the Coso Range. Most of the young fault scarps are embayed by cross-cutting drainage channels.

4.3 FAULT SCARP PROFILES

4.3.1 Coso Hot Springs Segment of the Airport Lake Fault

Five profiles were measured on the Coso Hot Springs fault. The displaced material is old, alluvial fan material except for profile 5 which is a young, alluvial fan. Care was taken to avoid areas which may have been altered by human activity as well as trails made by feral burros.

The scarp profiles are presented in Figures 36 through 40. Each profile shows the upper and lower original surfaces, base and crest, free face (where not removed by erosion), debris slope, and wash slope. Features such as grabens at the base of the scarp and mulitiple bevels can be identified.

Profiles 1, 2, and 4 were measured generally along medium-grained, hydrothermally-altered alluvium (see Coso Hot Springs segment of the Airport Lake fault). Profiles 3 and 5 were located on the northeast end of the fault where the offset material is a coarse, alluvial debris.

4.3.2 Southern Segment of the Airport Lake Fault

Figures 41 and 42 are profiles on the southern segment of the Airport Lake fault. Profile 1 is on the exact location of Trench A. The fault scarp formed in coarse-grained, poorly-consolidated alluvial

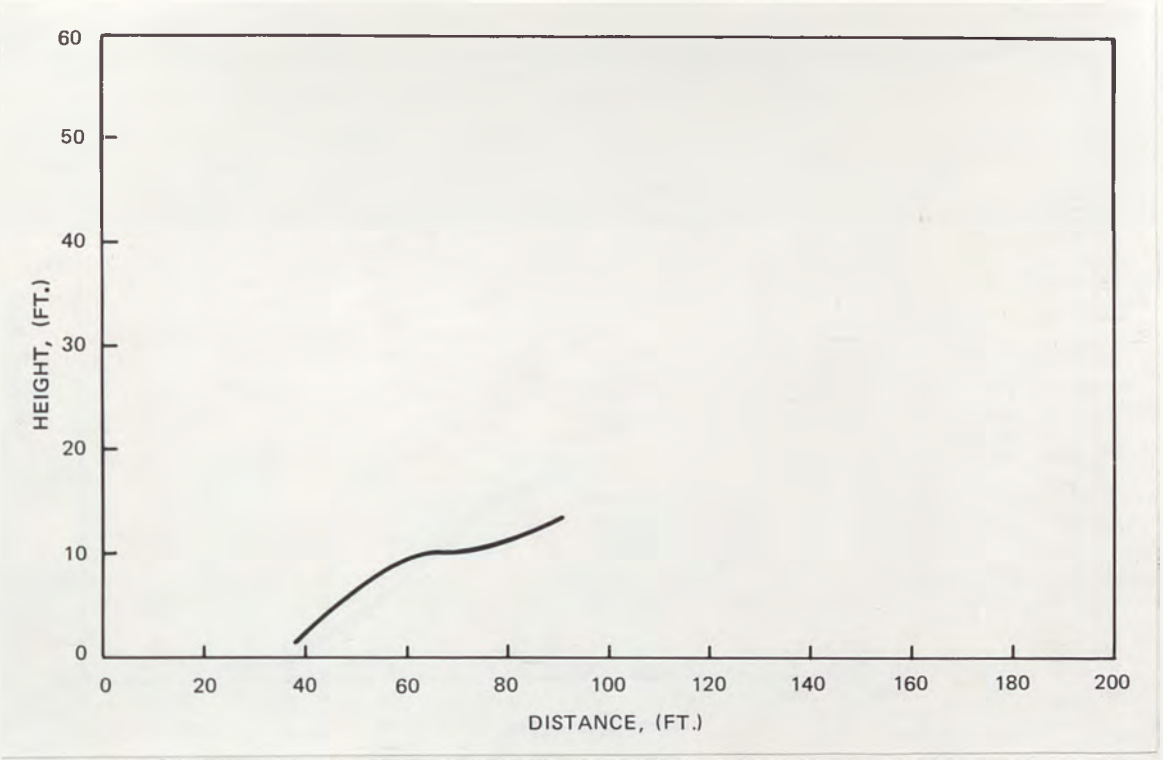

FIGURE 36. Scarp profile No. 1 on the Coso Hot Springs segment of the Airport Lake fault.

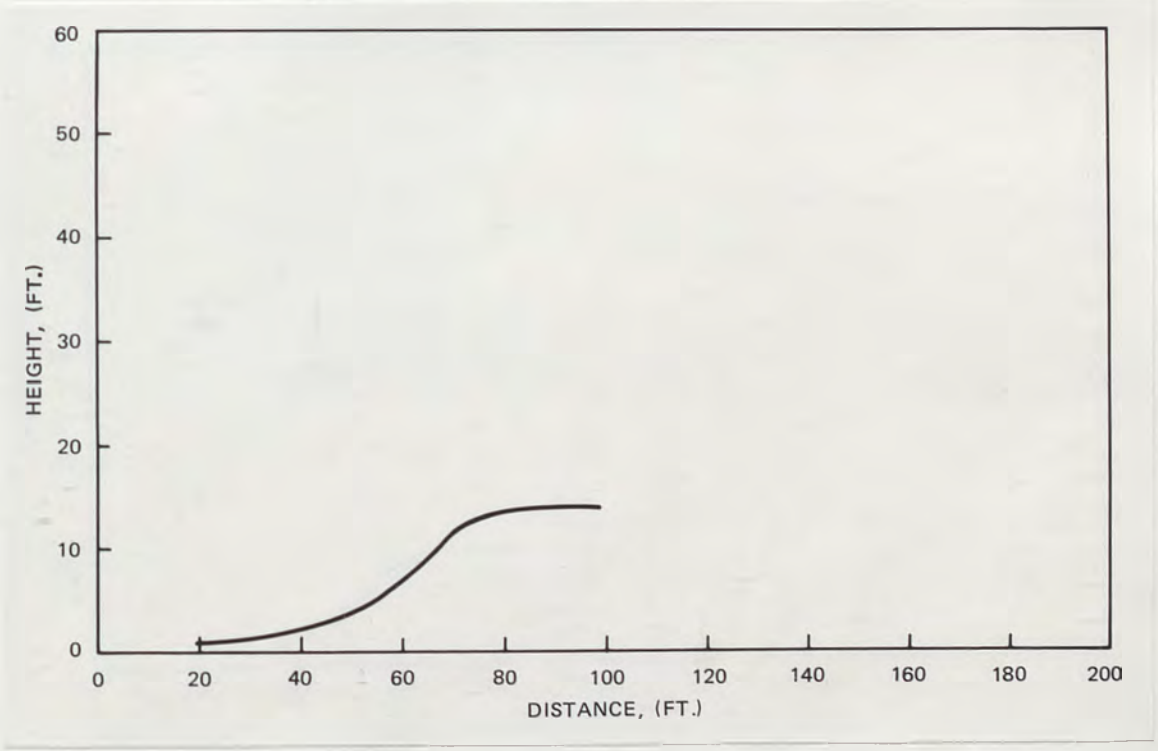

FIGURE 37. Scarp profile No. 2 on the Coso Hot Springs segment of the Airport Lake fault.

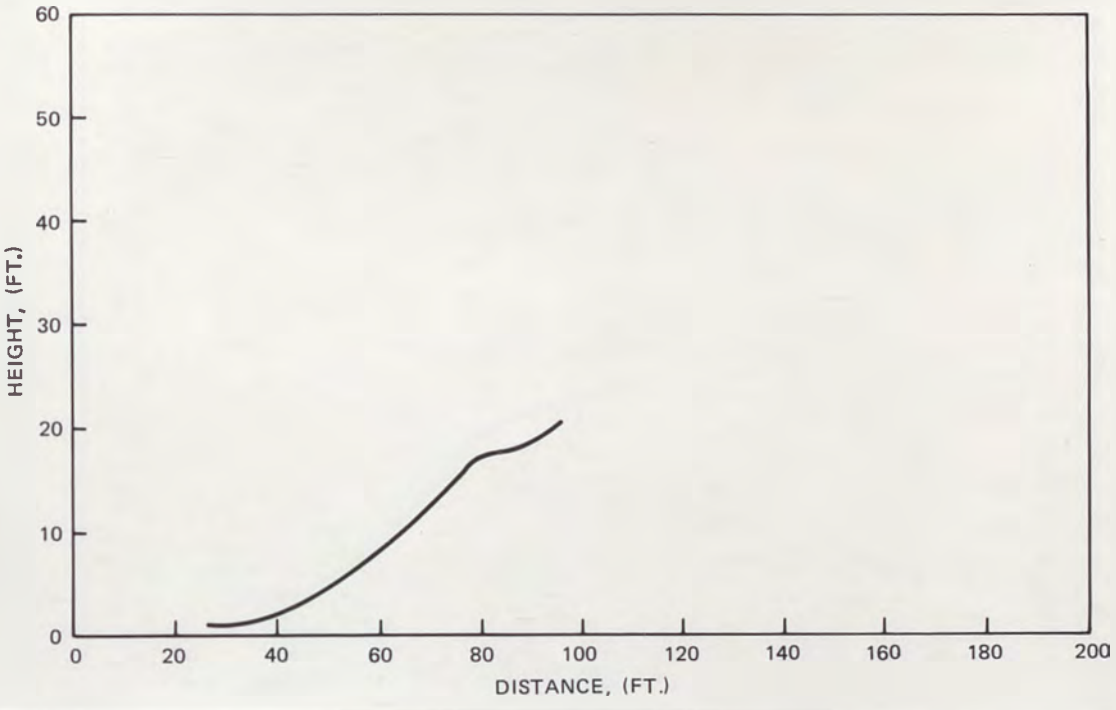

FIGURE 38. Scarp profile No. 3 on the Coso Hot Springs segment of the Airport Lake fault.

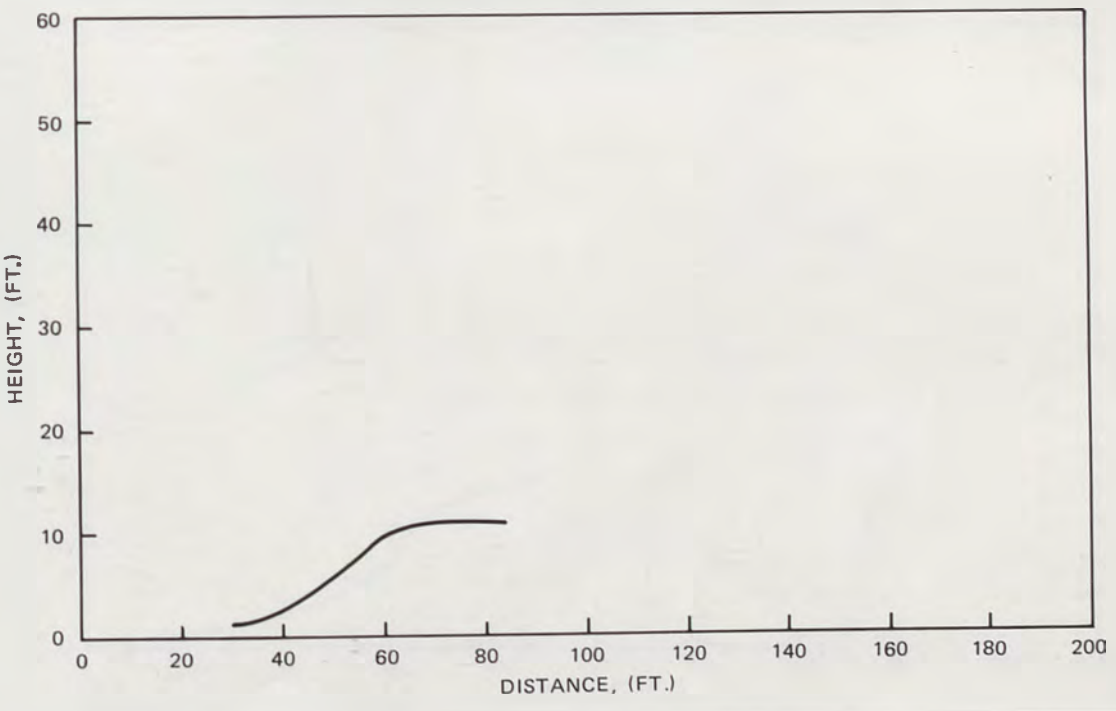

FIGURE 39. Scarp profile No. 4 on the Coso Hot Springs segment of the Airport Lake fault.

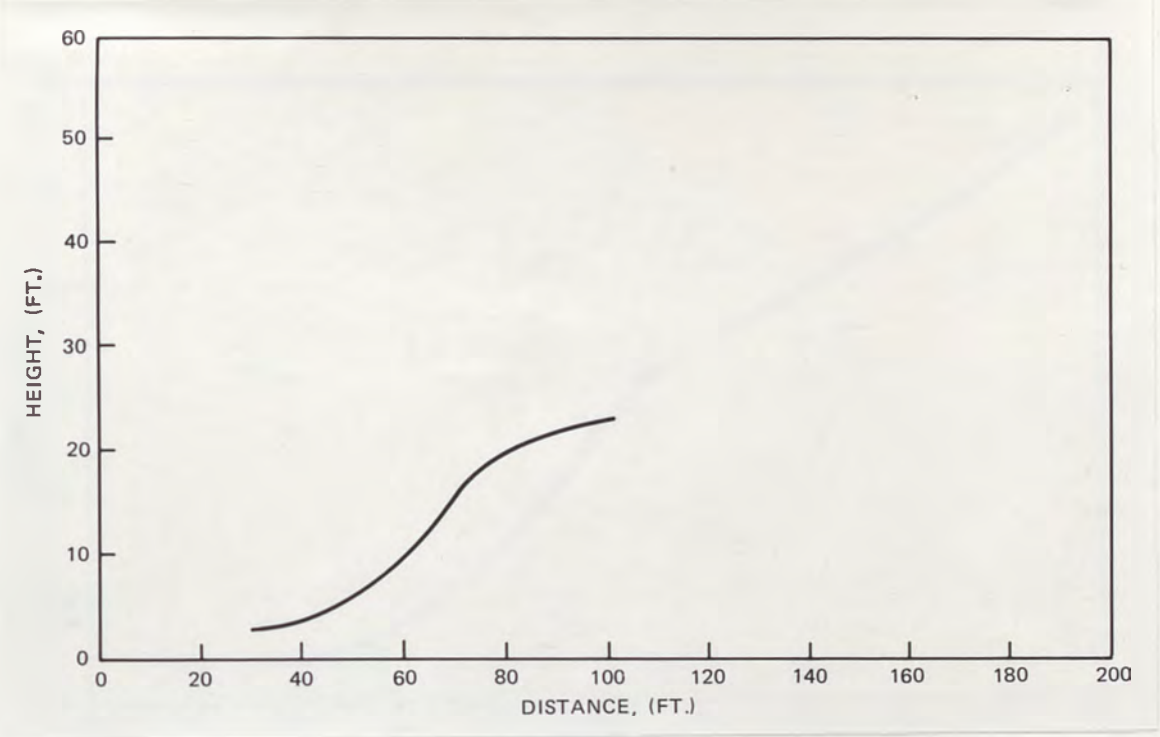

FIGURE 40. Scarp profile No. 5 on the Coso Hot Springs segment of the Airport Lake fault.

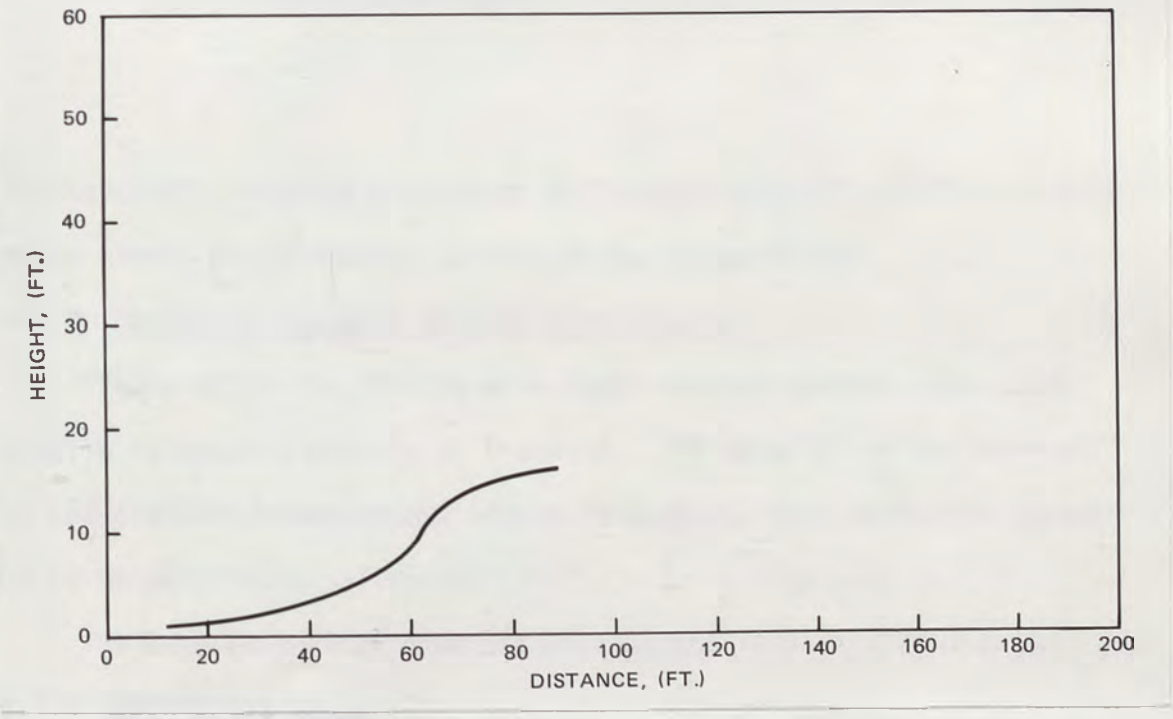

FIGURE 41. Scarp profile No. 1 on the southern segment of the Airport Lake fault.

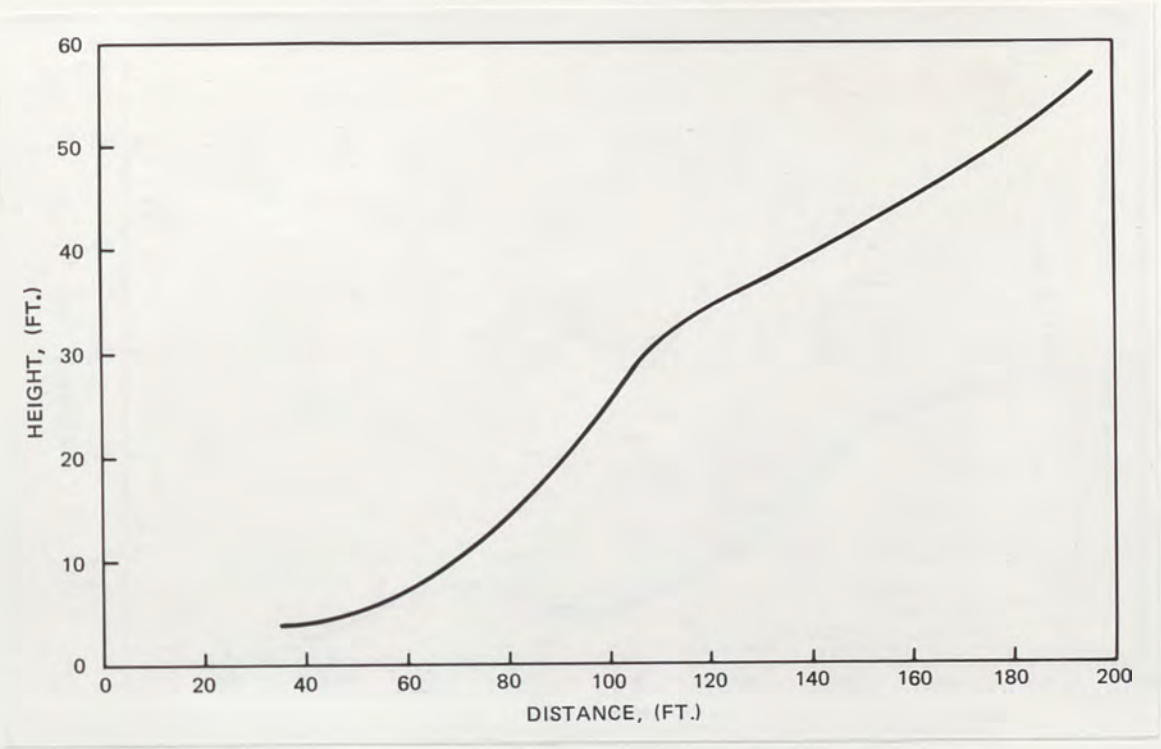

FIGURE 42. Scarp profile No. 2 on the southern segment of the Airport Lake fault.

fan material. Profile 2 is about 200 meters north of profile 1 and is on an older, consolidated, coarse-grained alluvial fan.

4.3.3 Faults on the East Side of Airport Lake

Figure 43 is the profile of a fault east of Airport Lake. The profile is located exactly at Trench B. The material on the headwall of the scarp is highly-consolidated, subaqueous tuff while the footwall is in unconsolidated alluvium.

The details derived from all of the profiles are listed in Table 1.

4.3.4 Back-Crest Swale

In the Coso Range, a swale is often found on the upthrown block near the crest of normal faults. Swales similar to these can be found

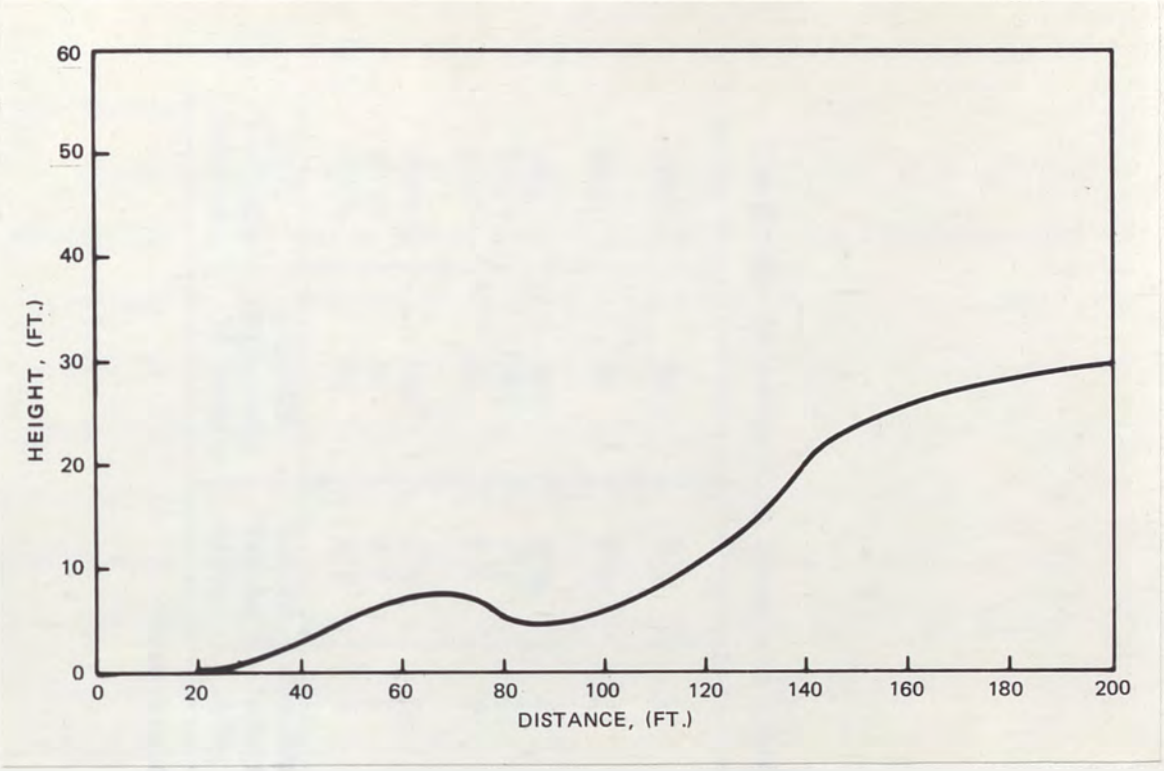

FIGURE 43. Scarp profile No. 1 on the east side of Airport Lake.

in Owens Valley, according to Dave Findley* in an oral communication in 1979, and in Saline Valley according to John Zellmer* in an oral communication in 1979. This feature also occurs in other regions such as the Atacama Desert in Chile according to Pierre St. Amand in an oral communication in 1979.

Possible mechanisms for this feature are:

1. Rotational slumping of the free face.

2. Open fracturing parallel to the free face caused by gravitational forces.

---

*Dave Findley and John Zellmer were graduate students at the University of Nevada at Reno at the time of their conversations with this author.

TABLE 1. Fault scarp profile data.

Profile location	Profile number	Freeface, degrees	Debris slope, degrees	Wash slope, degrees	Scarp height, meters	Number of identified events*	Age-years (Wallace, 1977)
Coso Hot Springs fault	1	...	29	5	4.1	2B	∿500
Coso Hot Springs fault	2	...	37	3	4.3	2H	∿100
Coso Hot Springs fault	3	...	26	10	6.2	2BH	∿1000
Coso Hot Springs fault	4	...	34	16	3.4	1B	∿100
Coso Hot Springs fault	5	...	31	15	7.1	2BH	∿500
Airport Lake fault	1	49	33	8	16.9	3BH	∿40
Airport Lake fault	2	69	35	7	4.8	2H	<100
Unnamed fault on the east side of Airport Lake	1	34	17	3	9.0	2H	∿100

*B = Event determined by the presence of multiple bevels; H = event determined by the height of the scarp based on a 3.5-meter average (Wallace, 1977).

3. Open fracturing parallel to the free face caused by multiple faulting.

Possible reasons for the formation of back-crest swales can be derived from exploratory trenching, especially if the stratification of sediment in the trench is rotated (slumped). In the Coso Range, trenches have not shown this to be the case. However, the trenches do show an abundance of cracking on the upthrown side of the fault which could be caused by gravity fractures parallel to the free face. These cracks are usually not filled. Finally, if the swale is due to multiple parallel faulting, the phenomenon should be pervasive all along the length of the scarp. The profiles do not show this to be the case. Therefore, evidence suggests that slope failure is the most likely mechanism to produce the swale. Furthermore, since near vertical, fault scarps are common in the Basin and Range province, slumping would be expected when the scarp is freshly formed.

4.4 SUMMARY AND CONCLUSIONS

Based on fault scarp profile data, the Coso Hot Springs segment of the Airport Lake fault has undergone displacement as recent as about a hundred years ago. The highest scarp reaches 7.1 meters.

The Wallace (1978) method of fault age dating leads to the conclusion that the southern segment of the Airport Lake fault has undergone displacement as recently as about forty years ago; however, this is certainly anomalous because the last likely event that could have displaced faults in the Coso Range was the 1872 Owens Valley earthquake, and indeed profile 2 suggests movement of about that age. An earthquake

since that time, large enough to produce the scarp, would not have gone unnoticed.

Profile data on the east side of Airport Lake suggest displacement about a hundred years ago.

5.0 SEISMICITY

5.1 INTRODUCTION

The eastern Sierra Nevada zone has long been recognized as having rapid tectonism and the associated high rate of seismicity. Earthquakes in the Owens Valley, the Walkers Pass, and the Tehachapi areas have shaken Indian Wells Valley. The following text is a description of these earthquakes as well as a discussion of the local seismicity.

5.2 DESCRIPTION OF NOTABLE EARTHQUAKES

5.2.1 1872 Owens Valley Earthquake

Most of the damage and loss of life from this earthquake was at Lone Pine, California. The seismologic details of this earthquake remain unknown because no seismograph was operating at that time. Most of the known information was made available by local residents and subsequent field studies (Whitney, 1872; Hobbs, 1910).

Fifty-two out of fifty-nine buildings in the town of Lone Pine were either wholly or partially destroyed. The ground ruptured for a distance of about a hundred miles between the town of Big Pine and Haiwee. The average vertical displacement at Lone Pine was 13 feet (Oakshott et al., 1972).

The Owens Valley earthquake is believed to be the greatest earthquake on record in the western United States, excluding Alaska (Oakshott, 1972). Damage was noted as far as about three hundred miles from the epicenter. The Indian Wells Valley comprised several small farms and ranches as well as an adobe building (which served as a stagecoach

stop and general store) located in the mouth of Indian Wells Canyon. Whitney (1872) states that this adobe building was partially destroyed during the Owens Valley earthquake.

Information pertaining to the recurrence interval along the Owens Valley fault zone is still incomplete. However, according to Oakshott et al., 1972, geologists and seismologists working on the problem state that strain builds up in that area to the point of rupture in a few hundred years.

5.2.2 1917 Owenyo Earthquake

The details of this event consist of information tainted by ambiguity. According to the Professor in charge of Seismological Investigations, W. J. Humphreys (1917), there was an earthquake on 7 July 1917, located at latitude 36°40' and longitude 118°01' (Owenyo) which was of intensity seven. Humphrey states in his report that the Los Angeles aqueduct was broken in the earthquake. This report was submitted to the Weather Bureau, Washington, D.C., 2 February 1918. There was no other mention of the earthquake in this report.

Andrew H. Palmer, observer, U.S. Weather Bureau, in a report entitled "California Earthquakes During 1917" (Palmer, 1918), stated that an earthquake occurred on 6 July, latitude 36°40', longitude 118°01' (Owenyo) with an intesity of seven. The following is from his report: (Editorial note: the following articles are reproduced herein exactly as they were published originally. No attempt has been made to edit them in order to preserve the original meanings and flavor.)

Some of these questions, however, are answered in the following excerpt from Palmer's paper:

> "The earthquake hazard is well recognized by residents of California, and it is a factor which is considered by careful investors. Earthquake insurance is in growing demand. However, owing to the absence of trustworthy statistics in the past, rates have been more or less arbitrary, and most of them have no scientific basis. Moreover, through a gentlemen's agreement among California newspaper editors the subject of earthquakes is tabooed in the daily press. The general public promptly plunges into a kind of hysteria when a severe earthquake occurs, but soon relapses into complacement indifference to the subject when the immediate danger is over. A seismologist can therefore expect but little sympathy or support in the serious investigation of earthquakes."

5.2.3 1946 Walker Pass Earthquake

March 15, 1946, the principal earthquake occurred at 35°44' N, 118°02' SW; origin time = 05:49:36. A total of 20 measured (Chakrabarty, 1949) aftershocks followed through 1 February 1947. The magnitude of the main shock was 6.3. The location can be found on Figure 44.

The following is a news story which appeared in the Naval Ordnance Test Station (NOTS) *Rocketeer*, Tuesday, 19 March 1946.

> "Station residents were jolted from their sleep last Friday morning at 0521 when a sharp earthquake rocked the entire desert area in the first of four perceptible tremors felt that day.
>
> The second shock came 18 minutes later at 0539 when the day's most severe quake set more than a few people to worrying whether their roof would hold up under much more of that kind of treatment.
>
> A third and mild trembler put in its appearance at 0600 while still another rocked the earth at 1121 later in the day. A number of slight settling quakes occurred Friday night and Saturday morning.
>
> This is important to the people of this city, for we also are preparing to bring water from the Sierra. It is known that there is an old fault between us and

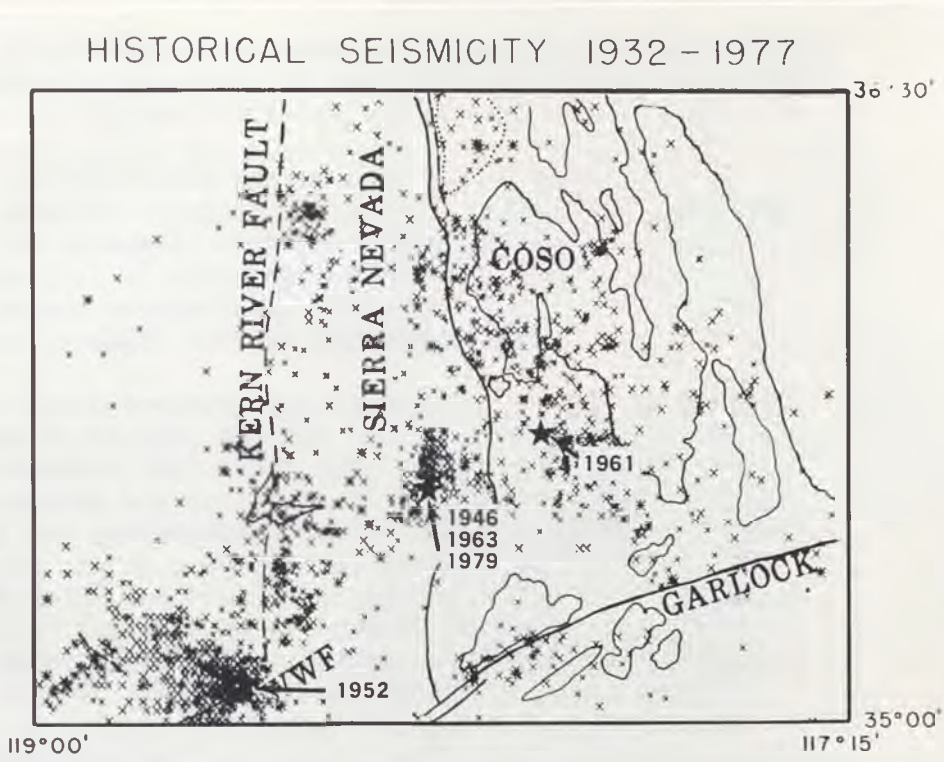

FIGURE 44. Plot of the regional historical seismicity from 1932-1977. The major events are called out by date. WWF is the White Wolf fault. (Modified from Walter and Weaver, 1980.)

> the Sierra and in the earlier plans for the Hetch-Hetchy enterprise two conduits were planned through the danger zone as insurance against interruption of supply.
>
> It if should appear that these breaks in the Los Angeles aqueduct, occurring on the same day, were due to seismotic disturbances we should know it in order that in building our own works we may take the necessary precautions, which may be two conduits and extra strength through the danger zone.
>
> Since we have come to understand that an earthquake is nothing but the slipping of the earth for a few hundred feet along some fault in the rocks that phenomenon has lost most of its terror. The mischief that any earthquake of which there is human experience can do can be prevented by proper construction. The burning of San Francisco was due to improper construction of the main water conduit supplying this city. We must take no more chances. If it appears that an earthquake damaged the Los Angeles tunnel, we must see to it that the danger is guarded against in our own enterprise."

The paradox surrounding this earthquake begins with a paper written by Mr. William Mulholland entitled, *Earthquakes in Their Relation to the Los Angeles Aqueduct* (Mulholland, 1918), and published in the same journal issue (BSSA, Vol. VIII, 1918) as was Palmer's paper. No mention is made by Mulholland of the Owenyo earthquake. Furthermore, no mention of the earthquake was made in any of the local Owens Valley newspapers nor does the Los Angeles Department of Water and Power have any record of the event. The University of California at Berkeley was the recording station for the Weather Bureau, and there is no record of the earthquake there.

> "July 6th. What was probably the most severe earthquake of the year occurred in the Owens Valley at 3:01 a.m. on this date. This shock had an intensity estimated at VII. It caused a break 160 feet long in the concrete flume of the Los Angeles aqueduct at a point between the Haiwee Reservoir and Owens Lake, in Inyo County. Under the direction of Mr. William Mulholland, Chief Engineer

of the aqueduct, the damage was temporarily repaired by bridging the break with steel pipe. Since that time the flume has been rebuilt and reinforced. The water supply in Los Angeles was not cut off, because the break occurred above the Haiwee Reservoir, which has a capacity sufficient for the storage of several weeks' supply of water for the city. In commenting upon this earthquake the *San Francisco Chronicle* published the following editorial on July 17th:"

At this point, Palmer reproduced part of the story printed by the *San Francisco Chronicle*. Several paragraphs were omitted by Palmer that are important to the story. The entire story is reproduced in the following.

THE LOS ANGELES AQUEDUCT

Occasional Breaks May Be Expected From Natural Causes

"There are two very serious breaks in the Los Angeles aqueduct, which some are disposed to attribute to a "plot" If the I.W.W. or German intrique.

There is no doubt of the hatefulness of the I.W.W or of their desire to do anything to hurt anybody. Whether the foreign public enemies are spending money for such work is more doubtful, as it apparently would not pay.

Just now it is becoming the habit to attribute all calamities to the public enemy, foreign or domestic. But there are misfortunes even in peace, and they will occur from natural causes during the war. The cause of these breaks should be ascertained if possible and made public.

They may be the result of the earthquake of a few days ago which disturbed the ground in part of the Sierra foothills and if that is the cause of these breaks it should be made known. A moderate seismotic disturbance acting upon some weak point might make a good deal of trouble.

According to seismologists at the California Institute of Technology, the earthquakes were centered about ten miles north of Inyokern in the Sand Canyon area where falling rocks tore gapping holes in the Owens River Aqueduct. The aqueduct carries water to Los Angeles and also supplies NOTS, but officials said no water shortage would

occur as present reserves would last until the pipeline could be restored to service.

Although the quake was considered as severe as the tremor that devastated Long Beach in 1933, slight cracking of a few walls was the the only damage that could immediately be ascertained at NOTS."

5.2.4 1952 Kern County Earthquakes

The main shock of the Kern County earthquake occurred on the White Wolf fault (WWF, Figure 44) with a magnitude of 7.7 (California Division of Mines and Geology, CDMG, 1955). Significant aftershocks occurred through June 1953 (Richter, 1955). The effects on Indian Wells Valley are written in the following newspaper account from the NOTS *Rocketeer*, Wednesday, July 23, 1952.

"One of the strongest earthquakes in state history rocked most of California at 4:55 a.m. Monday.

Damage to the Station was slight. A vane in a section of overhang at the extreme west portion of Michelson Laboratory shop area was broken off with an estimated $10 damage. A safety valve was popped in the Public Works garage, releasing live steam.

Several water lines were reported broken in the housing area by the trouble board. Circuit breakers were tripped and electricity flow was momentarily halted on a few lines when wires were swung together. No serious or permanent damage was reported however.

An undetermined amount of china and glassware was broken to Station residences, particularly in the trailer areas. One unconfirmed report described the floor of a house as having split open. LCDR W. R. Pool, housing officer, reported a lamp broken and John Richmond, Community Manager, told of the chimes on his grandfather clock ringing from the shake.

A lighting fixture was shaken loose in the housing office directly over the rent collection counter and another fixture was knocked loose in the Public Works building.

Confusion of waking suddenly in the night was responsible for two minor casualties here.

Harold C. Berry, a leadingman sheetmetal worker, was limping around at work Monday as the result of bruising his big toe when he ran into the closet instead of out the bedroom door when the earthquake shook him awake and he decided it would be safer out of doors than in his house.

Ray E. Smith, assistant fire chief, was awakened by a tiny bell ringing in the cage of his pet parakeet.

Thinking something might be after the bird, he leaped out of bed about the time the room started to rock and roll. He was pitched against the wall where he recieved a small cut on the nose.

Canned goods were thrown to the floor in the Commissary Store and several bottles were broken. Three fire alarm boxes, one at Armitage Field and two in the housing area were touched off. Most serious damage from the quake occurred in Tehachapi, approximately 75-80 miles from the Station on the road to Bakersfield.

Eleven persons including nine children, were killed in their beds by collapsing walls. A major part of the business section was destroyed and an outbuilding at the women's prison was made unusable.

The railroad water tower at Tehachapi collapsed into the street, crushing a car and ramming it against a telephone pole in a 'V' shape. The city water tower was also severely damaged and residents suffered from a water shortage.

Two ambulances, five medical corpsmen, and Dr. Arthur Shufro, of the Station infirmary, were dispatched with medical supplies to the stricken town. An R4D, a twin-engine transport plane, flew to Tehachapi air strip from Armitage Field in case air evacuation of casualties was necessary.

It was piloted by LT W. L. Cranney, instrument training and special devices officer at NAF, with H. A. Johnson, enlisted pilot first class, as co-pilot. LT Cranney reported the hospital there had lost the use of its sterilizing equipment and that Edwards Air Force Base was setting up field kitchens and trucking in water.

Two other R4Ds and two Beechcrafts were put on standby service at NAF in case they were needed.

The five corpsmen were Raymond Loveless and Robert J. Wallace, HMls; Rodney Rollo, HM2; Jerome Ciecmierowski, HM3, and Everett Hidlebaugh, HM.

Four security policemen were dispatched from the Station to Tehachapi for possible use in directing traffic, keeping the peace and guarding against looting. They were officers C. E. Ball, J. C. Phillips, C. D. Zills and H. O. Creech.

Officer Zills, in an eye-witness account to the *Rocketeer*, described damage to the women's prison, at first reported on the radio as untenable, as slight. Peace Officers from the California Highway Patrol, Bakersfield, and Tehachapi itself numbered an estimated 50, he stated.

The back porch of the hospital had caved in, he added and patients had been moved to the front lawn. There was no panic anywhere in the town, he observed. Walker Pass, the road from Bakersfield and Highway 466 from Mojave were all closed until they could be checked for damage and earthslides.

The Ridge Route was also closed by the Highway Patrol because of slides from the quake. Highway crews estimated that three days will be required to open the highway, the *Bakersfield Californian* reported.

Liberty was held up in the Station Marine barracks in case Marines were needed as firefighters or guards against looting in Tehachapi. All fire stations in the desert area were ordered to stand by and off-duty men were called in at Inyokern Fire Department.

The Tehachapi damage was declared a major disaster by the Red Cross and the Station Red Cross unit offered its services and went on a standby basis.

Two railroad tunnels between Tehachapi and a nearby town were collapsed and eight miles of track in Tehachapi Canyon were twisted out of shape.

Highway Patrol officers reported the Kern River Canyon closed at the mouth. Thousands of tons of rock and earth are blocking both ends of the canyon, according to a (GAP IN NEWSPAPER ACCOUNT).

The quake was given a rating of 7 1/2 by Caltech seismologists. This compares with the 1906 San Francisco earthquake, 8 1/4, and the Long Beach quake of March 10, 1933, of 6 1/2 in which 127 were killed and 4150 injured.

This rating scale has zero slightly less than the magnitude of the smallest recorded shocks. Magnitude of an earthquake is the common logarithm of the maximum displacement, expressed in microns, of the trace written by a standard torsion seismometer at an epicentral distance of 100 kilometers.

A reading was taken on a seismograph in tower 13 on G-2 range Monday morning. A photograph of the reading has been sent to Caltech for interpretation. The instrument here is one of the most sensitive in the world because of the solid foundation of surrounding country and consequent lack of 'background noise.'

According to Nelson R. Williams, head of the atmospheric studies branch of Test Department, who with Quenton Dalton is in charge of the seismograph, the local instrument has recorded quakes as far as 6000 miles away.

Tehachapi is approximately 5-6 miles north of the Garlock fault, which runs through the Tehachapi Mountains. This fault, which branches off the San Andreas Fault at Gorman, passes south of Tehachapi and the Station and through the Randsburg - Johannesburg - Red Mountain triangle. It is named after the village of Garlock, a few miles west of Randsburg and approximately 25 miles south of the Station.

This is the second major earthquake in the last six years in this area. A series of shocks ranging up to 6.3 magnitude rocked the Walker Pass area about 12 miles west of Highway 6 on March 15, 1946."

5.2.5 1961 Brown Earthquake

On October 19, 1961, an earthquake of magnitude 5.2 occurred east of Brown, approximately 10 kilometers northwest of Ridgecrest (Figure 44). The earthquake was felt at China Lake, Ridgecrest, Independence, Bakersfield, and Los Angeles. A foreshock of magnitude 3.4 was felt at China Lake about 8 minutes before the main shock (Richter et al., 1962).

The following is taken from an account of the local effects noted by Roland von Huene (a geologist at NWC).

"...(1) Little Lake (Mrs. Sullivan): Hot water gas vent pipe pulled out of wall, bottles knocked off of shelves, apparently no structural damage. Felt first event quite well - then about 10 min later a second event was shaking then a sharp jolt occurred.

(2) Nine Mile Canyon and Route 6 (Mr. Julian): Figurines knocked off shelves. No structural damage. Felt a first slight shaking then about 10 min later (9:10) a sharp jolt accompanied with shaking. Trailer rocked.

(3) Richfield Station Route 6, approximately 7/10 mile north of Kern-Inyo County Line (Mr. Hornbeck): Trailer swayed. Trees rustling and rumbling noise. No structural damage. Very slight 1st event, but approximately 10 min later a good shaking occurred followed by a sharp jolt.

(4) Brown Road and Route 6 (Dr. Flagg): Was in bed at time of quake. Shaking and jolt woke him up. No structural damage.

(5) Brady (Mr. Ernst): Didn't notice 1st event. But felt a good jolt and shaking about 9:10 p.m. Heard a loud rumbling noise. No structural damage. An employee who resided at Homestead was in bed and was awakened by the first quake.

(6) Mobil Gas Station in Inyokern: Just felt a strong jolt accompanied by shaking. Several cans of oil knocked off shelves (2nd quake).

(7) One mile south Leliter (Mrs. Jean Durling): Beds moved. Swaying motion. No noticeable vertical movement just a sharp jolt. No damage.

(8) Two miles north Leliter (Duel-Berg Farms): Bottles knocked off shelves. China fell to south side of building. No structural damage..."

The following was obtained by Glenn Roquemore from an interview.

LB Range, Naval Ordnance Test Station: Fluorescent lights hung by "S" chains were stretched down to shoulder level. Machine lathe was rotated 180 degrees. Cabinets fell to the floor, blocks in block wall were shifted and

cracked (Figure 45), water pipe was pulled from concrete foundation (Figure 46). Telephones poles were tilted (Figure 47).

5.2.6 1962 Walker Pass Earthquake

On September 16, 1962, a magnitude 4.9 earthquake occurred near Walker Pass about 10 kilometers west of Ridgecrest. Near the Sierra front, rocks fell and the quake was felt in a area that included Inyo-kern, the southern Sierra Nevada, the southern San Joaquin Valley, Fresno, and Los Angeles (Richter et al., 1962).

The following is an account of the local effects adapted from notes taken by R. T. Zbur (Naval Ordnance Test Station) and W. R. Moyle (U. S. Geological Survey):

"ON EARTHQUAKE - 16 September 1962 at 0536
R. T. Zbur and W. R. Moyle

No Name Canyon: Approximately 1/2 mi in canyon, Los Angeles road. South wall of canyon - 1 ft-diameter boulders traveled about 15 ft down a 45 deg slope. Cracks in road several millimeters wide - striking SSE. Along with cracks on sand band (slumping). Many small rocks and boulders slid down sand back (40 deg slope). North wall of canyon (along Los Angeles aque-duct road) - six ft by 2 ft boulders in road- 40 deg slope. Two ft by two ft boulder moved appoximately 5 ft off a 5 deg slope.

Sand Canyon: Approximately 1/2 mi west of Los Angeles aqueduct siphon at canyon constriction. South-southeast wall of canyon - slope approximately 50 deg - cracks visible in thin fan. Fault zone approximately 2 ft wide and about several hundred feet long, extending from a crack through a dike. Minor landsliding. Same pattern of cracks observed on north wall of canyon and directly across from south-southeast wall cracks. On north wall landsliding and slumping more pronounced. However, the slope is about 55 deg. Cracks resembled an erosion phe-nomemena from a distance - closer inspection shows cracks discontinuous.

Nine Mile Canyon: Small rocks and boulders up to 1 ft-diameter found along road - slope is very steep

FIGURE 45. Closeup view of machine shop wall showing cracking and grouting along the foundation where the wall shifted about 2 centimeters off the foundation.

FIGURE 46. Water pipe and concrete retainer wall. The water pipe pulled from the concrete which was patched. Later, however, events have begun to remove the patch.

FIGURE 47. View of the 1961 epicentral region showing tilted telephone poles.

tho' - about 75 to 80 deg in places. Slide material apparently less severe here than in canyons to the south. Cracks - on north wall about 1/2 mi west of aqueduct siphon and along road - cracks in an indurated sand ungoing saltation deflation.

Homestead (Dr. J. C. Shrader): Felt shock - was standing outside by auto - car swayed. Audible rumble similar to a subway train - estimated motion of ground to be about 2 oscillations per second. Motion was apparently uniform - no sharp movement like October 16, 1961, quake. Dr. and wife felt two smaller tremors between 2:00 a.m. and 4:00 a.m. No audible sound. Slight shaking. No damage observed.

Brady's Cafe (Hwy 6 and 395): Felt shock - lights swayed in cafe and a few dishes and cupboards rattled. Heard a rumbling sound that appeared to come from under the cafe - no damage.

Nine Mile Canyon and Hwy 6 and 395: Felt shock - was sitting in chair reading newspaper (no name given in notes)- no household articles fell - large objects swayed a little- small noise heard, like a semitruck pulling into driveway."

5.2.7 February 1977 Ridgecrest Earthquake

On February 14, 1977, two small earthquakes occurred along the same fault (Airport Lake fault) as the 1961 event. The magnitudes were 3.2 and 3.7. Both quakes were felt in both Ridgecrest and China Lake (Derr et al., 1977). The following account is taken from the *Daily Independent*, Monday and Tuesday, February 14 and 15, 1977.

RIDGECREST - Earthquake activity beginning about midnight has been rattling the Indian Wells Valley all morning, but as of press time, has resulted in no reported damage.

Seismologists at Cal-Tech report that the strongest of the quake was at 5:58 a.m. with a Richter reading of 3.8. The epicenter of the earthquake, according to Cal-Tech, is at China Lake.

Most of the earthquakes, occurring at 15 to 30 minute intervals, are not noticable, according to China Lake Naval Weapons Center spokesman Harry Parode, who reports that the strongest jolt awakened his wife, Helen.

Bill Finnegan, at China Lake's Earth and Planetary Sciences Division, says that it is not yet known precisely where the quake is centered.

Jack Crawford, head of the Weapons Department at China Lake, said he felt the earthquake as a mild shock followed by a stronger one.

MILD AFTERSHOCKS BEING FELT LOCALLY
15 February 1977

RIDGECREST - Mild aftershocks from the China Lake earthquake early Monday were continuing into the pre-dawn hours this morning.

The main shock of the 3.8-Richter-scale quake was recorded at 5:58 a.m. Monday. It was preceded by several small foreshocks, seismographs show.

The first aftershock came about two minutes after the main spike, according to Fred Davis, a physicist from the Earth and Planetary Sciences Division of the Naval Weapons Center.

The aftershocks, which "might be felt, but just barely," began to space out at 10 to 15 minute intervals until 11:00 a.m. when they dropped to approximately hourly intervals, Davis said.

The United States Geological Survey (USGS) from Menlo Park has reported the earthquake epicenter at approximately two miles north of the Naval Air Facility at Armitage Field.

USGS scientists are still attempting to detect the approximate depth of the quake, with such information to be used when later scouting the area for signs of physical fracturing or telephone pole realignment.

The Garlock fault is believed innocent of causing the quake through slippage, with the blame more likely falling on one of many small, unnamed faults under the valley.

Several local residents reported waking from their sleep when the quake struck. Some reported feeling motion for up to four seconds, which is not at all unusual according to Cal Tech graduate student Carl Johnson. In fact, it would be unusual if no one was awakened, he said.

5.2.8 March 1977 Ridgecrest Earthquakes

On March 7, 1977, two earthquakes occurred in the Ridgecrest area. The first earthquake was magnitude 3.0 and the second was magnitude 3.2 (Derr et al., 1977).

The following is a newspaper account of the earthquake from the *Daily Independent*, Tuesday, March 8, 1977.

> RIDGECREST - Seismographs were not working yesterday afternoon at the China Lake Naval Weapons Center's Earth and Planetary Sciences Lab, but it didn't matter.
>
> When the first of two earthquakes jarred the building about 2 p.m., the people working there felt it.
>
> "I was sitting in a chair and there was a small jolt that just lasted a second or so," said Harold Cronin.
>
> Secretary Reta Roquemore, whose earthquake-expert boss, Dr. Pierre St. Amand was out of town and missed the local show, agreed, "We felt it."
>
> "My desk moved forward," said Mrs. Roquemore, who noted that some of her co-workers mentioned hearing a noise before they felt the shock.
>
> She noticed people beginning to move towards the seismograph, too, unaware that the machinery was not working.
>
> Cal Tech reported that the first jolt about 2 p.m. measured 3.2 on the Richter scale. A second earthquake at 3:16 p.m. measured 3.0.
>
> Epicenter of the earthquakes was believed to be about five miles southwest of China Lake, perhaps in the vicinity of the White Star Mine. At Hi-Desert Sauna and Spa, however, at the White Star Mine, Ruth Kirley reported that no one there felt the earthquake.
>
> At the Daily Independent, the earthquake jarred desks and set an entryway hanging light swaying.
>
> No damage was reported.

5.2.9 1979 Walker Pass Earthquake

On June 14, 1979, there was a magnitude-4.3 earthquake near Walker Pass (Figure 44). Reports from Ridgecrest and China Lake residents include moderate shaking of houses, about 60% of the residents were awakened, and there were reports of audible rumbling. No damage was reported.

5.2.10 Local Seismicity

One of the first indications of high seismicity on the southeast side of the Sierra Nevada came in a paper by Allen et al., (1965). Figure 48, shows the relative location of a few earthquakes larger than magnitude 6 that have occurred near Indian Wells Valley. Figure 49, is a strain release map using earthquakes of magnitude 3 and larger in the strain calculations (Allen et al., 1965). When both Figures 48 and 49 are taken into account, it becomes obvious that an abundance of high-magnitude earthquakes as well as low-magnitude earthquakes occur in the region including Indian Wells Valley. After this work, little research was accomplished until seismicity for geothermal exploration became important in the Coso Range.

Walter has completed the most thorough examination of local seismicity to date. Walter found that fault-plane solutions show a regional north-south compression. Also, earthquakes located in northwest-striking zones generally have right-slip focal mechanisms, those in northeast-striking zones have left-slip focal mechanisms, and those in north-south striking zones have both normal-slip and lateral-slip focal mechanisms. These conclusions are in strong agreement with the geologic evidence that demonstrates dominant northwest-striking, right-slip faults with northeast-striking, left-slip and north-south striking, conjugate faults.

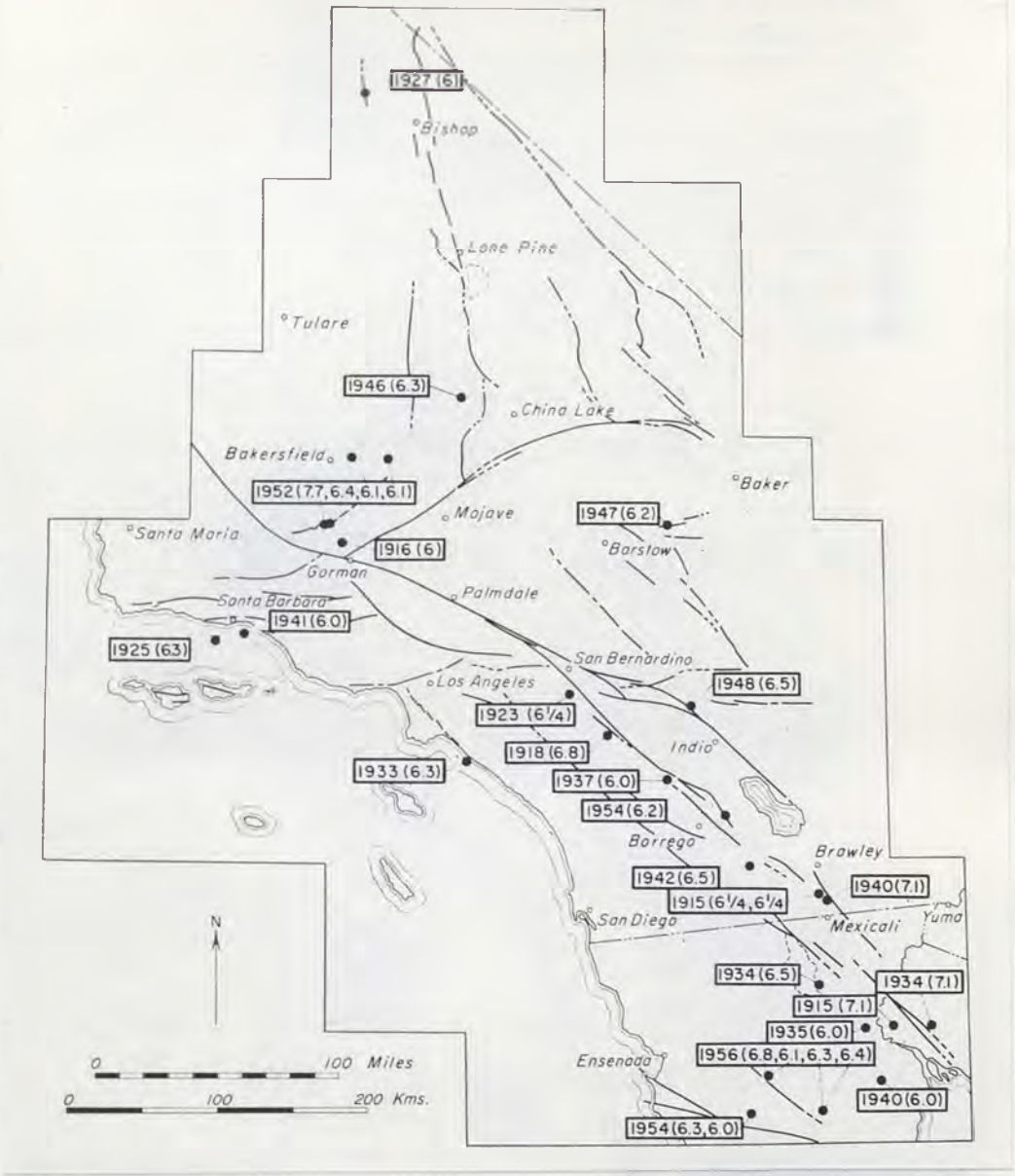

FIGURE 48. Geographic plot of southern California region showing locations of earthquakes larger than magnitude 6.0. (Modified from Allen et al., 1965.)

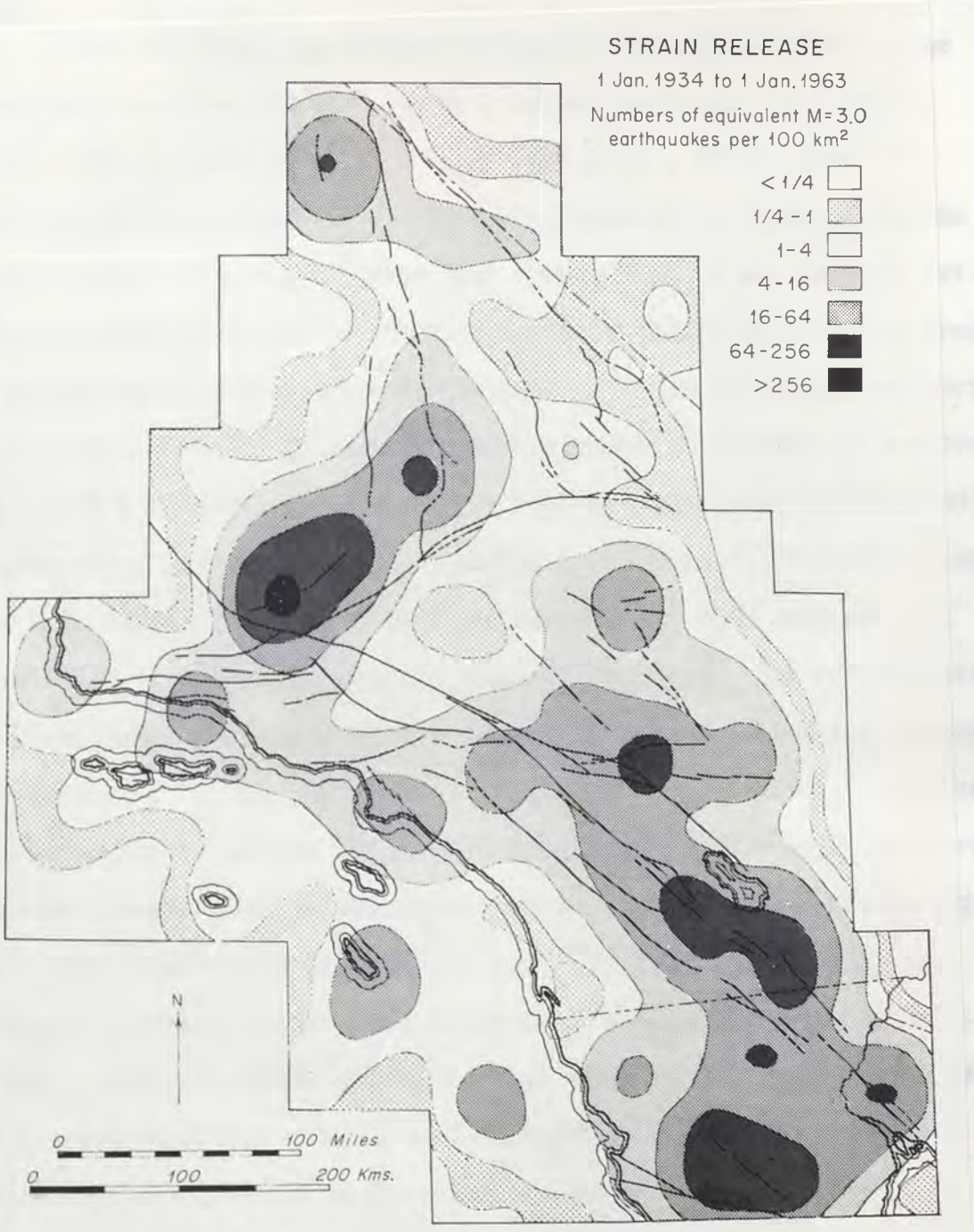

FIGURE 49. Strain-relief map of the southern California region. (Modified from Allen et al., 1965.)

Figure 44, shows the regional seismicity from 1932 to 1977. The epicenters are from Cal Tech and USGS seismic networks (Fuis et al., 1977, 1978; Friedman et al., 1976; Hileman et al., 1973). The dominant northeast band of seismicity in Figure 44 is identical to the trend shown in Figure 49. These data further support the geologic evidence of rapid tectonism in the Coso Range and Indian Wells Valley areas. Figure 50 shows several epicenter alignments in the Coso Range and northern Indian Wells Valley. Relatively speaking, there is somewhat of a seismic gap about 5 kilometers wide along the Sierran front (seen in Figure 50) except for a band of seismicity trending in a northeast direction across the Coso Range. Data presented later suggest that this zone may be a thrust and is consistent with the regional tectonics. The seismic pattern conforms very well with the fault pattern of the area. The area around the letter "I" is the north end of Indian Wells Valley which is a closed basin sandwiched between the north-south-trending Sierra Nevada and Argus mountain ranges. The seismicity in this area forms a north-south alignment with normal-fault focal mechanisms. The seismicity and the geomorphology suggest an east-west extensional mechanism for Indian Wells Valley. Where the south end of the Coso Range begins, south of the letter "B," there is a discontinuity in the orography. The range fronts and associated valleys bend to the west. This can be seen to the east in Panamint Valley as well. As the geomorphology changes, the dominant focal mechanism shifts to northwest trending, right-lateral strike-slip. The strike of the focal-mechanism-derived fault planes parallel the northwest trend of the valleys almost identically. About 2 kilometers east of the letter "B," there is a major north-south trend in the

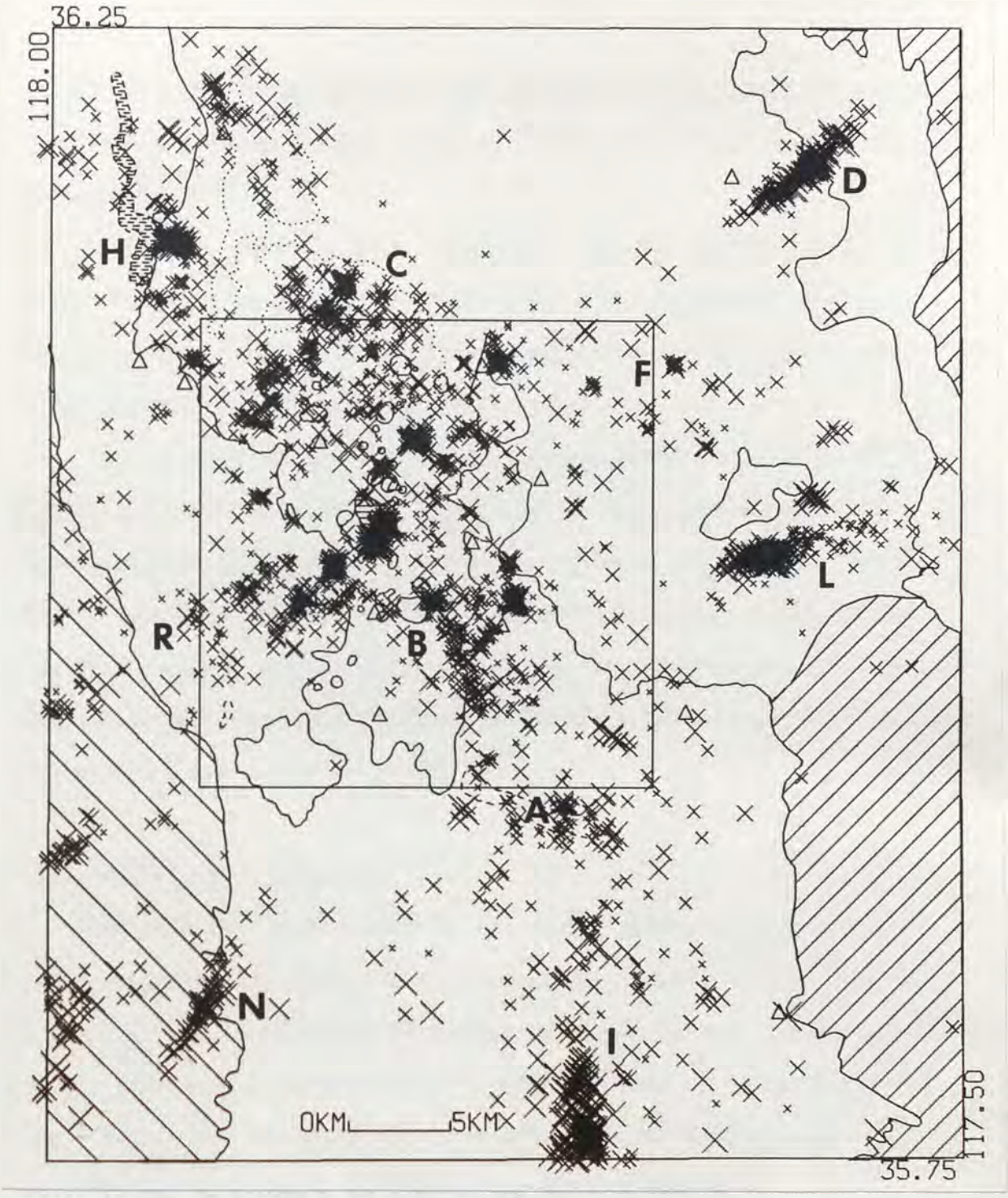

FIGURE 50. Plot of local microseismicity from September 1975 to September 1977. (I) Indian Wells Valley, (N) Nine Mile Canyon, (B) southern Coso Range, (R) Rose Valley, (L) Louisiana Butte, (F) northeast Coso Range, (H) Haiwee Reservoir, (C) northern Coso Range, (D) Darwin. The box indicates the location of the geothermal area. (Modified from Walter and Weaver, 1980.)

seismicity. The valley in which this seismicity occurs is north-south trending and, not so surprisingly, the normal fault focal mechanisms are north-south as well.

Figure 51, shows the focal mechanisms from October 1975 to September 1977. The northwest-trending, right-slip, focal mechanisms are dominant with the normal-slip, focal mechanisms occurring as conjugate systems resulting from the primary right-slip tectonics.

The tectonics of the Coso Range, as demonstrated by the seismicity, suggest east-west spreading brought about by the right-slip movement. This opening begins at the Garlock fault and continues northward at least 400 kilometers. The Coso Range may represent a pressure ridge in the regional picture. Indian Wells Valley and the closed basin which contains Owens Lake both represent regional sag ponds in this scenario. These observations are discussed in Chapter 8.

5.3 SUMMARY AND CONCLUSIONS

Regional and local seismicity has caused damage to communities of China Lake and Ridgecrest. One of the largest earthquakes in California history occurred within 100 kilometers of the study area. Microseismicity occurs every day and demonstrates a very high rate of tectonism in the Coso Range. The potential for large magnitude earthquakes near Indian Wells Valley is probably as high as anywhere in California.

The alignment of epicenters and focal mechanism plots both agree with the geologically-obtained data on the local tectonic mechanism.

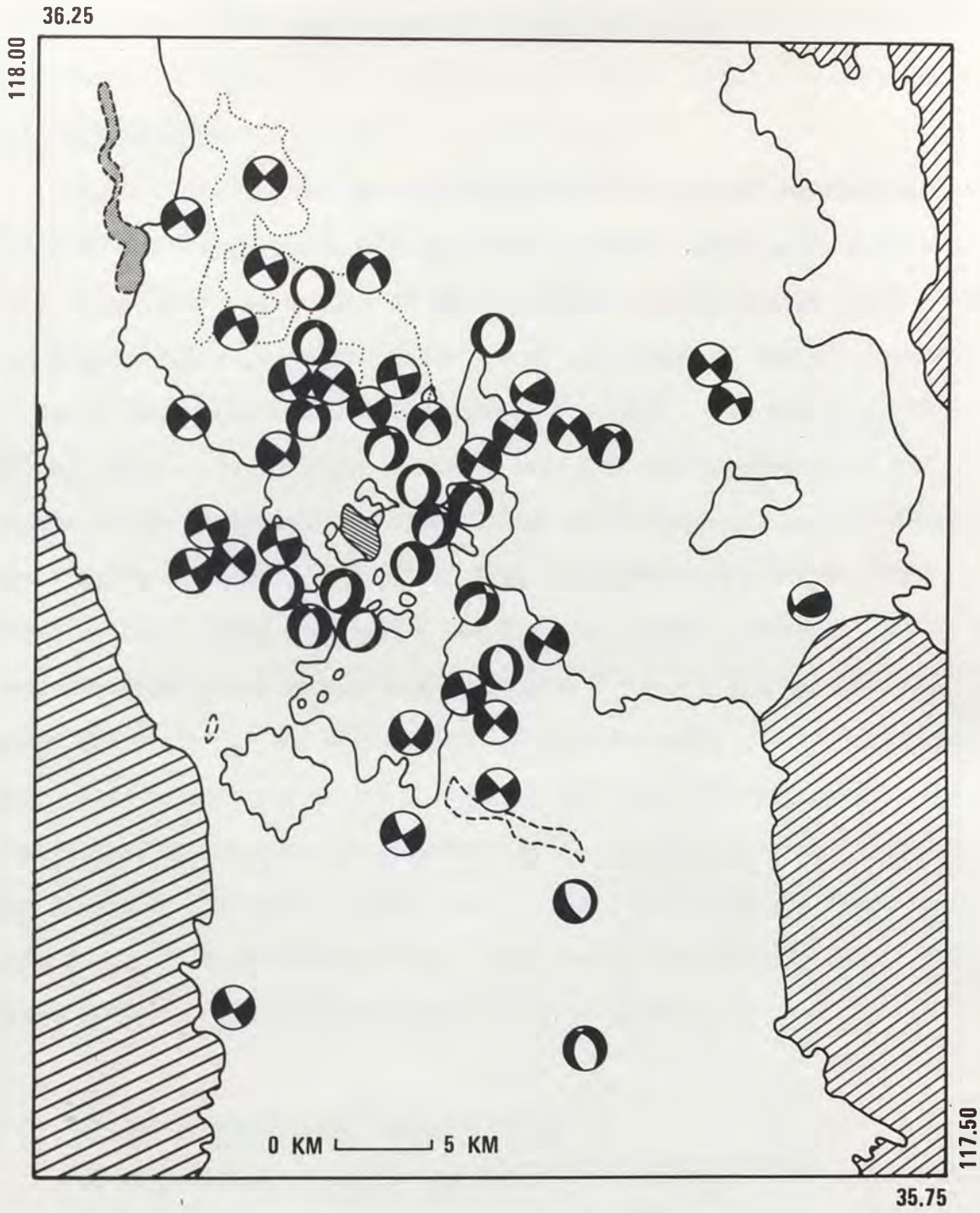

FIGURE 51. Plot of focal mechanisms for the Coso Range. (Modified from Walter and Weaver, 1980.)

6.0 CALCULATION OF DESIGN EARTHQUAKE

6.1 INTRODUCTION

When a fault has not produced significant historical earthquakes, calculation of a *design earthquake* proves useful. The *design earthquake* is defined as the earthquake of highest, credible magnitude a given fault can produce based on either statistics of the length or the displacement of faults that have historical earthquakes or both. The representation of this data is in the form of curves that plot the parameters of magnitude versus length and magnitude versus displacement as well as other modifications (Tocher, 1958; Iida, 1959, 1965; Albee and Smith, 1966; Bonilla, 1967, 1970; and Bonilla and Buchanan, 1970). Slemmons (1977) has normalized these curves in the equation $M = a + b \log x$, that becomes the basis for the calculations presented herein. In the equation, log x will be replaced by log L (length) and log D (displacement). The statistical calculations by Slemmons (1977), include groupings of data for faults of all types in North America (NA), faults of all types worldwide (WW), all lateral-slip faults (LS), and all normal-slip faults (NS). These data can be used to calculate a *design earthquake*.

6.2 DESIGN EARTHQUAKE (LITTLE LAKE FAULT)

For calculations done for the Little Lake fault, a length of 24 kilometers was used. The limitations to this length designation are that the Little Lake fault merges with the Sierra Nevada frontal fault and could be considered much longer, and the Little Lake fault has not been mapped

to the south. Therefore, 24 kilometers is a minimum length. The displacement value used in the calculations is based on 250 meters of right-slip displacement on a 400,000-year-old basalt.

In Table 2, the Little Lake fault results are listed by type of fault, magnitude, and recurrence interval based on 250 meters of displacement in the last 400,000 years. All magnitudes were calculated using length only.

TABLE 2. Design earthquake data for the Little Lake fault.

Fault type	Magnitude	Displacement, meters	Return interval, years
NA	6.4	0.49	784
WW	6.8	1.05	1680
LS	6.5	0.675	1080

6.3 DESIGN EARTHQUAKE (AIRPORT LAKE FAULT)

The length of 30 kilometers chosen for the Airport Lake fault is a minimum length. The fault is dispersed in lava flows at its north end and, therefore, arbitrarily ended there for this study. The south end of the fault was not mapped in this study. The displacement on the fault is based on 3.4 meters on normal-slip seen in the exploratory trench, and 125 meters of right-slip in a basalt assumed to be 400,000-years-old. The age of the basalt has not been determined. The flow has been placed in the geologic column between two flows dated by potassium-argon as 400,000 and 1 x 10^6 years (Duffield and Bacon, 1977).

The magnitude of the design earthquake on the Airport Lake fault was calculated from the length and the displacement. The date of the

3.4 meters of offset is not known and, therefore, not used in the return interval calculations. Table 3 lists the results of these calculations for the Airport lake fault.

TABLE 3. Design earthquake data for the Airport Lake fault.

Fault type	Magnitude vs displacement	Displacement, meters	Return interval, years
NA	7.3	3.4	...
WW	7.4	3.4	...
NS	7.4	3.4	...

Fault type	Magnitude vs length	Displacement, meters	Return interval, years
NA	6.6	0.65	2080
WW	6.9	1.25	4000
NS	7.0	...	...
LS	6.6	0.83	2656

6.4 DESIGN EARTHQUAKE (EAST SIDE AIRPORT LAKE FAULT)

For the fault on the east side of Airport Lake, a length of 11 kilometers is probably very close to reality; however, further study could extend the fault to the south. The displacement chosen is 3.4 meters of normal slip as seen in the exploratory trench. The age of this displacement is unknown and, therefore, a recurrence interval is not provided. Table 4 lists the calculated results for these faults.

TABLE 4. Design earthquake data for the faults on the east side of Airport Lake.

Type of fault	Magnitude	Displacement, meters	Return interval, years
NA	7.3	3.4	...
WW	7.4	3.4	...
NS	7.4	3.4	...
NA	5.9	3.4	...
WW	6.4	3.4	...
NS	6.5	3.4	...
LS	6.1	3.4	...

6.5 SUMMARY AND CONCLUSIONS

The design earthquake is often used when no historical earthquake information is available on a specific fault. According to the design earthquake formulas, the average magnitudes (M), displacements (D), and return intervals (RI) are as follows: The Little Lake fault, M = 6.6, D = 0.74 meter, RI = 3000 years; faults east side of Airport Lake M = 6.7, D = 3.4 meters.

Other faults in the area such as the Garlock, Sierra Nevada, and Kern faults are much longer. These faults are capable of producing an earthquake much larger than those mapped in this study.

7.0 PRESENT LOCAL TECTONIC PATTERN

7.1 INTRODUCTION

This chapter, based primarily on original geologic and geomorphic information, provides the basis for a synthesis of present-day tectonics in the Coso Range region of southeast California. This interpretation is relevant to the assessment of the structure development of the Basin and Range province. Presented is a view of important observations based on the patterns of faulting, geomorphology, and geochronology; a synthesis drawing from these evidences is presented.

Four major points that relate to the tectonic interpretation of the Coso Range are listed as follows:

1. The structure is consistent with the Basin-and-Range stress patterns.

2. The rate and style of vertical and horizontal displacement suggest transition between strike-slip tectonics to the west and extensional tectonics to the east.

3. Arcuate faulting in the Coso Range results from the strike-slip component of regional stress there.

4. The fumerolic activity is controlled largely by faults with a significant oblique-slip component, and thus is unrelated to caldera formation as suggested by earlier workers (see Chapter 1). Each of these points is discussed in the following paragraphs.

7.2 STRUCTURE CONSISTENT WITH BASIN AND RANGE STRESS PATTERNS

7.2.1 Graben Valleys and Tilted Blocks

Rose Valley (Figure 52) separates the Coso Range from the Sierra Nevada. According to Healy and Press (1964), it represents a southward extension of the Owens Valley graben. Their interpretation is consistent with later work carried out by Slemmons (personal communication), who found that faults mapped in the southern Owens Valley connect with those mapped by Allen et al., (1965) and by Roquemore (1977), (Naval Weapons Center Technical Publication 6036, being published). The valley fill in the center of Rose Valley is over 1670 meters thick, which indicates substantial down-faulting on the valley margins. Basin structures of this type are typical of a 240-kilometer zone along the Sierra front (Healy and Press, 1964). The west side of Rose Valley is bounded by the northeast-striking Sierra Nevada frontal fault zone, where Duffield and Smith (1978) report over 1200 meters of vertical movement. To the east of Rose Valley, there are several step-faulted, west-tilted blocks of the Pliocene Coso Formation (Power, 1958). The faulting in Rose Valley is high-angle, normal-slip and results in low- to moderately-tilted fault blocks.

Coso Valley (Figure 52) is in the south-central portion of the Coso Range. This graben valley is bound on the west by the Airport Lake fault, which is a left-stepping, *en echelon*, range-front fault. Two asymmetrical graben structures, one of which is nearly 2 kilometers wide, are within the zone of faulting. The Airport Lake fault strikes north 10 degrees to north 20 degrees east and dips from 50 degrees east

FIGURE 52. Fault map of the Coso Range. (AP) Airport Lake, (LLF) Little Lake fault, (LL) Little Lake, (SLM) Sugarloaf Mountain, (CHS) Coso Hot Springs, (CP) Cactus Peak, (UCF) Upper Cactus Flat, (MF) McCloud Flat, (CF) Cactus Flat. The shaded area marks the topography above 5000 feet. The hatched areas are rhyolite domes.

to vertical. Bounding the east side of Coso Valley is the highly step-faulted Wild Horse Mesa. Along this zone, thin sheets of basalt and andesite lava flows are broken by high-angle, normal faults with a sinuous, left-stepping, *en echelon* pattern. The Coso Hot Springs fault (east of Coso Hot Springs in Figure 52) strikes north 25 degrees east with a dip of 45 degrees to 55 degrees southeast and bounds Coso Valley on the north. It probably connects the Airport Lake fault and Haiwee Springs faults in a single *en echelon* zone. The right-oblique-slip displacement along this zone is consistent with orientation of the maximum compressive stress at north 15 degrees to north 25 degrees east, and the minimum compressive stress at north 65 degrees to north 75 degrees west. These stresses are shown, together with a detailed schematic drawing of faults in the Coso Basin graben, in Figure 53. The direction of extension stress is rotated about 25 degrees clockwise from that obtained by Carr (1974) for the Nevada test site to the east.

7.2.2 Strike-Slip Faults

Most of the normal faults in the Coso Range are generally north-trending and have right-slip displacement associated with them either as right-oblique-slip or as left-stepping, *en echelon* pattern. Examples of right-slip faults include the Airport Lake fault, Wild Horse Mesa, and the Little Lake faults. The Airport Lake fault is a prime example of an *en echelon* fault associated with right-slip movement, as evidenced by a right-slip, offset basalt flow and by the typical, left-stepping *en echelon* pattern in Coso Valley. On Wild Horse Mesa (Figure 54) a pattern of sinuous, left-stepping fractures stair-step-down west to the Coso Basin (see Coso Hot Springs, Figure 52). The Little Lake fault (Figure 53) is

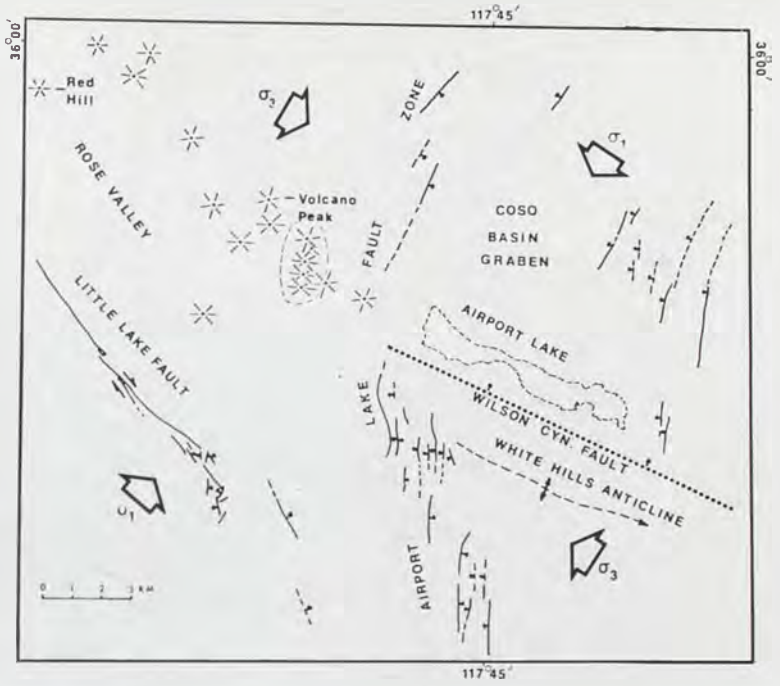

FIGURE 53. Schematic diagram of the southern Coso Range showing the local stress orientation. σ_3 is the direction of least compressive stress, and σ_1 is the direction of maximum compressive stress. The star symbols are cinder cones. The cones enclosed by a dashed line are the same age and composition.

FIGURE 54. Aerial view of Wild Horse Mesa showing abundant step-faults.

perhaps the most spectacular example in this part of the Basin and Range province; it has many of the typical landforms characteristic of strike-slip faults (Slemmons, 1977), including rhombic depressions, benches, side-hill ridges, linear troughs, and shutter ridges. Such clear manifestations of horizontal movement are rare east of the Walker Lane in the Basin and Range province, as evidenced by the lack of its being mentioned in the literature of the area.

7.2.3 White Hills Anticline

The White Hills anticline, which strikes north 65 degrees to north 75 degrees west, is a clear example of a primary fold. Its orientation is perpendicular to the direction of maximum compressive stress which is inferred by the faulting pattern (north 15 degrees to north 25 degrees east, Figure 53). The Wilson Canyon fault, running parallel to this fold and north of it, was active in pre-Quarternary time and had left-slip movement (Zbur, 1963). At present, this fault is seismically inactive (Walter and Weaver, 1980).

7.2.4 Alignment of Volcanoes

Nakamura (1977) found that the orientation of average tectonic stress may be determined by utilizing dike patterns and the alignment of volcanic cones. With equidirectional tectonic stress the dikes often extend radially from a central source, but with differential horizontal stress, they tend to be parallel to the direction of maximum horizontal compressive stress. Assuming a single source of the magma of the basaltic cones near Volcano Peak (Figure 53), the lineup of cinder cones (north 50 degrees west) indicates the same general direction of minimum compressive stress as shown by the faults and the White Hills anticline.

Evidence for the single magma source for these cones is (1) Close spatial relation along a line and (2) similar composition of the basalts (Duffield and Bacon, 1977).

7.3 RATE AND STYLE OF VERTICAL AND HORIZONTAL DISPLACEMENTS

7.3.1 Vertical Displacements

Vertical displacements are expresed in the Coso Range as horst-and-graben structures, tilted blocks, and step faults. As two examples here show, vertical rates are very rapid. A distinctive, capping rhyodacite flow above the Coso Formation is offset 600 meters at a site on the west flank of the Coso Range (Roquemore, 1977). Duffield and Bacon (1977) give an age of about 2.5 million years for this flow. This determination of offset is based on the present position atop the Coso Range and the location of the same flow buried in Rose Valley, identified by geophysical methods (Healy and Press, 1964). The inferred rate of vertical movement based on this offset is 1.8 millimeters per year. Similarly, on Wild Horse Mesa, another area of tectonic extension and associated step faults has been dated at about 3 million years by Duffield and Bacon (1977). The total offset of this flow has not been determined because the lowest down-dropped block is buried in the Coso Basin alluvium, but the offset is at least 600 meters. This gives a minimum rate of vertical deformation on Wild Horse Mesa at 0.2 millimeter per year.

7.3.2 Horizontal Displacements

Geomorphologic evidence can be used to estimate horizontal rates of offset on both the Little Lake and Airport Lake faults. The Little Lake fault strikes north 40 degrees west from near the Garlock fault. It is

best exposed near the settlement of Little Lake where a young lava flow is offset. The Little Lake fault is predominantly right-slip, and offsets a basalt flow dated at 440,000 years (Duffield and Smith, 1978) by 250 meters. This indicates an average slip rate of 0.6 millimeter per year. Since the lava flow is modified by stream erosion, this is probably a minimum estimate. A shutter ridge along the fault is offset only 30 meters, but wash channels are diverted which contain highly-crushed, landslide material from the Sierra Nevada. This landslide material is determined to be younger than the 440,000-year-old basalt because it has not been eroded by the ancient Owens River as has the basalt. Similar drainage offsets along the Airport Lake fault cannot be used for calculation rate-of-movement, because they are highly modified by seasonal flash floods. An offset basalt flow, which has not been potassium-argon dated, provided a measured displacement of 125 meters on this fault. Based on potassium-argon dating and field relations, Duffield and Bacon (1977) have placed this flow on their geologic column between two others with ages of about 0.400 and 1.0 million years, respectively. These numbers imply offset rates ranging between 0.3 and 0.1 millimeter per year on this fault.

7.4 FUMEROLIC ACTIVITY ALONG BASIN AND RANGE FAULTS IN THE COSO RANGE

Austin et al., (1971) and Koenig et al., (1972) noted the presence of radial faults projecting outward toward the circumference of a feature in the Coso Range that they identified as a ring structure. In this interpretation, one would expect fumerolic activity to concentrate along these radial faults, and that motion on them should be normal faulting

because they are extensional. Among the dozens of known hot springs in the Coso Range, all but two are associated with faults; the two exceptions are in the Sugarloaf Mountain area shown on Figure 52, and in the Devils Kitchen area 1 mile to the east. However, most of the faults in the Coso Range that are associated with hot springs have significant components of oblique-slip. (See the foregoing discussion on lateral faults.) Two examples are the Airport Lake fault with right-slip offset of a basalt flow and the Coso Hot Springs fault with a left-stepping *en echelon* pattern. Both of these faults have the main concentration of hot springs in the region. These faults have a strike-slip displacement of a sense consistent with the local tectonic stress pattern as seen in Figure 53. The strike-slip character shown is not required by ring fault or caldera-like features, nor is ring faulting consistent with the tectonic regime.

7.5 ARCUATE FAULTS IN THE COSO RANGE

In the area around McCloud Flat (Figure 55), a set of short segmented, and slightly curved faults define a crude arch. These faults have been interpreted (Austin et al., 1971 and Koenig et al., 1972) as a structure which resembles those associated with calderas. Chinnery (1966) has proposed that secondary faults forming at the ends of large-scale, strike-slip, master faults are often arcuate (Figure 55). This is a plausible concept for the arcuate faults in the Coso Range because the Coso Range is located at the south end of a long zone of right-slip as evidenced by the Owens Valley fault zone. Also south of the Coso Range is a very different tectonic style as evidenced by the east-west trending,

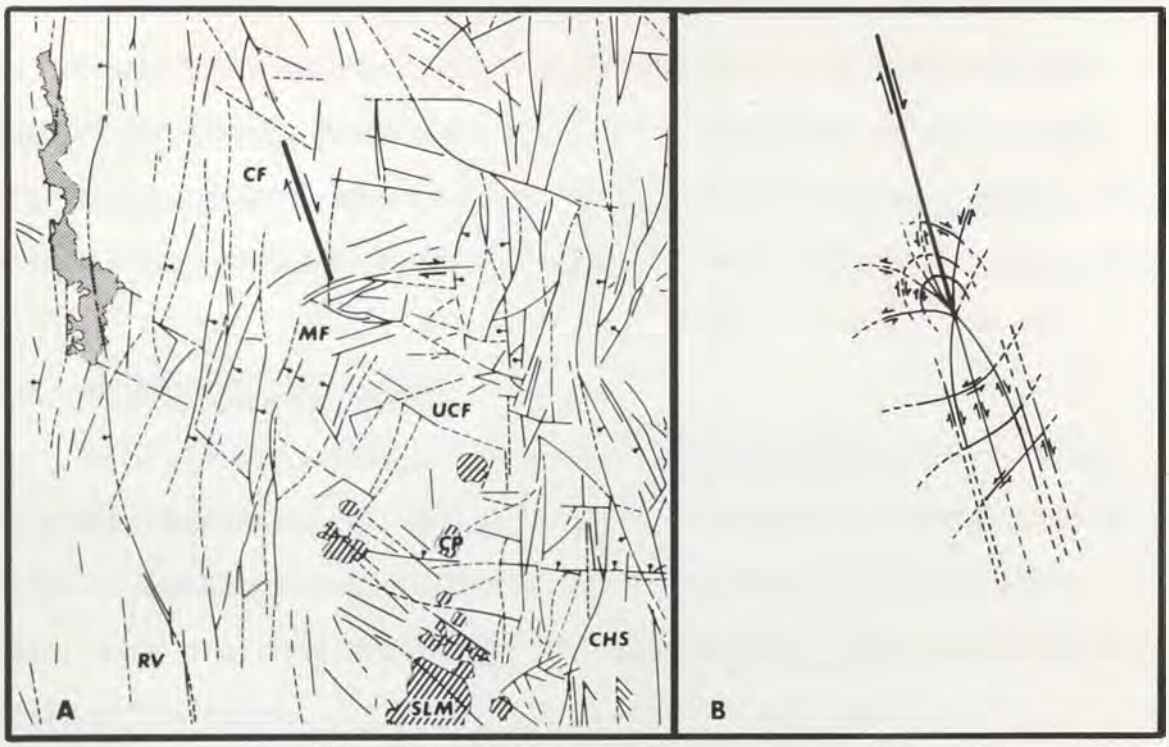

(a)

Existing fault pattern in the Coso Range.

(b)

Fault patterns predicted by Chinnery to occur at the end of right-slip master faults.

FIGURE 55. Diagram showing how Chinnery's concept of arcuate faults apply to the Coso Range.

left-slip, Garlock fault. There is no requirement for arcuate faults to be directly associated with volcano-genic origins. In the Coso Range, some of the arcuate faults have strike-slip striations on fault planes (St. Amand, personal communication) as predicted by Chinnery (1966). Ring dikes or other volcanic features cannot be linked with these arcuate faults.

7.6 SUMMARY AND CONCLUSIONS

Austin et al., (1971), Koenig et al., (1972), and Duffield (1975) have all interpreted the arcuate features of faulting in the Coso Mountains in terms of recent subsidence within a caldera-like structure. Thus, under these interpretations, volcanism controls the structural features of the region.

In this paper, it has been shown that the sense of faulting is consistent with the predominant principal stress directions of the Basin and Range (i.e., east-west extension and northeast-southwest compression). The volcanic and fumerolic activity are clearly associated with features that relate to these stresses, and thus manifestations of them rather than indicators of the dominant tectonic mechanism of the area. Also, it follows then, the overall assessment of the geothermal potential may be reduced by these factors.

The pattern of regional stress developed in this paper is consistent with that stress expected in the southwest Basin and Range province; graben structures and normal faulting running north-south. This paper documents a significant component of right-lateral, strike-slip motion that is consistent with San Andreas-Garlock tectonism to the west and south. Therefore, the area fits Wright's (1976) classification of Basin

and Range province "Deformation Field II" as he predicted it would: The Coso Range area is a region of transition between San Andreas-Garlock and Basin and Range province, with recent folding and faulting showing characteristics of each of these provinces, and some peculiar to itself.

8.0 REGIONAL TECTONICS

8.1 INTRODUCTION

Allen et al. (1965) state that the faults of the Owens Valley-Death Valley region probably represent features that are transitional between true San Andreas and true Basin and Range tectonic patterns. Wright (1976) identified two deformational fields within the Basin and Range province based on his observations as follows: (1) Field I encompasses most of Nevada and is characterized by steeply-dipping, normal faults oriented north-northeast, (2) Field II is bound approximately on the east by the Walker Lane and bound on the west by the Sierra Nevada block, (3) Field II contains gently-dipping, normal faults oriented north-south, and abundant conjugate shears, and (4) Deformational Field II is topographically and structurally distinct from the rest of the Great Basin because most of the mountain ranges trend northwestward. Wright goes on to state that this region is incompletely studied. Slemmons (1967) noted that the Walker Lane, a zone 10 to 20 miles wide and 450 miles in length, separates northwest-southeast topographic trends to the west and north-south to north-northeast, south-southeast trends to the east. Roquemore (1978) found evidence for structures compatible with a Basin and Range/Sierra Nevada transition zone in the Coso Range.

Troxel et al. (1972) suggested that the area north of the Garlock fault had been stretched. Davis and Burchfiel (1973) conclude that the Garlock fault is a transform structure, that the southern Basin and Range province is spreading faster than its northern counterpart, and that the Basin and Range province is still being formed by east-west extension

without significant right shear. This model, however, does not totally explain the structural anomaly found in the western Basin and Range province. New data allow us to build upon the hypothesis of Davis and Burchfiel to explain the anomalous structure found in the western Basin and Range province. A discussion of a possible structural mechanism follows.

Zoback and Zoback (1980) report that the Sierra Nevada Block has a least-principal, horizontal-stress direction oriented west-northwest to northwest and is a region of stress transition from strike-slip deformation on the San Andreas to extensional deformation in the Basin and Range province. Zoback and Zoback (1980) also state that the least-principal, horizontal stress direction for the Basin and Range is west-northwest and is a region of active, crustal spreading by distributed normal and oblique-slip, normal faulting. However, the westernmost part of the province exhibits both strike-slip and normal faulting (Slemmons et al., 1979).

My observations indicate that the structure of the Coso Range in the western Basin and Range province exhibits a change in properties between the San Andreas and Basin and Range province, based on (1) a nearly east-west orientation in the least-principal, horizontal-stress direction, and (2) abundant northwest-oriented, right-slip faults. This seems to be true for the remainder of the transition area between the Walker Lane and the Sierra Nevada from Mono Lake to the Garlock fault (Carr, 1974; Wright, 1976). This observation, if true, suggests the hypothesis discussed in the following paragraphs.

8.2 TECTONIC MODEL FOR THE AREA BETWEEN THE SIERRA NEVADA AND THE WALKER LANE

The fault pattern of the western United States and parts of Mexico is shown in Figure 56 (modified from Atwater, 1970). The area in question is located east of the Sierra Nevada and west of the Walker Lane. The region is roughly triangular in shape with the sides of the triangle formed by the Sierra Nevada, Walker Lane, and Garlock fault. The distinct difference in structural trend between the Sierra Nevada, Walker Lane, and the Basin and Range province is clearly seen in Figure 56. The faults in the Basin and Range province are north-northeast trending. The faults along the Walker Lane are northwest trending. The faults in the study area are slightly more north than those in the Walker Lane.

If the Walker Lane were a conjugate shear to the deep-seated, north-south, compressional forces that extend the Basin and Range province, the Sierra Nevada Block would migrate northwestward along the Walker Lane failure plane. If the San Andreas fault increased its slip-rate or had a higher rate of slip than the Walker Lane, a drag-rotation (clockwise) of the Sierra Nevada might be expected to occur. This rotation would explain (1) the bend in southern end of the Kern Canyon fault, (2) the existence of the Garlock fault, and (3) the structural anomaly between the Walker Lane and the Sierra Nevada Block, the abundant compressional structures west of the Sierra Nevada Block, and the bend in the San Andreas where the Garlock fault intersects it.

Figure 57 is a schematic diagram of Figure 56, showing part of the Basin and Range province with a set of opposing arrows representing the direction of least-principal, horizontal stress. Arrow V_3 indicates the

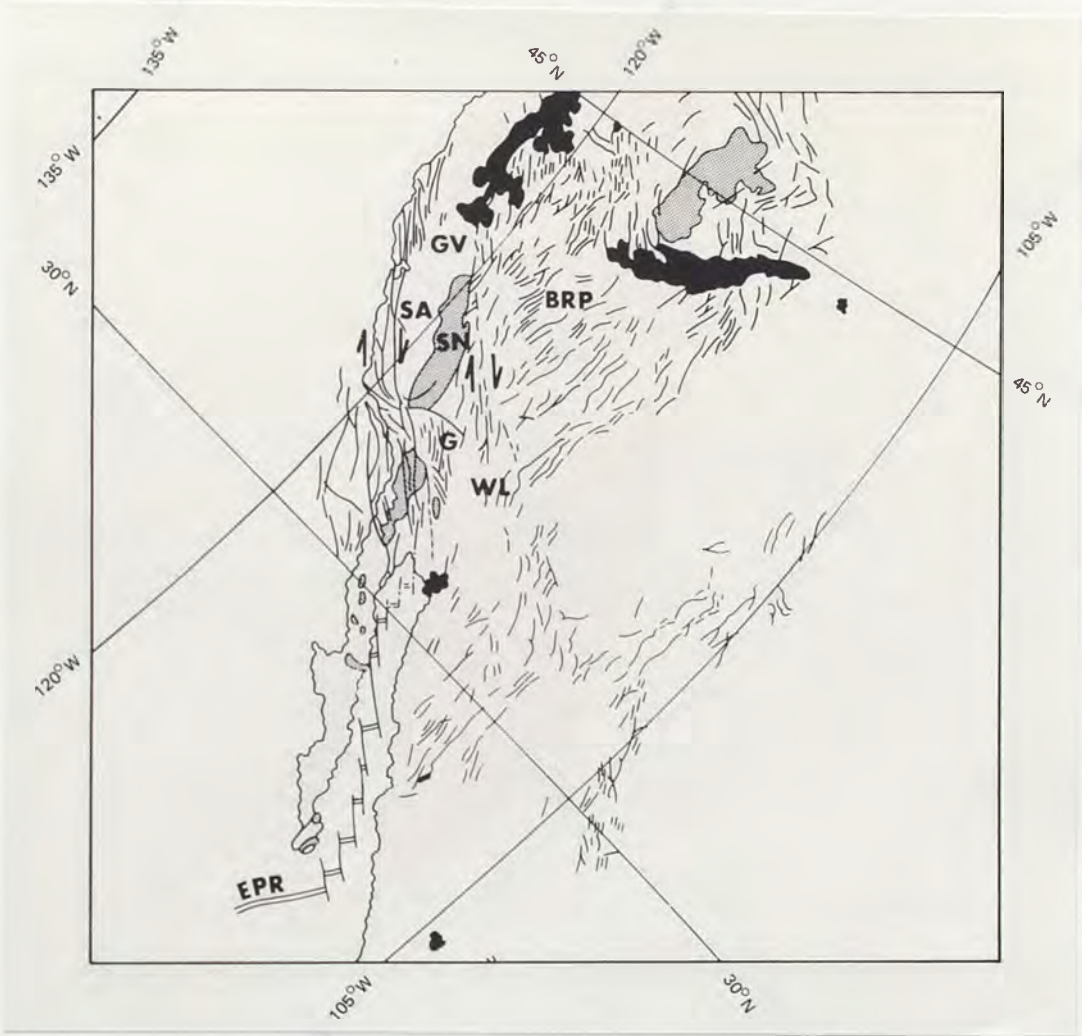

FIGURE 56. Fault map of the western United States and Mexico. (EPR) East Pacific rise, (WL) Walker Lane, (G) Garlock fault, (SN) Sierra Nevada, (SA) San Andreas fault, (BRP) Basin and Range province, (GV) Great Valley. Block areas are Quarternary volcanic rocks. Stippled areas are granitic plutonic rocks. (Modified from Atwater, 1970.)

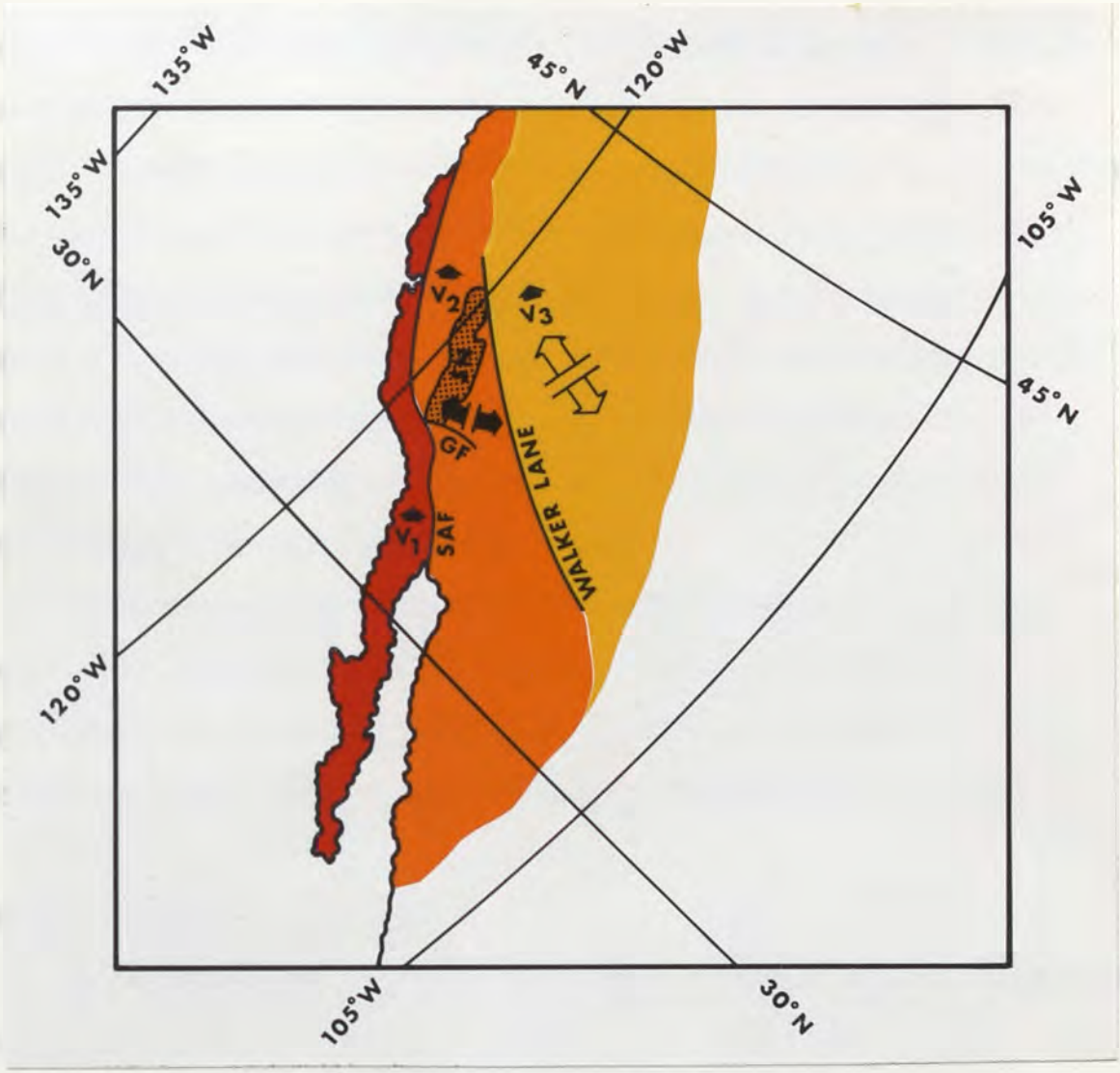

FIGURE 57. Schematic of Figure 56. (SAF) San Andreas fault, (GF) Garlock fault, (SN) Sierra Nevada. This schematic shows the northwestward migration of three sections of crust. The slowest movement is seen in yellow. The orange area has an intermediate northwest migration velocity. The red area has the highest northwest migration velocity and corresponds with movement on the San Andreas fault.

slowest rate of northwest migration. Walker Lane separates the zone of east-west extension from areas to the west. A set of opposing arrows shows the direction of least-principal, horizontal stress in the area that includes the Garlock fault, Sierra Nevada, and the transitional zone (seen here as a wedge shape bound by the Sierra Nevada, Garlock fault, and the Walker Lane). Also shown is another arrow that denotes the area as having an intermediate rate (V_2) of northwest migration. The San Andreas fault separates the V_2 zone and the V_1 zone. The V_1 zone has the highest rate of northwest migration.

Assuming the Sierra Nevada drag-rotated under the above proposed conditions, the Garlock fault, the bend in the San Andreas, the compressional structures west of the Sierra Nevada block, and the different structural style of the transition zone could have been the result.

8.3 SUMMARY AND CONCLUSIONS

The zone between the Sierra Nevada and the Walker Lane has long been noticed as being structurally different than that of the main Basin and Range province. Wright (1975) showed that most of the structures in his Deformational Field I (Basin and Range proper) are north-northeast trending and dominated by normal-slip faulting. This report presents evidence that Wright's Deformational Field II (zone between the Sierra Nevada and Walker Lane) contains abundant northwest, right-slip faults and north-south trending, normal-slip faults and that the Walker Lane is boundary between the two structural styles. A plausible hypothesis is a clockwise rotation about the northern tip of the Sierra Nevada block.

9.0 SUMMARY AND CONCLUSIONS

The Coso Range is a highly-active, tectonic area with a potential to produce major earthquakes. All active faults within the Coso Range were observed in the field to obtain fault-morphology data. The data were compiled to help determine activity, style, and amount of displacement for each fault.

The Little Lake fault is the only purely right-slip fault in the study area. The morphology includes shutter ridges, linear troughs, sag ponds, and pressure ridges. Thirty meters of right-slip displacement were found in undated material of probable Holocene age. Two hundred fifty meters of right-slip displacement were found in a 400,000-year-old basalt flow.

The southern segment of the Airport Lake fault proved to have right-slip displacement based on left-stepping, *en echelon* patterns and on associated tension grabens. Recency of displacement is indicated by flipped stones found near the fault scarps. The faulting generally adheres to the mountain front, however, occasional scarps are formed along young alluvial fans. It has been estimated the fans can be no older than 10,000 years. Displacement in the fans are dip-slip with scarps up to 3 meters in height.

The Coso Hot Springs and Haiwee segments of the Airport Lake fault have abundant offset stream channels and ridges. The overall pattern is left-stepping *en echelon* with normal-slip displacement on the *en echelon* segments up to 3 meters. The north end of the fault dissipates in lava

flows and is not seen as a continuous, mappable fault until it reaches the far northern end of the Coso Range.

The faulting on the east side of Airport Lake is left-stepping, *en echelon* faults with dip-slip displacement on each *en echelon* segment reaching 3 meters. The fault crosses recent fan development (thought to be less than a hundred years old), and displaces it by 0.5 meter. The overall, mapped length is 24 kilometers; however, evidence suggests that it could be much longer in a southerly direction.

The Airport Lake trench (Trench A) was located on a young, alluvial fan. The displacement in the trench was seen as 3 meters of dip-slip offset of two cinder-rich, obsidian-rare layers. The age of these layers, based on volcaniclastic chronology, is between 88,000 and 90,000 years. A 2-centimeter soil layer forming the surface is thought to be no more than 10,000 years old. There was no evidence in the trench of multiple events.

A trench located on faults along the east side of Airport Lake (Trench B) exposed a graben with a minimum of 3.4 meters of dip-slip displacement. There was no evidence of multiple events in this trench. Based on the soil stratigraphy, the faulting is thought to have occurred in the last few thousand years.

The trench located on the Little Lake fault, although incompletely studied, exposed a 4-meter wide, crushed zone. The fault plane dips to the southwest. Abundant liquefaction features, probably mud volcanoes, were identified along one stratigraphic horizon. This horizon is dated at about 2500 years and records a massive earthquake since that time.

Based on fault-scarp-profile data, the Coso Hot Springs segment of the Airport Lake fault has undergone displacement as recent as a hundred years ago. The highest scarp reaches 7.1 meters.

The method of Wallace leads to the conclusion that the southern segment of the Airport Lake fault has undergone displacement as recently as 40 years ago; however, this is certainly an anomalous result because the last likely event that could have displaced faults in the Coso Range was the 1872 Owens Valley earthquake; and indeed Profile 2 suggests movement of about that age. Profile data on the east side of Airport Lake suggest displacement about a hundred years ago. These data suggest the possibility that displacement occurred on these faults during the 1872 Owens Valley earthquake.

Regional and local seismicity has caused damage in China Lake and Ridgecrest. The largest earthquake in California history occurred within 100 kilometers of the study area. Microseismicity occurs every day and deomnstrates a very high rate of tectonism in the Coso Range. The potential for large magnitude earthquakes near Indian Wells Valley is probably as high as anywhere in California.

The alignment of epicenters and focal mechanism plots both agree with the geologically-obtained data on the local tectonic mechanism.

Austin (1971), Koenig (1972), and one of Duffield's earlier papers (1975) have interpreted the arcuate features of faulting in the Coso Mountains in terms of recent subsidence within a caldera-like structure. Thus, under these interpretations, volcanism controls the structural features of the region.

In this paper, it has been shown that the sense of faulting is consistent with the predominant, principal stress directions of the Basin and Range (i.e., east-west extension and northeast-southwest compression). The volcanic and fumerolic activity are clearly associated with features that relate to these stresses, and thus are manifestations of them rather than indicators of the dominant tectonic mechanism of the area. Also, it follows then, the overall assessment of the geothermal potential may be reduced by these factors.

The pattern developed in this paper of regional stress is consistent with that expected in the southwest Basin and Range province; graben structures and normal faulting running north-south. This paper documents a significant component of right-lateral, strike-slip motion that is consistent with San Andreas-Garlock tectonism to the west and south. Therefore, the area fits Wright's (1976) classification of Basin and Range province "Deformational Field II" as he predicted it would: The Coso Range area is a region of transition between San Andreas-Garlock and Basin and Range provinces, with recent folding and faulting showing characteristics of each of these provinces, and some peculiar to itself.

The zone between the Sierra Nevada and Walker Lane has long been noticed as structurally different than that of the Basin and Range province proper. Wright (1975) provided evidence that most of the structures in his Deformational Field I (Basin and Range proper) are north-northeast trending and dominated by normal-slip faulting. This report presents evidence that Wright's Deformational Field II (zone between the Sierra Nevada and Walker Lane) contains abundant northwest, right-slip faults and north-south trending, normal-slip faults and that the Walker Lane provides

a discontinuity between the two structural styles. A plausible hypothesis to explain the regional structure is a clockwise rotation about the northern tip of the Sierra Nevada Block.

10.0 REFERENCES

Albee, A. L., and Smith, J. L., 1966, Earthquake characteristics and fault activity in southern California: Engineering Geology in Southern California, R. Lung and R. Proctor, eds., Associated Engineering Geologists, Glendale, California, p. 9-33.

Allen, C. R., St. Amand, P., Richter, C. F., and Nordquist, J. M., 1965, Relationship between seismicity and geologic structure in the southern California region: Seismological Society of America Bulletin, v. 55, p. 753-797.

Austin, C. F., and Pringle, J. K., 1970, Geologic investigations at the Coso thermal area: U. S. Naval Weapons Center, China Lake, NWC TP 4878.

Austin, C. F., Austin,, W. H., and Leonard, G. W., 1971, Geothermal science and technology - a national program: U. S. Naval Weapons Center, China Lake, California, Technical Series 45-029-72.

Atwater, T., 1970, Implications of plate tectonics for the Cenozoic tectonic evolution of western North America: Geol. Soc. Amer., Bull., V. 81, p. 3513-3536.

Bonilla, M. G., 1967, Historic surface faulting in continental United States and adjacent parts of Mexico: U. S. Geological Survey Open-File Report; also Atomic Energy Commission Report TID-24124.

Bonilla, M. G., 1970, Surface faulting and related effects in earthquake engineering: Earthquake Engineering, Englewood Cliffs, N. J. Prentice-Hall, Ch. 3, p. 47-74.

Bonilla, M. G., and Buchanan, J. M., 1970, Interim report on worldwide historic surface faulting: U. S. Geological Survey Open-File Report.

California Division of Mines and Geology, 1955, Earthquake in Kern County, California, during 1952: Bulletin 171.

Campbell, M. R., 1902, Reconnaissance of the borax deposits of Death Valley and Mojave Desert: U. S. Geological Survey Bulletin 200.

Carr, W. G., 1974, Summary of tectonic and structural evidence for stress orientations at the Nevada Test Site: U. S. Geological Survey Open-File Report 74-176, p. 53.

Chakrabarty, S. K., and Richter, C. F., 1949, The Walker Pass earthquakes and structure of the southern Sierra Nevada: Seismological Society of America Bulletin, v. 53, p. 1075-1083.

Chesterman, C. W., 1956, Pumice, pumicite, and volcanic cinders in California: California Division of Mines Bulletin, p. 174.

Chinnery, M. A., 1966, Secondary Faulting - Geological aspects: Canadian Journal of Earth Sciences, v. 3, p. 175-190.

Clark, M. M., 1973, Map showing recently active breaks along the Garlock and associated faults, California: Miscellaneous Geology Investigation Map I-741, Scale 1:24,000, U. S. Geological Survey, Washington, D. C.

Cluff, L. S., and Slemmons, D. B., 1972, Wasatch fault zone - Features defined by low-sun-angle photography: Publication 1, Utah Geological Association, Salt Lake City, Utah, p. 61-69.

Comb, J., 1975, Heat flow and microearthquake studies, Coso geothermal area, China Lake, California: Final Report to Advanced Research Projects Agency (ARPA), p. 65.

Combs, J., and Rotstein, Y., 1976, Microearthquake studies at the Coso geothermal area, China Lake, California: Proceedings of the 2nd United Nations Symposium on the Development and Use of Geothermal Resources, U. S. Government Printing Office, v. 2. p. 909-916.

Combs, J., and Jarzabek, D., 1977, Seismic evidence for a deep heat source associated with the Coso geothermal area, California: U. S. Energy Research Development Administration Coso Geothermal Project Technical Report 4, p. 13.

Davis, G. A. and Burchfiel, D. C., 1973, Garlock fault: An intracontinental transform structure, southern California: Geological Society of America Bulletin, v. 84, p. 1407-1422.

Derr, J. S., Gordon, D., Irby, L. W., Kangas, R., Minsch, J., Person, W. J., Presgrave, B., 1977, Preliminary determination of epicenters, March 1977: U.S. Geological Survey Publication.

Duffield, W. A., 1975, Late Cenozoic ring faulting and volcanism in the Coso Range area of California: Geology, v. 3, p. 335-338.

Duffield, W. A., and Bacon, C. R., 1977, Preliminary geologic map of the Coso volcanic field and adjacent areas, Inyo County, California, with a table of new K/Ar dates by G. B. Dalrymple: U. S. Geological Survey Open-File Report, Scale 1:50,000, p. 77-311.

Duffield, W. A., and Smith, G. I., 1978, Pleistocene history of volcanism and the Owens River near Little Lake, California: U. S. Geological Survey Journal of Research, v. 6, p. 395-408.

Fairbanks, H. W., 1896a, Notes on the geology of eastern California: American Geologist, v. 17, p. 63-74.

Fairbanks, H. W., 1896b, The mineral deposits of eastern California: American Geologist, v. 17, p. 144-158.

Fournier, R. O., Thompson, J. M., Austin, C. F., 1978, Chemical analysis and preliminary interpretation of waters collected from the CGEH No. 1 geothermal well at Coso, California: U. S. Geological Survey Open-File Report 78-434, p. 10.

Fox, R. C., 1978a, Low-altitude aeromagnetic survey of a portion of the Coso Hot Springs, KGRA, Inyo County, California: Salt Lake City, Utah, University of Utah Research Institute, Earth Sciences Laboratory, p. 19.

Fox, R. C. 1978b. Dipole-dipole resistivity survey of a portion of the Coso Hot Springs, KGRA, Inyo County, California: Salt Lake City, Utah, University of Utah Research Institute, Earth Sciences Laboratory, p. 21.

Fraser, H. J., Wilson, H. D. B., and Hendry, N. W., 1942, Hot Springs deposits of the Coso Mountains: California Journal of Mines and Geology, v. 38, no. 3-4, p. 223-242.

Friedman, M. E., Whitcomb, J. H., Allen, C. R., and Hileman, J. A., 1976, Seismicity of the southern California region, 1 January 1972 to 31 December 1974: Pasadena, California Institute of Technology, Seismological Laboratory.

Fuis, G. S., Whitcomb, J. H., Johnson, C. E., Jenkins, D. K., Richter, K. J., Blanchard, A. C., Fisher, S. A., and Reed, B. A., 1978, Preliminary catalog of earthquakes in southern California, October 1976--September 1977: U. S. Geological Survey Open-File Report 78-678.

Furgerson, R. B., 1973, Progress report on electrical resistivity studies, Coso geothermal area, Inyo County, California: U. S. Naval Weapons Center, China Lake, California, NWC TP 5497, p. 38.

Galbraith, R. M., 1978, Geological and geophysical analysis of Coso Geothermal Exploration Hole No. (CGE#-1), Coso Hot Springs KGRA, California: Salt Lake City, Utah, University of Utah Research Institute, Earth Sciences Laboratory, p. 39.

Gilbert, G. K., 1875, Report of the geology of portions of Nevada, Utah, California, and Arizona: U. S. Geographical and Geological Surveys W. 100th Meridian Report, v. 3.

Goodyear, W. A., 1888, Inyo County: Report of the State Mineralogist (California), v. 8.

Hall, W. E., and MacKevett, E. M. Jr., 1962, Geology and ore deposits of the Darwin quadrangle, Inyo County, California: U. S. Geological Survey Professional Paper 368.

Healy, J. H., and Press, F., 1964, Geophysical studies of basin structures along the eastern front of the Sierra Nevada, California: Geophysics, v. 29, p. 337-359.

Hileman, J. A., Allen, C. R., and Nordquist, J. M., 1973, Seismicity of the southern California region, 1 January 1932 to 31 December 1972: Pasadena, California Institute of Technology, Seismological Laboratory.

Hobbs, W. H., 1910, Earthquake of 1872 in Owens Valley, California: Beitrage zur Geophysik, v. 10, p. 352-385.

Hopper, R. H., 1947, Geologic section from the Sierra Nevada to Death Valley, California: Geological Society of America Bulletin, v. 58, p. 393-432.

Hulen, J. B., 1978, Geology and alteration of the Coso geothermal area, Inyo County, California: Report N. IDO/78-1701.b.4.1, U. S. Department of Energy, p. 28.

Humphreys, W. J., 1918, Earthquakes felt in the United States during 1917: Monthly Weather Review (December 1917).

Iida, K., 1959, Earthquake energy and earthquake fault: Nagoya University, Journal of Earth Science, v. 7, no. 2, p. 98-107.

Iida, K., 1965, Earthquake magnitude, earthquake fault, and source dimensions: Nagoya University, Journal of Earth Science, v. 13, no. 2, p. 115-132.

Kelley, V. C., 1937, Origin of the Darwin silver-lead deposits: Economic Geology, v. 32, p. 987-1008.

Kelley, V. C., 1938, Geology and ore deposits of the Darwin silver-lead mining district, Inyo County, California: California Journal of Mines and Geology, v. 34, no. 4, p. 503-563.

Knopf, A., 1918, A geologic reconnaissance of the Inyo Range and the eastern slope of the southern Sierra Nevada, California: U. S. Geological Survey Professional Paper 110.

Koenig, J. B., Gawarecki, S. J., and Austin, C. F., 1972, Remote sensing survey of the Coso geothermal area, Inyo County, California: U. S. Naval Weapons Center, China Lake, California, NWC TP 5233, p. 32.

Lanphere, M. A., Dalrymple, G. B., and Smith R. L., 1975, K/Ar ages of Pleistocene rhyolitic volcanism in the Coso Range, California: Geology, v. 3, p 339-341.

LeSchack, L. A., Lewis, J. E., and Chang, D. C., 1977, Rapid reconnaissance of geothermal prospects using shallow temperature surveys: Report prepared under Department of Energy Contract EG-77-C-01-4021.

Mulholland, W., 1918, Earthquakes in their relation to the Los Angeles Aqueduct: Seismological Society of America Bulletin, v. 8, no. 1, p. 13-19.

Nakamura, K., 1977. Volcanoes as possible indicators of tectonic stress orientation: Journal Volcanology Geothermal Research, v. 2, p. 1-16.

Oakeshott, G. B., Greensfelder, R. W., Kahle, J. E., 1972, One hundred years later: California Division of Mines and Geology, California Geology, v. 25, no. 3, p. 55-61.

Palmer, A. H., 1918, California earthquakes during 1917: Seismological Society of America Bulletin, v. 8, no. 1, p. 13-19.

Power, W. R., Jr., 1958, Preliminary report on the geology and uranium deposits of Haiwee Ridge, Inyo County, California: U. S. Atomic Energy Commission Report, RME-2066, p. 37.

Power, W. R., Jr., 1959, Geology and petrology of Haiwee Ridge, Inyo County, California (Ph.D. thesis): Baltimore, Maryland, The Johns Hopkins University.

Richter, C. F., Gardner, J. K., Nordquist, J. M., 1962, Bulletin on local shocks, October-December 1961: Pasadena, California Institute of Technology, Seismological Laboratory.

Richter, C. F., 1962, Bulletin on local shocks, July-September 1962: Pasadena, California Institute of Technology, Seismological Laboratory.

Roquemore, G. R., 1977, Cenozoic history of the Coso Mountains as determined by tuffaceous lacustrine deposits (M. A. thesis): Fresno, California, California State University.

Roquemore, G. R., 1978a, Evidence for Basin and Range/Sierra Nevada transitional zone structures in the Coso Mountains, California: Geological Society of America Abstracts with Programs, v. 10, p. 144.

Roquemore, G. R., 1978b, Active faults and related seismicity of the Coso Mountains, Inyo County, California: Earthquake Notes, v. 49, p. 24.

Ross, C. P., and Yates, R. G., 1943, The Coso quicksilver district, Inyo County, California: U. S. Geological Survey Bulletin 935-Q.

Russell, R. J., 1926, Climates of California: University of California Publication in Geography 2 (4), p. 73-84.

Schultz, J. R., 1937, A late Cenozoic vertebrate fauna from the Coso Mountains, Inyo County, California: Washington, D. C., Carnegie Institute Publication 427, p. 75-109.

Slemmons, D. B., 1967, Pliocene and Quaternary crustal movements at the Basin-and-Range province, USA, J. Geosci., v. 10, p. 91-101.

Slemmons, D. B., 1977, State-of-the-art for assessing earthquake hazards in the United States: U. S. Army Eng. Water W. Exp. Stn., Misc. Paper S-73-1, Rep., v. 6, p. 129.

Slemmons, D. B., Van Wormer, D., Bell, E. J., and Silberman, M. L., 1979, Recent crustal movements in the Sierra Nevada-Walker Lane region of California-Navada: Part I, Rate and style of deformation. In: C. A. Whitten, R. Green, and B. K. Meade (eds.), Recent Crustal Movements, 1977: Tectonophysics, v. 52, p. 561-570.

Spurr, J. E., 1903, Descriptive geology of Nevada south of the fortieth parallel and adjacent portions of California: U. S. Geological Survey Bulletin 208.

St. Amand, Pierre, 1958, Circum-Pacific orogeny: Publication of the Dominion Observatory, v. 20, no. 2, p. 403-411.

Stinson, M. C., 1977, Geologic map and sections of the Haiwee Reservoir 15-minute quadrangle, Inyo County, California: California Division of Mines and Geology Map Sheet 37, scale 1:62,500.

Teledyne Geotech, 1972, Geothermal noise survey of the Coso Hot Springs area, Naval Weapons Center, China Lake, California: U. S. Naval Weapons Center, China Lake, California, NWC TP 72-6, p. 14.

Tocher, D., 1958, Earthquake energy and ground breakage: Seismological Society of America Bulletin, v. 48, no. 2, p. 147-153.

Troxel, B. W., Wright, L. A., and Jahns, R. H., 1972, Evidence for differential displacements along the Garlock fault zone, California: Geol. Soc. America Abs. with Programs, v. 4, p. 250.

von Huene, R. W., 1960, Structural geology and gravimetry of Indian Wells Valley, southeastern California (Ph. D. thesis): Los Angeles, California, Unversity of California, p. 138.

Wallace, R. E., 1977, Profiles and ages of young fault scarps, north-central Nevada: Geological Society of America Bulletin, v. 88, no. 9, p. 1267-1281.

Walter, A. W., and Weaver, C. S., 1980a, Catalog of earthquakes in the Coso Range and vicinity, Southern California: U. S. Geological Survey Open-File Report (in press).

Walter, A. W., and Weaver, C. S., 1980b, Seismic studies in the Coso geothermal area, Inyo County, California: Journal of Geophysical Research (in press).

Warner, T., 1930, Mercury deposit in Coso Range, Inyo County, California: Mining in California, v. 25, p. 58-63.

Whitney, J. D., 1865, Geology of California: Geological Survey of California, v. 1, p. 474.

Whitney, J. D., 1872, The Owens Valley earthquake: Overland Monthly, v. IX, no. 8, p. 130-140 and no. 9, p. 266-278.

Wright, L. A., 1976, Late Cenozoic fault patterns and stress fields in the Great Basin and westward displacement of the Sierra Nevada block: Geology, v. 4, p. 489-494.

Zbur, R. T., 1963, A geophysical investigation of Indian Wells Valley, California: U. S. Naval Ordnance Test Station, China Lake, NWC TP 2795, p. 98.

Zoback and Zoback, 1980, State in the conterminous United States: Journal of Geographical Research, v. 85, no. B-11, p. 6113-6156.